Structural studies on the membrane attack complex and staphylococcal immune evasion

C8α-MACPF, C5b6 and FLIPr-like-FcγRIIa

Michiel Arjan Hadders

ISBN: 978-90-3935472-8

Print: Ipskamp Drukkers B.V.

Cover: Impression of a MACPF domain

Structural studies on the membrane attack complex and staphylococcal immune evasion:

C8α-MACPF, C5b6 and FLIPr-like-FcγRIIa

Structurele studies aan het membraan aanvals complex en ontduiking van het immuunsysteem door stafylokokken*:*

C8α-MACPF, C5b6 en FLIPr-like-FcγRIIa

(met een samenvatting in het Nederlands)

Proefschrift

ter verkrijging van de graad van doctor aan de Universiteit Utrecht op gezag van de rector magnificus, prof. dr. J.C. Stoof, ingevolge het besluit van het college voor promoties in het openbaar te verdedigen op woensdag 1 december 2010 des middags te 2.30 uur

door

Michiel Arjan Hadders

geboren op 31 juli 1979 te Jubail, Saoedi-Arabië

Promoter: Prof. Dr. P. Gros

Het in dit proefschrift beschreven onderzoek werd gefinancierd door de Nederlandse organisatie voor Wetenschapelijk Onderzoek (NWO), gebied Chemische Wetenschappen (CW).

Science never solves a problem
without creating ten more.

George Bernard Shaw

Table of contents

Chapter 1

General Introduction

Michael A. Hadders

Crystal and Structural Chemistry, Bijvoet Center for Biomolecular Research, Department of Chemistry, Faculty of Science, Utrecht University, Padualaan 8, 3584 CH, Utrecht, Netherlands

The number of bacterial cells living in and on a human being is estimated to exceed the number of cells of an adult by at least tenfold. Most often these bacteria do not pose a threat and some are actually beneficial. The human host is protected from bacteria by the epithelial lining, which forms a physical barrier between the two. The breaching of this barrier results in a rapid immune reaction that typically clears the infection before any damage is done. This initial response is part of the innate immune system and is ready to strike immediately. However, sometimes an infection persists, requiring a much more specific reaction. This adaptive response may take up to a week to reach maximal effectiveness but it typically succeeds where the innate response failed. Although the innate and adaptive immune system differ in their specificity they ultimately call upon the same effectors to clear the infection. Bacteria on the other hand are under strong selective pressure to evolve strategies to evade and interfere with host immune detection. Indeed, invading bacteria have an awesome arsenal of weapons that may rival the host immune response.

The Complement System

The mammalian immune system must respond rapidly upon infection. The complement system forms one of the first lines of defense and is able to specifically recognize invading micro-organisms, altered host cells and debris (Walport 2001; Walport 2001). The system consists of over thirty large modular plasma and membrane associated proteins, which form an intricate molecular cascade (Gros, Milder et al. 2008). The activation of the complement system gives rise to a series of proteolytic events which result in the subsequent activation of downstream effector proteins. Together these proteins can then clear the foreign particles from circulation, initiate an inflammatory response and facilitate the full activation of an adaptive immune response. Moreover, complement proteins can also directly kill invading microbes through initiation of the terminal pathway, which leads to the formation of lytic pores called the membrane attack complex (MAC).

Activation

The complement system has three major pathways that lead to activation: the classical pathway, the mannose-binding lectin (MBL) pathway and the alternative pathway, allthough the initiation of complement by properdin is also becoming recognized as an independent activation pathway (**Figure 1**) (Kemper, Atkinson et al.; Muller-Eberhard 1988). These pathways all converge at the assembly and activation of protease complexes called C3 convertases which activate the central protein of the complement system, C3. The proteolytic activation of C3 results in C3b (**Box 1**), which is the main effector protein of the complement system. C3b attaches covalently to the pathogens surface through a reactive thioester and is involved in all major effector functions.

Complement activation is initiated by pattern recognition molecules such as antibodies and C1 in the classical pathway and MBL and ficolins in the MBL pathway (Wallis, Mitchell et al.; Ziccardi 1984; Ikeda, Sannoh et al. 1987). These recognition events result in the activation of proteases that can cleave and activate complement components C4 and C2, resulting in the active classical pathway convertase C4b2a (Muller-Eberhard, Polley et al. 1967). First, C4 is cleaved, resulting in C4b. The large conformational change that accompanies this conversion exposes the reactive thioester and a cryptic binding site for the zymogen C2. The thioester typically reacts with the target surface resulting in the

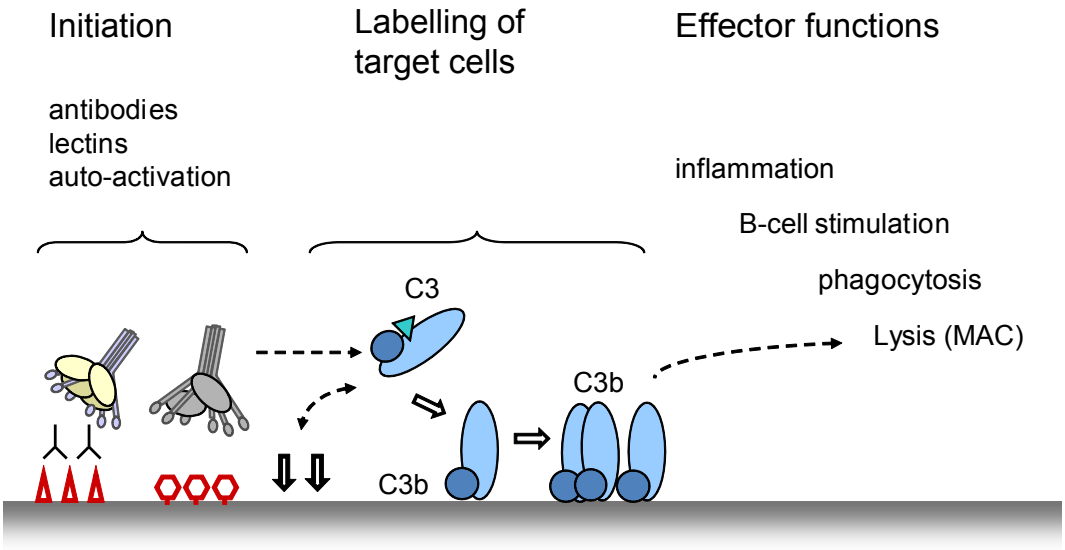

Figure 1 Schematic representation of the three stages of complement activation.

covalent attachment of C4b (Law, Dodds et al. 1984), while the binding of C2 makes it susceptible to proteolytic activation, resulting in the active convertase C4b2a. This surface attached protease complex can turn over C3 molecules to C3b, which again attach covalently to the target surface.

The alternative pathways is activated in a different manner. There are no pattern recognition proteins involved, instead the system is continuously activated by the spontaneous hydrolysis of the internal thioester in C3 (Pangburn, Morrison et al. 1980; Pangburn and Muller-Eberhard 1980). This results in an active form of C3, called C3(H_2O) and like in C4, activation of C3 exposes a cryptic binding site for a zymogen, in this case factor B (FB) (Pangburn, Schreiber et al. 1981; Smith, Vogel et al. 1984). Upon binding, FB becomes susceptible to proteolytic activation resulting in the alternative pathway C3 convertase C3(H_2O)Bb which can then turn over C3 to C3b which again attaches to target surfaces (Fishelson, Pangburn et al. 1984). Since C3b is both a cofactor and product of the C3 convertases the alternative pathway is not only important for initiating complement activation but also for amplification. Every C3b deposited on the surface can, through formation of new alternative pathway convertases, generate new C3b molecules. This results in a rapid amplification of the initial response and the opsonization of an entire bacterial cell in only minutes.

Regulation

The classical and MBL pathways can specifically recognize pathogens through antibodies and pattern recognition molecules. This results in a very local activation of the complement system that should prevent damage of surrounding host tissue. The alternative pathway on the other hand, is indiscriminate. The spontaneous hydrolysis of the internal thioester in C3 can lead to complement activation on any surface. Moreover, in certain pathological conditions host tissue may be recognized as foreign, resulting in antibody deposition and classical pathway complement activation. The complement system must therefore be tightly regulated (Liszewski, Farries et al. 1996; Kirkitadze and Barlow 2001).

Box 1

The protein C3 belongs to the α2-macroglobulin family, which also includes complement components C4 and C5 (Armstrong and Quigley 1999). These are large multidomain proteins with an intricate folding pattern (**figure 1A-C**). The complement family members consist of thirteen domains depicted schematically in **figure 2**: eight macroglobulin (MG) domains, a CUB domain, an anaphylotoxin domain, a C345C domain, a linker region and a thioester containing domain (TED) which contains the hallmark reactive thioester (with the exception of C5). During the secretion process the proteins are cleaved in a loop that connects the linker region with the anaphylotoxin domain. This results in a mature protein consisting of two chains called the α- and β-chain (depicted in purple and green in the figures below). The proteins can then be activated, by a second proteolytic event that removes the anaphylotoxin. It is though that this activation step leads to large conformational changes and, in the case of C3 this has been well established. Crystal structures and electron microscopy data of C3 and C3b show detailed snapshots of the rearrangements the protein undergoes during activation (Janssen, Huizinga et al. 2005; Fredslund, Jenner et al. 2006; Janssen, Christodoulidou et al. 2006; Nishida, Walz et al. 2006; Wiesmann, Katschke et al. 2006). In C3 the thioester is shielded from nucleophiles in a hydrophobic pocket while being kept in a less reactive conformation. Upon activation the TED swings out and down over a distance of 85Å (**figure 1A-B**), completely exposing the thioester. A concomitant conformational change in TED changes the conformation of the thioester into a highly reactive acyl-imidazole intermediate that readily reacts with available nucleophiles, like those present on the target surfaces of bacteria (Law and Levine 1977; Law, Lichtenberg et al. 1979; Dodds and Law 1998).

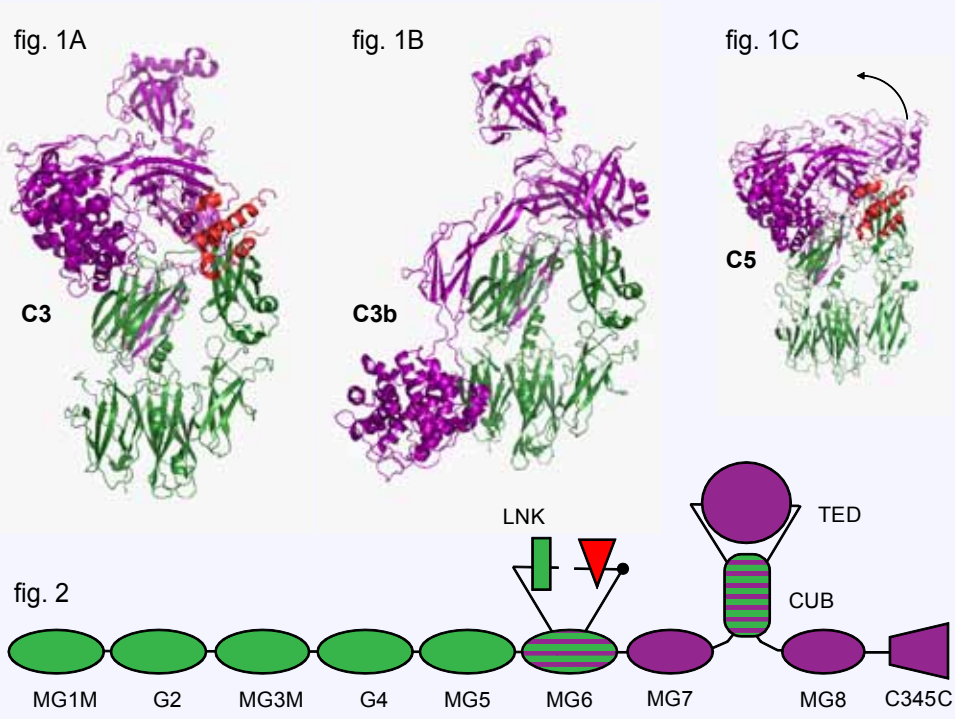

Cells of the host blood system carry a whole range of cell surface proteins that can down regulate inadvertent activation on host cells (**Table 1**). These proteins can disassociate the C3 convertases and/or serve as a cofactor for the proteolytic degradation of surface bound C3b. There are also soluble regulators to protect tissues that do not carry membrane bound regulators. Natural deficiencies or loss of function mutations in any of these regulators result in auto-immune diseases (**Table 1**) (Meri 2007).

Effector functions

When an invading bacteria is opsonized by C3b it becomes marked for destruction. C3b is involved in all effector functions of the complement system. Various cells of the immune system carry receptors that recognize surface bound C3b and/or its degradation products iC3b and C3d (**Table 1**) (Myones, Dalzell et al. 1988; Ehlers 2000; Krych-Goldberg and Atkinson 2001). These interactions mediate phagocytosis of the opsonized particles , which result in clearance from circulation. One of these receptors, CR2, is part of the B-cell co-receptor and binds to C3d on opsonized antigens. This interaction is necessary for full activation and proliferation of B-cells, leading to a ~10.000 fold enhancement compared to antigen binding alone (Dempsey, Allison et al. 1996; Fearon and Locksley 1996; Fearon and Carroll 2000). The activation of the complement system also results in the formation of the chemotactic peptides C3a and C5a (Guo and Ward 2005;

Table 1 List of complement receptors and their receptors

receptor	ligand	function
CR1/CD35	C3b/iC3b/ C4b	Mediates phagocytosis of opsonized particles. Accelarates the decay of the classical and alternative pathway convertase. Serves as a cofactor for the protease factor I to help in the degradation of surface bound C3b
CR2/CD21	iC3b/C3d	Part of the B-cell co-receptor complex. Ligation enhances B-cell proliferation upon antigen binding by 1.000-10.000 fold
CR3/ CD11b-CD18	iC3b	Mediates phagocytosis of opsonized particles
CR4/ CD11c-CD18	iC3b	Mediates phagocytosis of opsonized particles
CRIg	C3b/iC3b	Mediates phagocytosis of opsonized particles
C3aR	C3a	Initiation of a pro-inflammatory response. Mediates chemotaxis and activation of neutrophils
C5aR/CD88	C5a	Initiation of a pro-inflammatory response. Mediates chemotaxis and activation of neutrophils
MCP/CD46	C3b/C4b	Accelarates the decay of the classical and alternative pathway convertase. Serves as a cofactor for the protease factor I to help in the degradation of surface bound C3b and C4b
DAF/CD55	C3b	Accelarates the decay of the alternative pathway convertase
CD59	C8/C9	Prevents C8α and C9 insertion and assembly of the MAC
C4bBP	C4b	Serves as a cofactor for the protease factor I to help in the degradation of mainly fluid fase C4b
factor H	C3b	Serves as a cofactor for the protease factor I to help in the degradation of C3b

Haas and van Strijp 2007; Klos, Tenner et al. 2009). They result in the targeting of neutrophils to sites of infection and activates these cells, so that upon arrival the cells are ready to clear the invading pathogen. Moreover, C5a is a powerful mediator of inflammation. The complement system can also directly kill Gram-negative bacteria by initiation of the terminal pathway. This results in the assembly of cytolytic pores on target surfaces (Muller-Eberhard 1986; Esser 1994).

The Membrane Attack Complex

One of the most dramatic effector functions of the complement system is its ability to directly lyse and kill certain cells like Gram-negative bacteria but also host erythrocytes (Muller-Eberhard 1986; Esser 1994). Lysis takes place when the so called terminal or lytic pathway is initiated, resulting in the formation of the membrane attack complex (MAC). The MAC is a large (~1 MDa) pore forming structure and consists of five different proteins, C5b, C6, C7, C8 and C9 (Gotze and Muller-Eberhard 1970; Lachmann and Thompson 1970; Thompson and Lachmann 1970; Kolb, Haxby et al. 1972). Assembly of the MAC on a bacterial surface leads to a loss of membrane integrity resulting in lysis and cell death. With the exception of C5, all proteins of the MAC belong to the Membrane Attack Complex/PerForin (MACPF) family of proteins. These proteins all have a similar modular arrangement, consisting of a central MACPF domain with adjacent ancillary domains (**Figure 2**). The most important funtions have been ascribed to these central MACPF domains, however, nothing is known about how they function, in part due a lack of structural details.

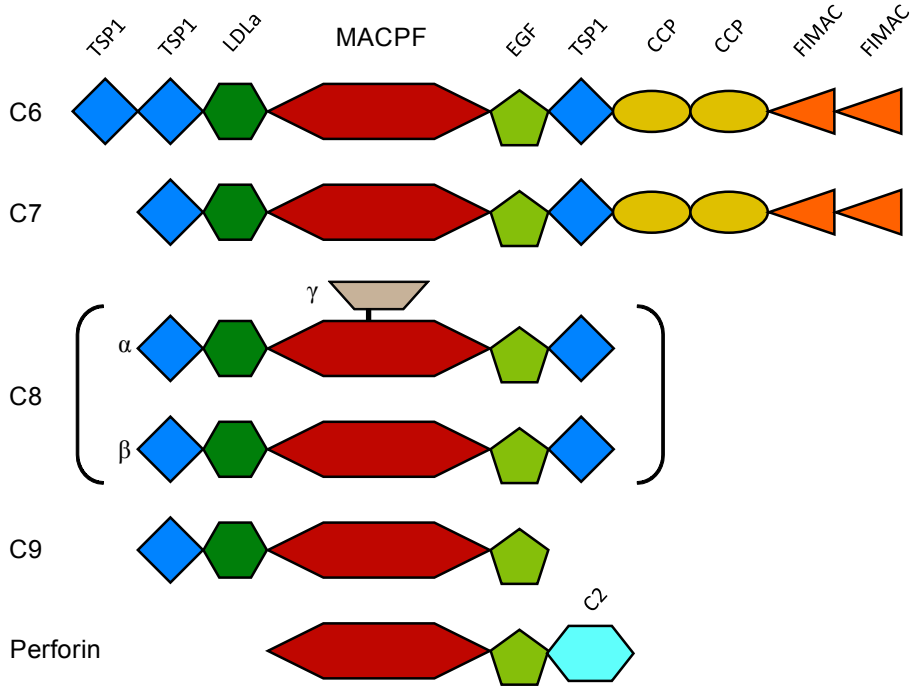

Figure 2 Domain organization of the known poreforming MACPF members.

Activation

When invading bacteria become tagged with C3b or C4b, convertases are formed that lead to the formation of more C3b. This results in rapid opsonization of the bacteria. When the number of C3b molecules on the surface exceeds a certain threshold both the classical and alternative pathway convertases change their specificity from C3 to C5. Most often the C5 convertase is denoted as C3bBbC3b or C4bBbC3b but the process of C5 activation is poorly understood and the exact molecular identity of the C5 convertase remains unclear (Pangburn and Rawal 2002). The C5 convertases cleave C5 resulting in the activation products C5a and C5b (Rawal and Pangburn 1998; Rawal and Pangburn 2000; Rawal and Pangburn 2003). The anaphylatoxin C5a initiates a powerful inflammatory response and plays an important role in resolving infections (Guo and Ward 2005). C5b on the other hand initiates the terminal pathway, resulting in formation of the MAC.

Assembly

The assembly of the MAC is an obligate sequential process (**Figure 3**). The terminal pathway is initiated by the formation of C5b and although C5 does not contain a reactive thioester like its homologues C3 and C4, the activation of C5 to C5b is thought to expose a similar cryptic binding site (Cooper and Muller-Eberhard 1970). When the first MACPF protein C6 binds to C5b, a binding platform for the second protein C7 is formed (Podack, Biesecker et al. 1978; Podack, Kolb et al. 1978). Upon binding of C7 the complex acquires an affinity for membranes, although C5b7 does not yet disrupt membrane integrity (Preissner, Podack et al. 1985). The C5b7 complex bound to the bacterial surface now forms a receptor for C8, a hetero-trimer consisting of two homologous chains called α and β, both belonging to the MACPF family, and a lipocalin called γ, which is covalently attached to the α-chain (Sodetz 1989). While C8β is responsible for binding to C5b7, the α-chain is the first protein to penetrate the membrane (Monahan and Sodetz 1980; Hu, Esser et al. 1981; Ishida, Wisnieski et al. 1982; Steckel, Welbaum et al. 1983; Stewart, Kolb et al. 1987). The loss of hemo-

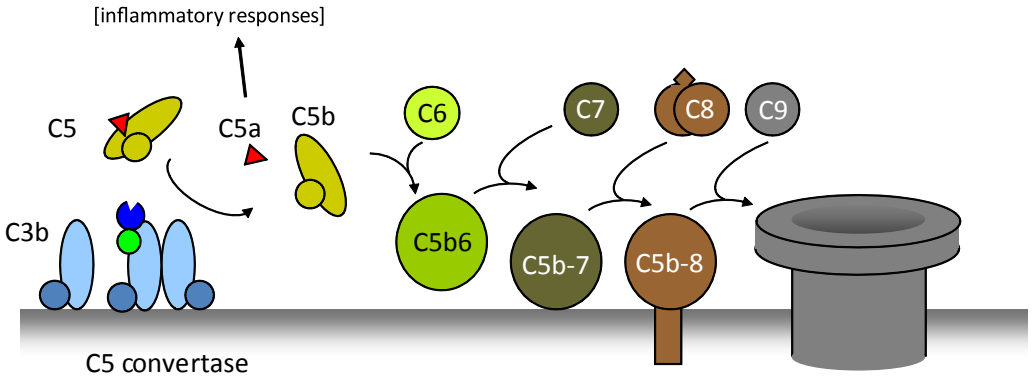

Figure 3 Schematic representation of formation of the membrane attack complex.

globin from erythrocytes on which C5b8 is assembled indicates this penetration leads to a significant loss of membrane integrity (Tschopp and Podack 1981). However, on bacteria this complex is not bactericidal and for full activity the pore forming protein C9 is needed (Joiner, Schmetz et al. 1985). In the final step C9 binds to the C5b8 complex which catalyzes it's polymerization and membrane insertion (Tschopp, Podack et al. 1985). It has been shown that the transition from the water soluble form to the membrane inserted state involves a substantial refolding of C9 (Laine and Esser 1989).

Membrane insertion

During assembly of the MAC, C7 (in C5b7) mediates the initial binding event to membranes. However C5b7 is a peripheral membrane protein and only very little membrane insertion could be detected using membrane restricted probes (Hu, Esser et al. 1981; Ishida, Wisnieski et al. 1982; Steckel, Welbaum et al. 1983). Studies with these probes have demonstrated that C8 and C9 insert into the membrane. The membrane inserted sequences have been mapped to the MACPF domains of C9 and the C8α-chain of C8, more specifically to a stretch of residues between 272-345 in C9. Based on this data Peitsch et al. proposed a model in which two predicted helical hairpins form the linings of protein pore, much like the bacterial alpha-helical colicins discussed below (Peitsch, Amiguet et al. 1990). These helices are however not hydrophobic but amphipathic with the connecting loops carrying several charges making it difficult to envision how these segments would insert or traverse a hydrophobic membrane. At this moment it is unclear how the MAC forms pores and it remains to be seen if the membrane inserting segments form the lining of a physical structure or cause a local distorion of lipids similar to honeybee mellitin (Esser, Kolb et al. 1979; Laine, Morgan et al. 1988; Laine and Esser 1989). This mechanism has also been proposed for other alpha helical poreforming proteins like the BCL2 family involved in apoptosis (Qian, Wang et al. 2008).

Pore formation and bacterial killing

In vivo, the C5b8 complex mediates membrane insertion and polymerization of C9 (Podack, Tschoop et al. 1982). However, in vitro C9 is able to form large ring-like structures with an internal diameter of ~10 nm, without the aid of C5b8. This process can be sped up by increased temperatures, detergents and divalent cations like Zn^{2+} (Tschopp 1984; Tschopp, Engel et al. 1984; Amiguet, Brunner et al. 1985). Although these ring-like structures are a logical candidate for the lytic moiety of the MAC they differ in their pore characteristics. Moreover, just three copies of C9 per C5b8 is enough to achieve full hemolytic and bactericidal activity (Joiner, Schmetz et al. 1985; Bhakdi and Tranum-Jensen 1986). Taken together, these data suggest that in vivo, MAC pores do not necessarily consist of the large ring-like structures observed for poly-C9 (Tschopp 1984). Regardless of the actual structural identity of the pore, the MAC is efficient in bacterial killing. The importance of MAC mediated killing is underscored by people deficient in any of the terminal components. These patients suffer from recurring infections, most notably of Neisserial origin (Harriman, Esser et al. 1981; Walport 2001; Botto, Kirschfink et al. 2009). Gram-positive bacteria are impervious to MAC attack due to the thick layer of peptidoglycan in their cell walls, but MAC assembly on Gram-negative pathogens leads to a rapid dissipation of membrane potential across the inner membrane (Wright and Levine 1981; Wright and Levine 1981; Joiner, Schmetz et al. 1985; MacKay and Dankert 1990). This results in target cell death but how the MAC is able to reach and damage the inner membrane is unclear. It has been observed that C9 alone, upon gaining acces to the periplasm, is also able to kill bacteria supporting a model in which surface as-

sembled C5b8 functions mainly as a receptor for C9 (Dankert and Esser 1987; Wang, Bjes et al. 2000). Initial loss of membrane integrity across the outer membrane would then lead to diffusion of more C5b8 and or C9 through the periplasm, where it could then damage the inner membrane.

Host protection

Since inadvertent complement activation can harm host tissue, the system must be tightly regulated. There are multiple cell surface proteins that regulate complement activation at steps upstream of the terminal pathway and one protein, CD59, that specifically interferes with reactive lysis (Zalman, Wood et al. 1986). CD59 is a cell surface protein that is attached to the membrane through a GPI-anchor. It is found on most cells of lymphoid origin and on erythrocytes and protects these cells by interfering with membrane insertion of both C8 and C9 (Lehto and Meri 1993; Farkas, Baranyi et al. 2002). Moreover, CD59 also prevents further incorporation of C9 into both C5b8 and C5b9. The protective function of CD59 is species specific, which has aided in identifying the segments in C8 and C9 that interact with CD59. Making use of recombinant human-horse and human-rabbit chimeras it was demonstrated that the CD59 binding site is located in a region between aa 334 -386 in C8α and 365-371 in C9 (Husler, Lockert et al. 1995; Tomlinson, Wang et al. 1995). The importance of CD59 protection is underscored by the acquired genetic disorder paroxysmal nocturnal haemoglobinuria (PNH) (Nishimura, Murakami et al. 1999; Botto, Kirschfink et al. 2009). In this disease patients have a genetic defect in the gene *PIGA* that encodes for the enzyme phosphatidylinositol N-acetylglucosaminyltransferase subunit A, which catalyzes the formation of the first biosynthetic intermediate of the GPI anchor. This results in a total absence of GPI anchored proteins on the cell surface with patients suffering from recurring outbreaks of anemia and thrombosis.

Perforin

Natural killer cells and cytotoxic T-cells also secrete a MACPF domain containing protein called perforin, which is able to form ring-like structures like C9 (Tschopp, Masson et al. 1986; Young, Cohn et al. 1986; Young, Hengartner et al. 1986; Young, Liu et al. 1986). Perforin is involved in the immune response against virally infected and transformed cells, the impotance of which is underscored by perforin mutations that lead to the severe disease familial hemophagocytic lymphohistiocytosis but also predispose to cancer (Voskoboinik, Smyth et al. 2006; Chia, Yeo et al. 2009). When natural killer cells and cytotoxic T-cells recognize their target an immune synapse is formed in which the contents of specialized secretory granules is released. These granules contain granzymes, that induce apoptosis in the target cell and perforin, which is necessary for the delivery of the granzymes. Perforin is able to form oligomeric ring-like structures that damage membrane integrity but unlike the MACPF proteins of the complement system perforin does not need any ancillary proteins. Instead, targeting to the membranes is achieved by its C-terminal C2 domain in a calcium dependent fashion (Voskoboinik, Thia et al. 2005). At this moment it is not clear whether perforin mediated pore formation results in direct diffusion of the granzymes into the target cell or mediates a membrane repair response that results in the internalization of the granzymes through endocytosis (Thiery, Keefe et al.; Keefe, Shi et al. 2005).

Bacterial pore forming toxins (PFTs)

Membrane attack through pore forming proteins is used not only in mammalian immune defense but also in bacterial attack. Bacteria secrete numerous toxins that are able to kill host cells by formation of pores that either result in direct lysis or facilitate the translocation of additional toxins that function inside the cell. These PFTs can be divided into two classes based on the secondary structure of their trans-membrane segments: the alpha-pore-forming toxins and the beta-pore-forming toxins (**Figure 4**) (Tilley and Saibil 2006). Like the proteins of the MAC and perforin these toxins are secreted as monomeric water soluble proteins that must transform into a multimeric integral membrane protein.

Alpha-pore-forming toxins

The mechanism of alpha-PFTs is poorly understood (Tilley and Saibil 2006). Although several structures of their pore-forming domains have been solved, not much is known about their oligomeric membrane inserted state. The pore-forming domains solved to date have a compact helical arrangement with two central helices that form a hydrophobic hairpin (**Figure 4**). It has been shown that upon binding of the toxin two a target receptor this domain unfolds, leading to membrane insertion of this helical hairpin. A similar mechanism has been proposed for the eukaryotic BCL-2 family of proteins and recently an alternative mechanism for both alpha-PFTs and BCL-2 family members has been proposed based on the way helical pore-forming peptides function (Qian, Wang et al. 2008; Martinez-Caballero, Dejean et al. 2009). Instead of the formation of an oligomeric ring-like structure, the inserted helical segments are thought to cause a rearrangement of lipid packing, leading to a disruption of membrane integrity. However, more detailed studies will have to clarify the exact nature of the pore of alpha-PFTs.

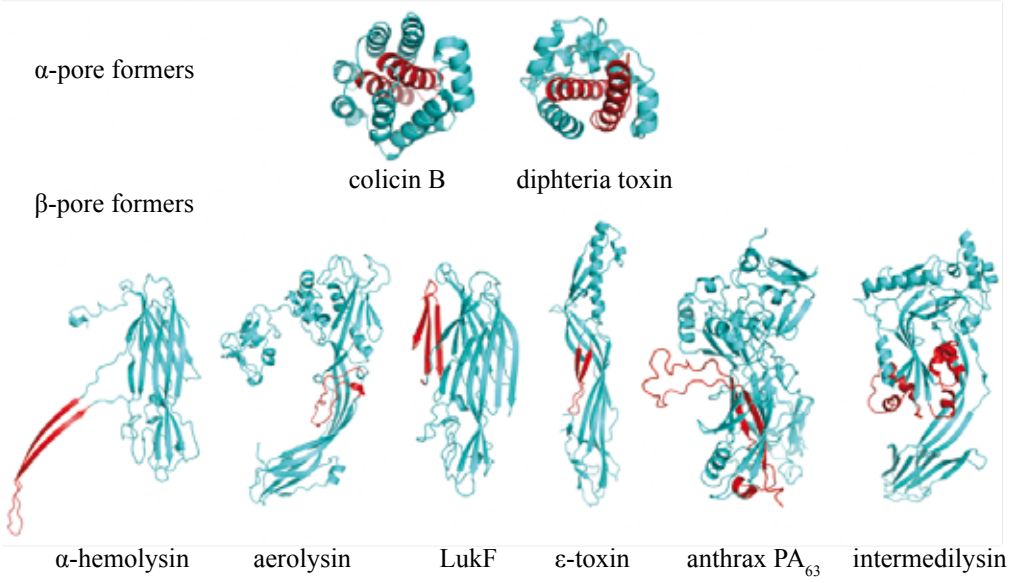

Figure 4 Structures of bacterial pore forming proteins colored in cyan with their membrane inserting regions colored in red..

Beta-pore-forming toxin

Much more is known about how beta-PFTs function. Several crystal structures and cryo-EM reconstructions of beta-PFTs have been solved, both in their monomeric state as well as in their oligomeric prepore and pore forms (Rossjohn, Feil et al. 1997; Tilley, Orlova et al. 2005). These structures, together with detailed biochemical and spectroscopic analysis have lead to a detailed understanding of the mechanism of PFTs. Typically the soluble monomeric toxins bind to a target membrane or receptor before oligomerizing to a non-lytic prepore (Shepard, Shatursky et al. 2000; Heuck, Tweten et al. 2003). This is followed by a substantial refolding of an amphipathic segment that ultimately drills a hole and forms the lining of a trans-membrane beta-barrel pore (**Figure 4**) (Shatursky, Heuck et al. 1999; Shepard, Shatursky et al. 2000; Czajkowsky, Hotze et al. 2004).

Immune Evasion

Bacteria secrete a range of proteins and apart from toxins that directly harm the host a large part of the secretome is dedicated to evasion of the host immune system (Lambris, Ricklin et al. 2008). Bacteria have evolved proteins that are able to modulate many steps of the immune response and new proteins and targets are continuously being discovered. These proteins are of interest not only because of the roles they play in disease pathogenesis. Their ability to specifically interfere with the function of certain proteins of our immune system makes them attractive leads for drug development in e.g. autoimmune disorders.

Staphylococcus aureus

Named after the golden color of the colonies it forms, *S. aureus* frequently inhabits the human skin, nose or throte as a commensal. It is however, one of the five most common nosocomial infections, often causing post surgical wound infections, with deeper infections leading to endocarditis, pneumonia, septic arthritis or bacteraemia. Outside of hospitals *S. aureus* is involved in a multitude of diseases as well. Breaching of the epithelial lining can lead to infection and *S. aureus* is often the causative agent of skin disorders like boils and atopic dermatitis. Other staphylococcal diseases are dependent on the presence of specific toxins. Some strains secrete an enterotoxin and can cause gasteroenteritis wherase others secrete the toxin TSST-1, which may cause toxic shock syndrome, a rare but potentially fatal condition associated with the use of tampons.

Complement inhibitors

The complement system plays a crucial role in the protection against invading microorganisms. Accordingly, it is of fundamental importance for bacteria to inhibit complement mediated immune defence. *S. aureus* secretes a whole range of proteins that intervene at several steps of the complement pathways.

Several of these poteins interfere with the assembly or function of the C3 convertases, thereby preventing efficient opsonization. Staphylococcal complement inhibitor (SCIN) for example binds to the active convertase C3bBb and inhibits the formation of an enzyme-substrate complex (Rooijakkers, Ruyken et al. 2005). SCIN binding results in dimerization of the C3bBbSCIN complex and although dimerization is not necessary for convertase inhibition it does prevent phagocytosis by interfering with surface bound C3b binding to CR1 and CRIg (Jongerius, Puister et al.; Rooijakkers, Milder et al. 2007; Rooijakkers, Wu et al. 2009). Staphylococcal proteins, Efb

and Ecb/Ehp, are also known to inhibit complement activation and amplification. Althgough the mechanism remains unclear, both proteins bind to the same site in C3 and this binding also disrupts the C3d-CR2 interaction, important for full B-cell activation (Jongerius, Garcia et al.; Hammel, Sfyroera et al. 2007; Hammel, Sfyroera et al. 2007; Jongerius, Kohl et al. 2007). Sbi disrupts complement through a different mechanism. It binds to C3 through its domains III and IV. This results in fluid phase complement activation and ultimately leads to futile complement consumption (Isenman, Leung et al.; Burman, Leung et al. 2008; Upadhyay, Burman et al. 2008).

Next to the inhibition of opsonization described above, *S. aureus* also sheads opsonins already accumulated on the bacterial surface. Two secreted proteins are known that make use of host proteases to directly cleave these opsonins. The first protein, clumping factor A (ClfA), makes use of the hosts protection mechanism that downregulates surface attached C3b (Hair, Echague et al.; Higgins, Loughman et al. 2006; Hair, Ward et al. 2008). ClfA binds to the host protease, factor I and serves as a cofactor for the degradation of surface bound C3b (Cunnion, Hair et al. 2004; Cunnion, Buescher et al. 2005). The second protein, staphylokinase (SAK) functions by modulating the function of the host protease plasmin (PL). *S. aureus* expresses several proteins on its surface that bind and recruit plasminogen (PLG), the PL zymogen, to the bacterial surface. Surface bound PLG can then be proteolytically activated by the 1:1 complex of PL and SAK, which switches PL into a PLG activator. This results in the covering of the bacteria with an active protease which cleaves the major opsonins C3b and IgG leading to a strong reduction of phagocytosis of the bacteria (Molkanen, Tyynela et al. 2002; Rooijakkers, van Wamel et al. 2005).

Chemotaxis inhibitors

Neutrophils and macrophages are the main effector cells of the innate immune system. They are recruited to sites of infection by sensing gradients of locally produced chemoattractants which can be both host-derived, like C5a, and bacterial-derived, like formylated peptides. These chemoattractants are typically recognized by G-protein coupled receptors (GPCRs) on phagocytic cells and mediate both cell recruitment and cell activation. To counteract this crucial step in immune defense *S. aureus* secretes several proteins which are able to bind to these GPCRs and block there activity (table 2) (Bestebroer, de Haas et al. 2009). Whereas CHIPS, FLIPr and FLIPr-like bind to their target GPCRs through a protein-protein interaction SSL5 recognizes the glycan present on the N-terminus of many GPCRs (de Haas, Veldkamp et al. 2004; Postma, Poppelier et al. 2004; Prat, Bestebroer et al. 2006; Prat, Haas et al. 2009). In this way SSL5 is able to inhibits neutrophil activation by all chemokines and anaphylatoxins which require the N-terminus of their GPCR for binding (Bestebroer, van Kessel et al. 2009). SSL7 on the other hand does not function by binding to a GPCR. Instead it binds to C5, thereby preventing C5 cleavage and formation of the anaphylotoxin C5a (Laursen, Gordon et al.; Langley, Wines et al. 2005).

Antibody inhibition

Antibodies play a crucial role in the clearance of infections. Together with C3b they are the major opsonins and signal various effector systems that result in the removal of the invading pathogen. *S. aureus* expresses several proteins that are known to bind to and thereby modulate the antibody response. Protein A (SpA) is a cell wall attached protein that is able to bind to IgG both in the Fc region as well as the VH3 domain in the Fab region. By binding to the Fc regions it recruits

IgG to the bacterial surface in an unproductive orientation where the IgG is unable to activate the classical pathway of complement or interact with Fc receptors on immune effector cells (Deisenhofer 1981; Langone 1982). Sbi is a secreted protein that is also able to bind to IgG. Although Sbi has been shown to downregulate the complement response the importance of the Sbi:IgG interaction remains unclear (Zhang, Jacobsson et al. 1998; Atkins, Burman et al. 2008). A third IgG binding protein is SSL10, which is also secreted. The interaction of SSL10 with IgG interferes with C1q binding and thereby inhibits the classical pathway of complement activation. *S. aureus* can also interfere with other types of antibodies like IgA (Itoh, Hamada et al.). IgA is the second most abundant serum immunoglobulin, next to IgG and staphylococcal SSL7 binds to both the serum and mucosal forms. It was shown that SSL7 binds to the Cα2-Cα3 interface of IgA and that this binding site overlaps with that of the FcαRI, thereby inhibiting IgA effector functions (Langley, Wines et al. 2005; Wines, Willoughby et al. 2006; Ramsland, Willoughby et al. 2007).

Scope of this Thesis

The membrane attack complex forms one of the effector arms of the complement system and functions in the direct killing of invading bacteria. On the other hand, bacterial pathogens host a vast array of immune evasion molecules to circumvent immune attack and succesfully infect the host. This thesis describes the structural characterization of several components of the membrane attack complex and an immune evasion molecule from *Staphylococcus aureus* using X-ray crystallography. Structural biology is an extremely powerfull tool in helping to understand complex biological systems. Allthough decades of research have led to a reasonably detailed understanding in the assembly of the MAC high resolution structures have remained absent. In **chapter 2** we describe the first structure of a MACPF domain, central to the functional proteins of the MAC. We show the fold is similar to cholesterol dependent cytolysins, a group of pore forming toxins, and based on the functional similarity, propose a mechanism for pore formation by the MAC. In **chapter 3** we describe the structure of the complex between C5b and C6 that initiates MAC formation. The structure gives clues about the activation of C5 and also reveals for the first time the domain architecture of a full-length MACPF protein. Finally, in **chapter 4** we describe the structure of a newly discovered bacterial inhibitor of phagocytosis, FLIPr-like, which is secreted by *S. aureus*. FLIPr-like mediates phagocytosis inhibition by binding to FcγRs. The structure of the complex between FLIPr-like and FcγRIIa revealed the FLIPr-like binding site almost completely overlaps with that of IgG. Moreover the structure, together with biophysical studies, revealed the molecular basis for previously observed receptor specificity. These results are summarized and discussed in **chapter 5**.

References

Amiguet, P., J. Brunner, et al. (1985). "The membrane attack complex of complement: lipid insertion of tubular and nontubular polymerized C9." Biochemistry 24(25): 7328-34.
Armstrong, P. B. and J. P. Quigley (1999). "Alpha2-macroglobulin: an evolutionarily conserved arm of the innate immune system." Dev Comp Immunol 23(4-5): 375-90.
Atkins, K. L., J. D. Burman, et al. (2008). "S. aureus IgG-binding proteins SpA and Sbi: host specificity and mechanisms of immune complex formation." Mol Immunol 45(6): 1600-11.
Bestebroer, J., C. J. de Haas, et al. (2009). "How microorganisms avoid phagocyte attraction." FEMS Microbiol Rev.
Bestebroer, J., K. P. van Kessel, et al. (2009). "Staphylococcal SSL5 inhibits leukocyte activation by chemokines and anaphylatoxins." Blood 113(2): 328-37.
Bhakdi, S. and J. Tranum-Jensen (1986). "C5b-9 assembly: average binding of one C9 molecule to C5b-8 without poly-C9 formation generates a stable transmembrane pore." J Immunol 136(8): 2999-3005.
Botto, M., M. Kirschfink, et al. (2009). "Complement in human diseases: Lessons from complement deficiencies." Mol Immunol 46(14): 2774-83.
Burman, J. D., E. Leung, et al. (2008). "Interaction of human complement with Sbi, a staphylococcal immunoglobulin-binding protein: indications of a novel mechanism of complement evasion by Staphylococcus aureus." J Biol Chem 283(25): 17579-93.
Chia, J., K. P. Yeo, et al. (2009). "Temperature sensitivity of human perforin mutants unmasks subtotal loss of cytotoxicity, delayed FHL, and a predisposition to cancer." Proc Natl Acad Sci U S A 106(24): 9809-14.
Cooper, N. R. and H. J. Muller-Eberhard (1970). "The reaction mechanism of human C5 in immune hemolysis." J Exp Med 132(4): 775-93.
Cunnion, K. M., E. S. Buescher, et al. (2005). "Serum complement factor I decreases Staphylococcus aureus phagocytosis." J Lab Clin Med 146(5): 279-86.
Cunnion, K. M., P. S. Hair, et al. (2004). "Cleavage of complement C3b to iC3b on the surface of Staphylococcus aureus is mediated by serum complement factor I." Infect Immun 72(5): 2858-63.
Czajkowsky, D. M., E. M. Hotze, et al. (2004). "Vertical collapse of a cytolysin prepore moves its transmembrane beta-hairpins to the membrane." EMBO J 23(16): 3206-15.
Dankert, J. R. and A. F. Esser (1987). "Bacterial killing by complement. C9-mediated killing in the absence of C5b-8." Biochem J 244(2): 393-9.
de Haas, C. J., K. E. Veldkamp, et al. (2004). "Chemotaxis inhibitory protein of Staphylococcus aureus, a bacterial antiinflammatory agent." J Exp Med 199(5): 687-95.
Deisenhofer, J. (1981). "Crystallographic refinement and atomic models of a human Fc fragment and its complex with fragment B of protein A from Staphylococcus aureus at 2.9- and 2.8-A resolution." Biochemistry 20(9): 2361-70.
Dempsey, P. W., M. E. Allison, et al. (1996). "C3d of complement as a molecular adjuvant: bridging innate and acquired immunity." Science 271(5247): 348-50.
Dodds, A. W. and S. K. Law (1998). "The phylogeny and evolution of the thioester bond-containing proteins C3, C4 and alpha 2-macroglobulin." Immunol Rev 166: 15-26.
Ehlers, M. R. (2000). "CR3: a general purpose adhesion-recognition receptor essential for innate immunity." Microbes Infect 2(3): 289-94.
Esser, A. F. (1994). "The membrane attack complex of complement. Assembly, structure and cytotoxic activity." Toxicology 87(1-3): 229-47.

Esser, A. F., W. P. Kolb, et al. (1979). "Molecular reorganization of lipid bilayers by complement: a possible mechanism for membranolysis." Proc Natl Acad Sci U S A 76(3): 1410-4.
Farkas, I., L. Baranyi, et al. (2002). "CD59 blocks not only the insertion of C9 into MAC but inhibits ion channel formation by homologous C5b-8 as well as C5b-9." J Physiol 539(Pt 2): 537-45.
Fearon, D. T. and M. C. Carroll (2000). "Regulation of B lymphocyte responses to foreign and self-antigens by the CD19/CD21 complex." Annu Rev Immunol 18: 393-422.
Fearon, D. T. and R. M. Locksley (1996). "The instructive role of innate immunity in the acquired immune response." Science 272(5258): 50-3.
Fishelson, Z., M. K. Pangburn, et al. (1984). "Characterization of the initial C3 convertase of the alternative pathway of human complement." J Immunol 132(3): 1430-4.
Fredslund, F., L. Jenner, et al. (2006). "The structure of bovine complement component 3 reveals the basis for thioester function." J Mol Biol 361(1): 115-27.
Gotze, O. and H. J. Muller-Eberhard (1970). "Lysis of erythrocytes by complement in the absence of antibody." J Exp Med 132(5): 898-915.
Gros, P., F. J. Milder, et al. (2008). "Complement driven by conformational changes." Nat Rev Immunol 8(1): 48-58.
Guo, R. F. and P. A. Ward (2005). "Role of C5a in inflammatory responses." Annu Rev Immunol 23: 821-52.
Haas, P. J. and J. van Strijp (2007). "Anaphylatoxins: their role in bacterial infection and inflammation." Immunol Res 37(3): 161-75.
Hair, P. S., C. G. Echague, et al. "Clumping Factor A interaction with complement factor I increases C3b cleavage on the bacterial surface of Staphylococcus aureus, and decreases complement-mediated phagocytosis." Infect Immun.
Hair, P. S., M. D. Ward, et al. (2008). "Staphylococcus aureus clumping factor A binds to complement regulator factor I and increases factor I cleavage of C3b." J Infect Dis 198(1): 125-33.
Hammel, M., G. Sfyroera, et al. (2007). "Characterization of Ehp, a secreted complement inhibitory protein from Staphylococcus aureus." J Biol Chem 282(41): 30051-61.
Hammel, M., G. Sfyroera, et al. (2007). "A structural basis for complement inhibition by Staphylococcus aureus." Nat Immunol 8(4): 430-7.
Harriman, G. R., A. F. Esser, et al. (1981). "The role of C9 in complement-mediated killing of Neisseria." J Immunol 127(6): 2386-90.
Heuck, A. P., R. K. Tweten, et al. (2003). "Assembly and topography of the prepore complex in cholesterol-dependent cytolysins." J Biol Chem 278(33): 31218-25.
Higgins, J., A. Loughman, et al. (2006). "Clumping factor A of Staphylococcus aureus inhibits phagocytosis by human polymorphonuclear leucocytes." FEMS Microbiol Lett 258(2): 290-6.
Hu, V. W., A. F. Esser, et al. (1981). "The membrane attack mechanism of complement: photolabeling reveals insertion of terminal proteins into target membrane." J Immunol 127(1): 380-6.
Husler, T., D. H. Lockert, et al. (1995). "Chimeras of human complement C9 reveal the site recognized by complement regulatory protein CD59." J Biol Chem 270(8): 3483-6.
Ikeda, K., T. Sannoh, et al. (1987). "Serum lectin with known structure activates complement through the classical pathway." J Biol Chem 262(16): 7451-4.
Isenman, D. E., E. Leung, et al. "Mutational analyses reveal that the staphylococcal immune evasion molecule Sbi and complement receptor 2 (CR2) share overlapping contact residues on C3d: implications for the controversy regarding the CR2/C3d cocrystal structure." J Immunol 184(4): 1946-55.

Ishida, B., B. J. Wisnieski, et al. (1982). "Photolabeling of a hydrophobic domain of the ninth component of human complement." J Biol Chem 257(18): 10551-3.
Itoh, S., E. Hamada, et al. "Staphylococcal superantigen-like protein 10 (SSL10) binds to human immunoglobulin G (IgG) and inhibits complement activation via the classical pathway." Mol Immunol 47(4): 932-8.
Janssen, B. J., A. Christodoulidou, et al. (2006). "Structure of C3b reveals conformational changes that underlie complement activity." Nature 444(7116): 213-6.
Janssen, B. J., E. G. Huizinga, et al. (2005). "Structures of complement component C3 provide insights into the function and evolution of immunity." Nature 437(7058): 505-11.
Joiner, K. A., M. A. Schmetz, et al. (1985). "Multimeric complement component C9 is necessary for killing of Escherichia coli J5 by terminal attack complex C5b-9." Proc Natl Acad Sci U S A 82(14): 4808-12.
Jongerius, I., B. L. Garcia, et al. "Convertase inhibitory properties of the staphylococcal extracellular complement binding protein." J Biol Chem.
Jongerius, I., J. Kohl, et al. (2007). "Staphylococcal complement evasion by various convertase-blocking molecules." J Exp Med 204(10): 2461-71.
Jongerius, I., M. Puister, et al. "Staphylococcal complement inhibitor modulates phagocyte responses by dimerization of convertases." J Immunol 184(1): 420-5.
Keefe, D., L. Shi, et al. (2005). "Perforin triggers a plasma membrane-repair response that facilitates CTL induction of apoptosis." Immunity 23(3): 249-62.
Kemper, C., J. P. Atkinson, et al. "Properdin: emerging roles of a pattern-recognition molecule." Annu Rev Immunol 28: 131-55.
Kirkitadze, M. D. and P. N. Barlow (2001). "Structure and flexibility of the multiple domain proteins that regulate complement activation." Immunol Rev 180: 146-61.
Klos, A., A. J. Tenner, et al. (2009). "The role of the anaphylatoxins in health and disease." Mol Immunol 46(14): 2753-66.
Kolb, W. P., J. A. Haxby, et al. (1972). "Molecular analysis of the membrane attack mechanism of complement." J Exp Med 135(3): 549-66.
Krych-Goldberg, M. and J. P. Atkinson (2001). "Structure-function relationships of complement receptor type 1." Immunol Rev 180: 112-22.
Lachmann, P. J. and R. A. Thompson (1970). "Reactive lysis: the complement-mediated lysis of unsensitized cells. II. The characterization of activated reactor as C56 and the participation of C8 and C9." J Exp Med 131(4): 643-57.
Laine, R. O. and A. F. Esser (1989). "Detection of refolding conformers of complement protein C9 during insertion into membranes." Nature 341(6237): 63-5.
Laine, R. O. and A. F. Esser (1989). "Identification of the discontinuous epitope in human complement protein C9 recognized by anti-melittin antibodies." J Immunol 143(2): 553-7.
Laine, R. O., B. P. Morgan, et al. (1988). "Comparison between complement and melittin hemolysis: anti-melittin antibodies inhibit complement lysis." Biochemistry 27(14): 5308-14.
Lambris, J. D., D. Ricklin, et al. (2008). "Complement evasion by human pathogens." Nat Rev Microbiol 6(2): 132-42.
Langley, R., B. Wines, et al. (2005). "The staphylococcal superantigen-like protein 7 binds IgA and complement C5 and inhibits IgA-Fc alpha RI binding and serum killing of bacteria." J Immunol 174(5): 2926-33.
Langone, J. J. (1982). "Protein A of Staphylococcus aureus and related immunoglobulin receptors produced by streptococci and pneumonococci." Adv Immunol 32: 157-252.

Laursen, N. S., N. Gordon, et al. "Structural basis for inhibition of complement C5 by the SSL7 protein from Staphylococcus aureus." Proc Natl Acad Sci U S A 107(8): 3681-6.
Law, S. K., A. W. Dodds, et al. (1984). "A comparison of the properties of two classes, C4A and C4B, of the human complement component C4." EMBO J 3(8): 1819-23.
Law, S. K. and R. P. Levine (1977). "Interaction between the third complement protein and cell surface macromolecules." Proc Natl Acad Sci U S A 74(7): 2701-5.
Law, S. K., N. A. Lichtenberg, et al. (1979). "Evidence for an ester linkage between the labile binding site of C3b and receptive surfaces." J Immunol 123(3): 1388-94.
Lehto, T. and S. Meri (1993). "Interactions of soluble CD59 with the terminal complement complexes. CD59 and C9 compete for a nascent epitope on C8." J Immunol 151(9): 4941-9.
Liszewski, M. K., T. C. Farries, et al. (1996). "Control of the complement system." Adv Immunol 61: 201-83.
MacKay, S. L. and J. R. Dankert (1990). "Bacterial killing and inhibition of inner membrane activity by C5b-9 complexes as a function of the sequential addition of C9 to C5b-8 sites." J Immunol 145(10): 3367-71.
Martinez-Caballero, S., L. M. Dejean, et al. (2009). "Assembly of the mitochondrial apoptosis-induced channel, MAC." J Biol Chem 284(18): 12235-45.
Meri, S. (2007). "Loss of self-control in the complement system and innate autoreactivity." Ann N Y Acad Sci 1109: 93-105.
Molkanen, T., J. Tyynela, et al. (2002). "Enhanced activation of bound plasminogen on Staphylococcus aureus by staphylokinase." FEBS Lett 517(1-3): 72-8.
Monahan, J. B. and J. M. Sodetz (1980). "Binding of the eighth component of human complement to the soluble cytolytic complex is mediated by its beta subunit." J Biol Chem 255(22): 10579-82.
Muller-Eberhard, H. J. (1986). "The membrane attack complex of complement." Annu Rev Immunol 4: 503-28.
Muller-Eberhard, H. J. (1988). "Molecular organization and function of the complement system." Annu Rev Biochem 57: 321-47.
Muller-Eberhard, H. J., M. J. Polley, et al. (1967). "Formation and functional significance of a molecular complex derived from the second and the fourth component of human complement." J Exp Med 125(2): 359-80.
Myones, B. L., J. G. Dalzell, et al. (1988). "Neutrophil and monocyte cell surface p150,95 has iC3b-receptor (CR4) activity resembling CR3." J Clin Invest 82(2): 640-51.
Nishida, N., T. Walz, et al. (2006). "Structural transitions of complement component C3 and its activation products." Proc Natl Acad Sci U S A 103(52): 19737-42.
Nishimura, J., Y. Murakami, et al. (1999). "Paroxysmal nocturnal hemoglobinuria: An acquired genetic disease." Am J Hematol 62(3): 175-82.
Pangburn, M. K., D. C. Morrison, et al. (1980). "Activation of the alternative complement pathway: recognition of surface structures on activators by bound C3b." J Immunol 124(2): 977-82.
Pangburn, M. K. and H. J. Muller-Eberhard (1980). "Relation of putative thioester bond in C3 to activation of the alternative pathway and the binding of C3b to biological targets of complement." J Exp Med 152(4): 1102-14.
Pangburn, M. K. and N. Rawal (2002). "Structure and function of complement C5 convertase enzymes." Biochem Soc Trans 30(Pt 6): 1006-10.
Pangburn, M. K., R. D. Schreiber, et al. (1981). "Formation of the initial C3 convertase of the alternative complement pathway. Acquisition of C3b-like activities by spontaneous hydrolysis of the putative thioester in native C3." J Exp Med 154(3): 856-67.

Peitsch, M. C., P. Amiguet, et al. (1990). "Localization and molecular modelling of the membrane-inserted domain of the ninth component of human complement and perforin." Mol Immunol 27(7): 589-602.
Podack, E. R., G. Biesecker, et al. (1978). "The C5b-6 complex: reaction with C7, C8, C9." J Immunol 121(2): 484-90.
Podack, E. R., W. P. Kolb, et al. (1978). "The C5b-6 complex: formation, isolation, and inhibition of its activity by lipoprotein and the S-protein of human serum." J Immunol 120(6): 1841-8.
Podack, E. R., J. Tschoop, et al. (1982). "Molecular organization of C9 within the membrane attack complex of complement. Induction of circular C9 polymerization by the C5b-8 assembly." J Exp Med 156(1): 268-82.
Postma, B., M. J. Poppelier, et al. (2004). "Chemotaxis inhibitory protein of Staphylococcus aureus binds specifically to the C5a and formylated peptide receptor." J Immunol 172(11): 6994-7001.
Prat, C., J. Bestebroer, et al. (2006). "A new staphylococcal anti-inflammatory protein that antagonizes the formyl peptide receptor-like 1." J Immunol 177(11): 8017-26.
Prat, C., P. J. Haas, et al. (2009). "A homolog of formyl peptide receptor-like 1 (FPRL1) inhibitor from Staphylococcus aureus (FPRL1 inhibitory protein) that inhibits FPRL1 and FPR." J Immunol 183(10): 6569-78.
Preissner, K. T., E. R. Podack, et al. (1985). "The membrane attack complex of complement: relation of C7 to the metastable membrane binding site of the intermediate complex C5b-7." J Immunol 135(1): 445-51.
Qian, S., W. Wang, et al. (2008). "Structure of transmembrane pore induced by Bax-derived peptide: evidence for lipidic pores." Proc Natl Acad Sci U S A 105(45): 17379-83.
Ramsland, P. A., N. Willoughby, et al. (2007). "Structural basis for evasion of IgA immunity by Staphylococcus aureus revealed in the complex of SSL7 with Fc of human IgA1." Proc Natl Acad Sci U S A 104(38): 15051-6.
Rawal, N. and M. K. Pangburn (1998). "C5 convertase of the alternative pathway of complement. Kinetic analysis of the free and surface-bound forms of the enzyme." J Biol Chem 273(27): 16828-35.
Rawal, N. and M. K. Pangburn (2000). "Functional role of the noncatalytic subunit of complement C5 convertase." J Immunol 164(3): 1379-85.
Rawal, N. and M. K. Pangburn (2003). "Formation of high affinity C5 convertase of the classical pathway of complement." J Biol Chem 278(40): 38476-83.
Rooijakkers, S. H., F. J. Milder, et al. (2007). "Staphylococcal complement inhibitor: structure and active sites." J Immunol 179(5): 2989-98.
Rooijakkers, S. H., M. Ruyken, et al. (2005). "Immune evasion by a staphylococcal complement inhibitor that acts on C3 convertases." Nat Immunol 6(9): 920-7.
Rooijakkers, S. H., W. J. van Wamel, et al. (2005). "Anti-opsonic properties of staphylokinase." Microbes Infect 7(3): 476-84.
Rooijakkers, S. H., J. Wu, et al. (2009). "Structural and functional implications of the alternative complement pathway C3 convertase stabilized by a staphylococcal inhibitor." Nat Immunol 10(7): 721-7.
Rossjohn, J., S. C. Feil, et al. (1997). "Structure of a cholesterol-binding, thiol-activated cytolysin and a model of its membrane form." Cell 89(5): 685-92.
Shatursky, O., A. P. Heuck, et al. (1999). "The mechanism of membrane insertion for a cholesterol-dependent cytolysin: a novel paradigm for pore-forming toxins." Cell 99(3): 293-9.

Shepard, L. A., O. Shatursky, et al. (2000). "The mechanism of pore assembly for a cholesterol-dependent cytolysin: formation of a large prepore complex precedes the insertion of the transmembrane beta-hairpins." Biochemistry 39(33): 10284-93.
Smith, C. A., C. W. Vogel, et al. (1984). "MHC Class III products: an electron microscopic study of the C3 convertases of human complement." J Exp Med 159(1): 324-9.
Sodetz, J. M. (1989). "Structure and function of C8 in the membrane attack sequence of complement." Curr Top Microbiol Immunol 140: 19-31.
Steckel, E. W., B. E. Welbaum, et al. (1983). "Evidence of direct insertion of terminal complement proteins into cell membrane bilayers during cytolysis. Labeling by a photosensitive membrane probe reveals a major role for the eighth and ninth components." J Biol Chem 258(7): 4318-24.
Stewart, J. L., W. P. Kolb, et al. (1987). "Evidence that C5b recognizes and mediates C8 incorporation into the cytolytic complex of complement." J Immunol 139(6): 1960-4.
Thiery, J., D. Keefe, et al. "Perforin activates clathrin- and dynamin-dependent endocytosis, which is required for plasma membrane repair and delivery of granzyme B for granzyme-mediated apoptosis." Blood 115(8): 1582-93.
Thompson, R. A. and P. J. Lachmann (1970). "Reactive lysis: the complement-mediated lysis of unsensitized cells. I. The characterization of the indicator factor and its identification as C7." J Exp Med 131(4): 629-41.
Tilley, S. J., E. V. Orlova, et al. (2005). "Structural basis of pore formation by the bacterial toxin pneumolysin." Cell 121(2): 247-56.
Tilley, S. J. and H. R. Saibil (2006). "The mechanism of pore formation by bacterial toxins." Curr Opin Struct Biol 16(2): 230-6.
Tomlinson, S., Y. Wang, et al. (1995). "Chimeric horse/human recombinant C9 proteins identify the amino acid sequence in horse C9 responsible for restriction of hemolysis." J Immunol 155(1): 436-44.
Tschopp, J. (1984). "Circular polymerization of the membranolytic ninth component of complement. Dependence on metal ions." J Biol Chem 259(16): 10569-73.
Tschopp, J. (1984). "Ultrastructure of the membrane attack complex of complement. Heterogeneity of the complex caused by different degree of C9 polymerization." J Biol Chem 259(12): 7857-63.
Tschopp, J., A. Engel, et al. (1984). "Molecular weight of poly(C9). 12 to 18 C9 molecules form the transmembrane channel of complement." J Biol Chem 259(3): 1922-8.
Tschopp, J., D. Masson, et al. (1986). "Structural/functional similarity between proteins involved in complement- and cytotoxic T-lymphocyte-mediated cytolysis." Nature 322(6082): 831-4.
Tschopp, J. and E. R. Podack (1981). "Membranolysis by the ninth component of human complement." Biochem Biophys Res Commun 100(3): 1409-14.
Tschopp, J., E. R. Podack, et al. (1985). "The membrane attack complex of complement: C5b-8 complex as accelerator of C9 polymerization." J Immunol 134(1): 495-9.
Upadhyay, A., J. D. Burman, et al. (2008). "Structure-function analysis of the C3 binding region of Staphylococcus aureus immune subversion protein Sbi." J Biol Chem 283(32): 22113-20.
Voskoboinik, I., M. J. Smyth, et al. (2006). "Perforin-mediated target-cell death and immune homeostasis." Nat Rev Immunol 6(12): 940-52.
Voskoboinik, I., M. C. Thia, et al. (2005). "Calcium-dependent plasma membrane binding and cell lysis by perforin are mediated through its C2 domain: A critical role for aspartate residues 429, 435, 483, and 485 but not 491." J Biol Chem 280(9): 8426-34.
Wallis, R., D. A. Mitchell, et al. "Paths reunited: Initiation of the classical and lectin pathways of complement activation." Immunobiology 215(1): 1-11.

Walport, M. J. (2001). "Complement. First of two parts." N Engl J Med 344(14): 1058-66.
Walport, M. J. (2001). "Complement. Second of two parts." N Engl J Med 344(15): 1140-4.
Wang, Y., E. S. Bjes, et al. (2000). "Molecular aspects of complement-mediated bacterial killing. Periplasmic conversion of C9 from a protoxin to a toxin." J Biol Chem 275(7): 4687-92.
Wiesmann, C., K. J. Katschke, et al. (2006). "Structure of C3b in complex with CRIg gives insights into regulation of complement activation." Nature 444(7116): 217-20.
Wines, B. D., N. Willoughby, et al. (2006). "A competitive mechanism for staphylococcal toxin SSL7 inhibiting the leukocyte IgA receptor, Fc alphaRI, is revealed by SSL7 binding at the C alpha2/C alpha3 interface of IgA." J Biol Chem 281(3): 1389-93.
Wright, S. D. and R. P. Levine (1981). "How complement kills E. coli. I. Location of the lethal lesion." J Immunol 127(3): 1146-51.
Wright, S. D. and R. P. Levine (1981). "How complement kills E. coli. II. The apparent two-hit nature of the lethal event." J Immunol 127(3): 1152-6.
Young, J. D., Z. A. Cohn, et al. (1986). "The ninth component of complement and the pore-forming protein (perforin 1) from cytotoxic T cells: structural, immunological, and functional similarities." Science 233(4760): 184-90.
Young, J. D., H. Hengartner, et al. (1986). "Purification and characterization of a cytolytic pore-forming protein from granules of cloned lymphocytes with natural killer activity." Cell 44(6): 849-59.
Young, J. D., C. C. Liu, et al. (1986). "The pore-forming protein (perforin) of cytolytic T lymphocytes is immunologically related to the components of membrane attack complex of complement through cysteine-rich domains." J Exp Med 164(6): 2077-82.
Zalman, L. S., L. M. Wood, et al. (1986). "Isolation of a human erythrocyte membrane protein capable of inhibiting expression of homologous complement transmembrane channels." Proc Natl Acad Sci U S A 83(18): 6975-9.
Zhang, L., K. Jacobsson, et al. (1998). "A second IgG-binding protein in Staphylococcus aureus." Microbiology 144 (Pt 4): 985-91.
Ziccardi, R. J. (1984). "The role of immune complexes in the activation of the first component of human complement." J Immunol 132(1): 283-8.

Chapter 2

Structure of C8α-MACPF Reveals Mechanism of Membrane Attack in Complement Immune Defense

Michael A. Hadders, Dennis X. Beringer, Piet Gros

Crystal and Structural Chemistry, Bijvoet Center for Biomolecular Research, Department of Chemistry, Faculty of Science, Utrecht University, Padualaan 8, 3584 CH, Utrecht, Netherlands

Science, **317**, 1552 – 1554 (2007)

Membrane attack is important for mammalian immune defense against invading microorganisms and infected host cells. Proteins of the complement membrane attack complex (MAC) and the protein perforin share a common MACPF domain that is responsible for membrane insertion and pore formation. We determined the crystal structure of the MACPF domain of complement component C8α at 2.5 angstrom resolution and show that it is structurally homologous to the bacterial, pore-forming, cholesterol-dependent cytolysins. The structure displays two regions that (in the bacterial cytolysins) refold into transmembrane b hairpins, forming the lining of a barrel pore. Local hydrophobicity explains why C8α is the first complement protein to insert into the membrane. The size of the MACPF domain is consistent with known C9 pore sizes. These data imply that these mammalian and bacterial cytolytic proteins share a common mechanism of membrane insertion.

Protection in blood against Gram-negative bacteria critically depends on the cytolytic activity of the terminal pathway of the complement system (Walport 2001; Walport 2001). Deficiency in components of the terminal pathway results in recurrent bacterial infections in humans [in particular, meningococcal infections (Wurzner, Orren et al. 1992)]. The terminal pathway is initiated when complement protein C5 is proteolytically activated into two fragments, C5a and C5b, in the complement cascade (Muller-Eberhard 1986). C5b then sequentially binds C6, C7, C8, and multiple copies of C9, forming a C5b–9 complex called the MAC. The complement proteins C6 to C9 are homologous and have a central MACPF domain of molecular mass ~40 kD, flanked by small regulatory domains at the N and C termini (fig. S1) (Esser 1994). C8 is a trimer made up of homologous proteins C8α and C8β, each of which contain a MACPF domain, and a lipocalin protein C8γ that is covalently linked to C8a through a disulfide bridge (Sodetz 1989). During assembly of the MAC, C7 mediates the initial binding to the membrane surface. However, the C8α component of C8 is the first protein that traverses the lipid bilayer (Steckel, Welbaum et al. 1983; Peitsch, Amiguet et al. 1990). C5b–8 complexes, obtained in the absence of C9, have hemolytic activity, indicating that C8 penetration leads to a loss of membrane integrity (Gee, Boyle et al. 1980). After C5b–8 assembly, multiple C9 molecules bind and oligomerize into pores, consisting of 12 to 18 C9 monomers, that are 100 ± 10Å wide and 160 Å high (Tschopp, Muller-Eberhard et al. 1982; Tschopp 1984; DiScipio and Hugli 1985). Host cells are protected from this membrane attack by CD59, which binds to C8α and C9 during MAC assembly, preventing pore formation (Huang, Qiao et al. 2006). Cytotoxic T lymphocytes and natural killer cells secrete granules containing perforin, which (like the complement proteins C6 to C9) has a central MACPF domain. Perforin multimerizes, forming similar pores composed of ~20 monomers (Dennert and Podack 1983; Podack and Dennert 1983; Podack, Hengartner et al. 1991). Perforin, however, does not use accessory proteins for membrane binding (Podack, Hengartner et al. 1991). The mechanism of membrane insertion and pore formation by these proteins of the immune system is unclear.

We expressed and crystallized the human C8α-MACPF domain (residues 103 to 462). The C8α-MACPF domain retains its ability to form heterotrimeric C8 (with full-length C8β and C8γ) that is functionally active in membrane attack and pore formation (Slade, Chiswell et al. 2006). The structure was determined to 2.5 Å resolution by experimental phasing (see the Materials and Methods, table S1, and fig. S2 in the supporting online material). The overall structure consists of a central kinked four stranded β sheet surrounded by α-helices and β-strands, forming two structural segments (which we call d1 and d3 for reasons discussed below) (Fig. 1A). Overall, the molecule has a thin L shaped appearance with dimensions 67 Å by 55 Å by 24 Å.

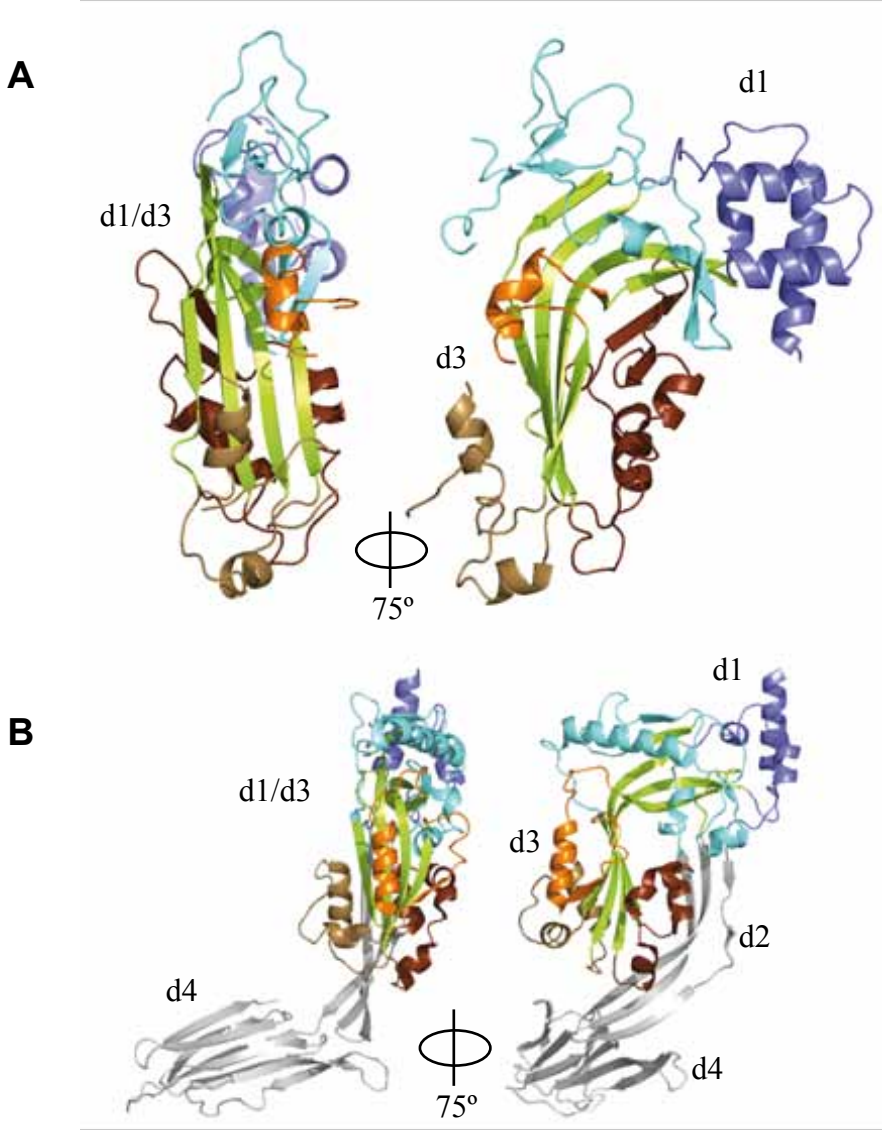

Fig. 1. Structure of human C8α-MACPF. Cα representation of C8α-MACPF (**A**) and intermedilysin (PDB accession code 1s3r) (**B**) in two views. The top and bottom halves of the moleculeare denoted d1 (blue) and d3 (brown), respectively. The central kinked β sheet (part of both d1 and d3) is shown in green. The additional domains d2 and d4 in intermedilysin are shown in gray. Figures are produced with PyMOL (30).

The observed fold of C8α-MACPF with its central kinked β-sheet resembles the fold of domains d1 and d3 of intermedilysin and perfringolysin, which are cholesterol-dependent cytolysins (CDCs) secreted by the Gram-positive bacteria (Rossjohn, Feil et al. 1997; Polekhina, Giddings et al. 2005) (Fig. 1B and fig. S3). CDCs undergo substantial refolding of part of their structure in transforming from monomeric soluble proteins to multimeric membrane pores [reviewed in (Tilley and Saibil

2006)]. CDCs are built up of four domains: d1 to d4. Domain d4 is responsible The observed fold of C8α-MACPF with its central kinked β-sheet resembles the fold of domains d1 and d3 of intermedilysin and perfringolysin, which are cholesterol-dependent cytolysins (CDCs) secreted by the Gram-positive bacteria (Rossjohn, Feil et al. 1997; Polekhina, Giddings et al. 2005) (Fig. 1B and fig. S3). CDCs undergo substantial refolding of part of their structure in transforming from monomeric soluble proteins to multimeric membrane pores [reviewed in (Tilley and Saibil 2006)]. CDCs are built up of four domains: d1 to d4. Domain d4 is responsible for membrane binding (Giddings, Zhao et al. 2004; Tweten 2005), whereas d2 forms a linker to d1 and d3, which mediate pore formation (Parker and Feil 2005). Domains d1 and d3 correspond to the two halves of the kinked b sheet in the structure of C8α-MACPF, which is consistent with the membrane-insertion function of C8α-MACPF. The absence of the d2 and d4 domains in C8α-MACPF correlates, however, with marked topological differences in d1 (fig. S3, C and D). The modules flanking the C8α-MACPF domain [that is, the N-terminal thrombospondin type 1 (TSP1) and low-density lipoprotein receptor class a domains and the C-terminal epidermal growth factor–like and TSP1 domains] are linked on opposite sides to d1 (Fig. 1A). The covalent binding site for C8γ (Cys164) is located in a disordered surface loop on the N-terminal side of d1. In contrast, the topologies of d3 in C8α and CDCs are very similar and are characterized by an antiparallel b sheet (strands β1 to β4) with extended, connecting regions β1- β2 and β3- β4.

Residues from domain d3 in CDCs form the wall of the β-barrel pores. In CDCs, the antiparallel β-sheet (strands b1 to b4) in d3 has two helical connections (between strands β1- β2 and β3- β4). By means of multiple spectroscopic methods, these two helical regions have been shown to refold into amphipathic b hairpins [denoted transmembrane β-hairpin 1 (TMH1) and TMH2], which insert into the membrane, forming a β-barrel pore (Shepard, Heuck et al. 1998; Shatursky, Heuck et al. 1999). C8α-MACPF exhibits similar, but longer, regions in between strands β1- β2 and β3- β4. The first region spans 58 residues (residues 201 to 258) and forms two α-helices interspersed with a β-hairpin (Fig. 2A). The second region consists of 62 residues (residues 326 to 387). This region has two discernible α-helices in the electron density but is largely disordered. Like in CDCs, these regions show high sequence variation across species (fig. S4). In C8α, we observe a partitioning into three segments for these regions: (i) charged and amphipathic, (ii) hydrophobic, and (iii) charged and amphipathic (Fig. 2B and fig. S4). In the structure, the hydrophobic middle part (26 residues long) of region β1- β2 forms a β-hairpin that aligns with the central sheet of d1. The corresponding part in region β3- β4 is 25 residues long and is delimited by the disulfide bond Cys345-Cys369. This hydrophobic part has three charged residues positioned halfway between the cysteine residues. The hydrophobic character of the central β1- β2 and β3- β4 parts is consistent with membrane insertion without pore formation, as expected for the function of C8. Presumably, the central β3- β4 part would traverse the membrane completely and position the three charged residues on the inside of the target membrane. In contrast, the central parts of the β1- β2 and β3- β4 regions in C9 and perforin (Fig. 2B and fig. S4) have an alternating hydrophobic and hydrophilic character (like the TMHs of CDCs). This amphipathic character is consistent with forming a β-barrel pore with a hydrophilic inside and a hydrophobic outside that faces the lipid membrane. The flanking regions in C8α, C9, and perforin contain short stretches of consecutive charged residues indicative of a solvent-exposed character. We hypothesize that the central segments traverse the membrane (forming TMHs) and that the flanking parts protrude above the membrane.

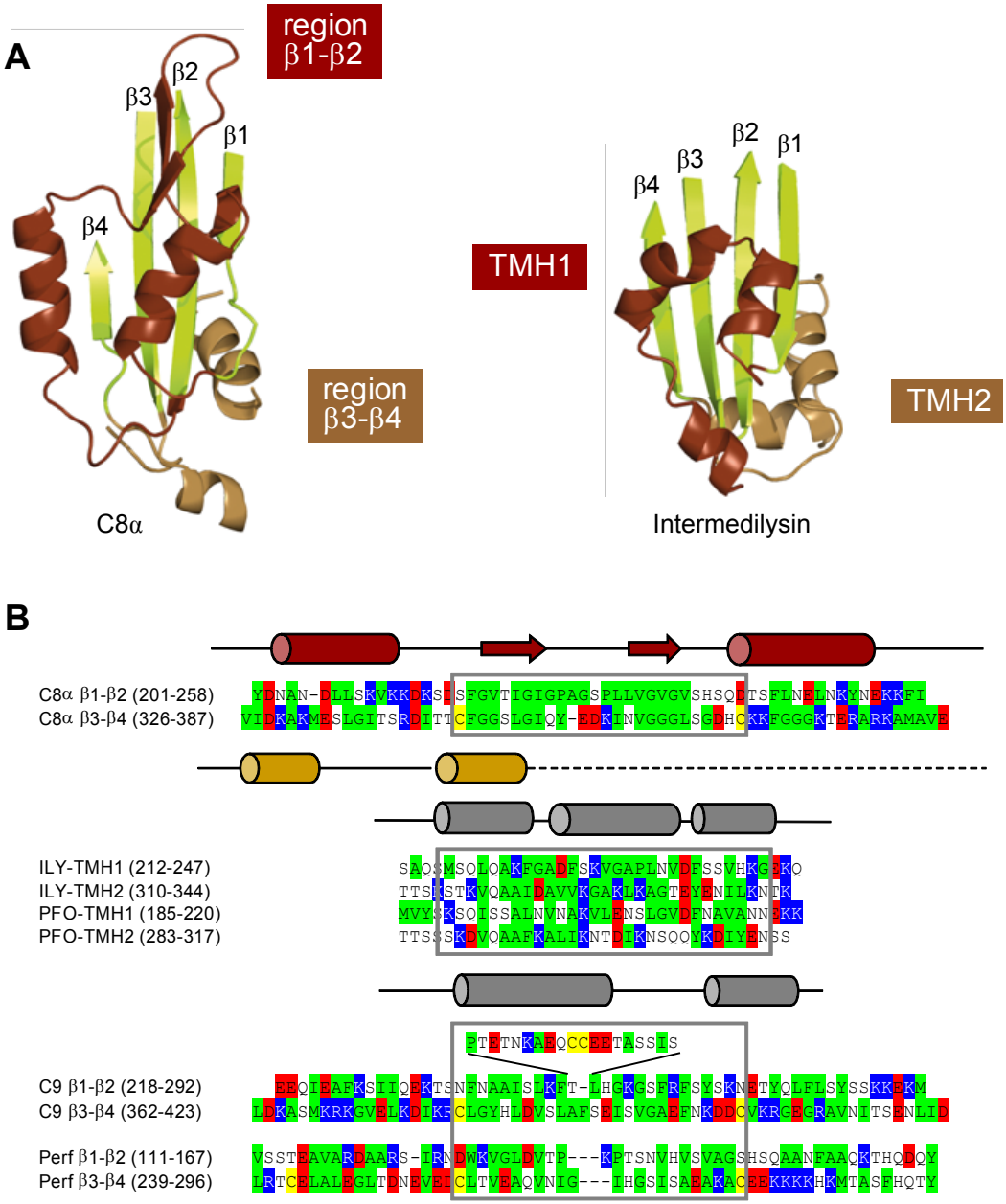

Fig. 2. Comparison of putative transmembrane regions. (**A**) Cartoon diagrams of domains d3 of C8α-MACPF and intermedilysin. The putative β hairpin regions β1-β2 and TMH1 are colored in darkbrown, and β3-β4 and TMH2 are colored in light brown. (**B**) Sequence alignmentof (i) the β1-β2 and β3-β4 regions of C8α, C9 and perforin (Perf) and (ii) TMH1 and TMH2 of perfringolysin (PFO) and intermedilysin (ILY). Residues (31) are colored according to character: hydrophobic (green), positively charged (blue), negatively charged (red), and hydrophylic (white). Yellow indicates cysteine residues. Secondary structure elements, as observed for C8α-MACPF and intermedilysin, are indicated. Putative transmembrane regions are indicated by gray boxes.

Electron micrographs of the MAC and poly (C9) reveal a pore (~100Å inner-diameter, ~160 Å height, and ~200 Å outer-diameter torus) and a small rim at the base of the pore (DiScipio and Hugli 1985). Our structure shows that a soluble, monomeric MACPF domain has a thin "L" shape. In analogy with CDCs, the β1- β2 and β3- β4 regions in d3 are expected to change into long β-hairpins upon membrane insertion, contributing four strands per monomer. Extending 60 residues into one straight β-hairpin yields a maximum length of ~100 Å; this structure would extend from the existing four-stranded β-sheet in d3. Together with the MACPF domain, this yields a total length of ~160 Å, which is consistent with the height measured for MAC and C9 pores by electron microscopy (EM). Similarly, modeling of the x-ray structure of perfringolysin into a cryo-EM map of a pneumolysin pore also indicated extended β-hairpins oriented parallel to the membrane normal (Tilley, Orlova et al. 2005). However, the β-strands are most likely twisted and tilted (as observed in many β-barrel structures of outer-membrane proteins); possibly, the missing N-terminal domains contribute to the height of the C9 pore. Furthermore, the putative TMH1 in C9 has a 17-residue extension which is consistent with the presence of a small rim at the bottom side of the pore. Based on the MACPF domain of C8α, we constructed a hypothetical model of the C9 pore torus. Sixteen and 18 copies of the molecule were placed in rings, with the β1 to β4 strands of d3 placed on the inside (Fig. 3). This simplistic modeling resulted in rings with an inner diameter of 97 and 110 Å and an outer diameter of 170 and 185 Å, respectively. The inner diameters of these models are close to the observed 100 Å; the smaller outer diameter (170 to 185Åversus 200 Å) is possibly caused by the missing C-terminal domains that are connected to the outer rim of the torus. Thus, based on a MACPF domain, the main characteristics of the C9 pore can be modeled.

Membrane recognition and pore formation by the complement proteins depend on a sequential assembly of the MAC. The C8α-MACPF and C8β-MACPF domains are sufficient for a functional C5b–8 complex, indicating that the flanking N- and C-terminal domains in C8 are not essential for complex formation (Slade, Chiswell et al. 2006; Brannen and Sodetz 2007). The flanking domains, however, possibly cover the putative TMHs in soluble C8. Soluble forms of the cell-surface protein CD59 do not bind soluble C8 or C9 (Huang, Qiao et al. 2006). CD59 binds residues 365 to 371 of C9 and residues 320 to 415 in C8α (Lockert, Kaufman et al. 1995), which map to the TMH2 region. Presumably, docking of C8 or C9 onto the MAC reorients the flanking domains exposing the TMHs, which are subsequently "caught in the act" by CD59 present on host cells, and hence the membrane insertion is blocked. In CDCs, membrane insertion only takes place after oligomerization [that is, a large oligomeric prepore is formed on top of the membrane before the membrane is perforated (Tilley, Orlova et al. 2005)]. C8α inserts without oligomerization, which is consistent with the hydrophobic character of the putative TMHs. Partial and incomplete pores are observed, when limiting numbers of C9 are available for binding to C5b–8 (Tschopp 1984). These data indicate that MAC pore formation is gradual and does not require oligomeric prepores. In this process, C8 plays an important role by binding to the membrane-bound C5b–7 complex, penetrating and destabilizing the membrane, thus readily enabling pore formation by C9.

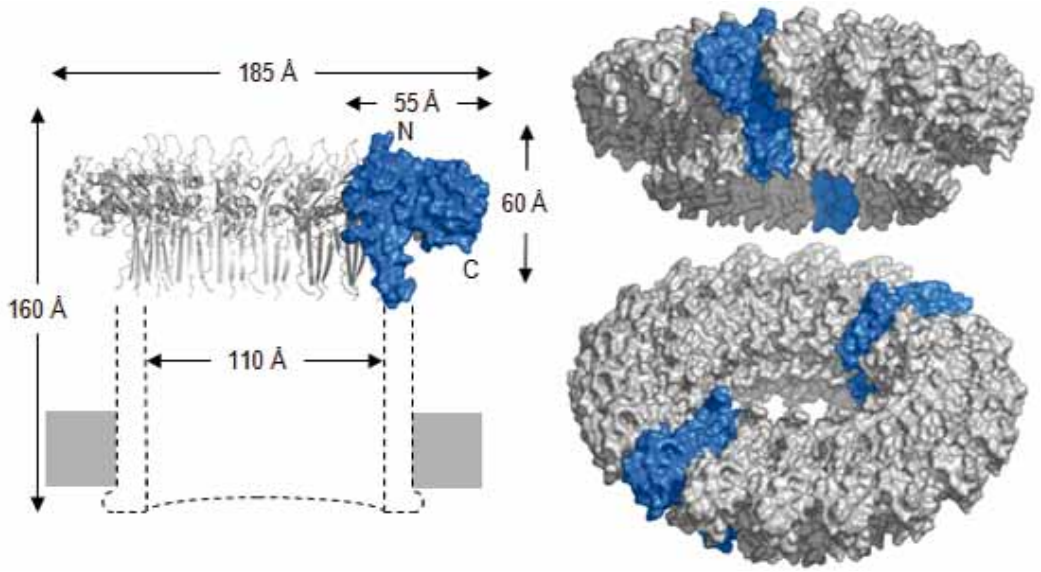

Fig. 3. Hypothetical model of the C9 pore. Shown is a pore model derived from a ring of 18 monomers of C8α-MACPF. (**Left**) Cross section of the pore, with MACPF domains forming the torus. (**Right**) Two orientations of the torus in surface representation, with two individual monomers highlited (in blue) for convenience.

Perforin, perhaps, acts more like CDCs. Membrane binding by perforin is Ca^{2+} dependent and is mediated by its C-terminal C2 domain (Voskoboinik, Thia et al. 2005). The C2 fold is closely related to the fold of the C-terminal d4 domain in CDCs (fig. S5). Notably, the "undecapeptide" membrane–binding site in d4 overlaps with the Ca^{2+}-dependent binding site in C2, indicating a common orientation when bound to a membrane. Like in CDCs and C9, the putative TMHs of perforin are amphipathic in character. The amphipathic regions presumably do not penetrate the membrane easily. We argue that unassisted pore formation [as for CDCs, perforin, and in vitro poly(C9)] hence requires formation of a large oligomeric prepore on the membrane to facilitate perforation of the membrane.

The MACPF domain of complement proteins C6 to C9 and perforin is similar to domains d1 and d3 of bacterial CDCs. This finding indicates a possible common evolutionary origin and a common mechanism of membrane insertion. The structural insights could be valuable in the design of therapeutics preventing inappropriate activation of the terminal pathway of complement, as in the case of paroxysmal nocturnal hemoglobinuria and hyper acute rejection of transplanted organs.

Materials and Methods

Protein expression and purification

Human C8α-MACPF (res. 103-462) was cloned from cDNA. A single free cysteine (Cys164) was mutated to serine using the Quickexchange kit (Stratagene). The sequence was then verified by sequencing and the gene cloned into a modified pET vector. This resulted in C8α-MACPF fused to an N-terminal tobacco etch virus protease (TEV)-cleavable hexa-histidine (His) tag. The construct was transformed to Origami (DE3) cells and protein expressed overnight by auto-induction (Studier 2005). In the morning a single colony was inoculated in LB containing 0.2 % w/v glucose, 25 mg/ml kanamycin and 50 mg/ml ampicilin. At the end of the afternoon the preculture was diluted 1:100 in LB supplemented with 50 mM phosphate buffer pH 6.9, 0.5 % v/v glycerol, 0.1 % w/v glucose, 0.01 % w/v lactose, 5 mM $MgCl_2$ and antibiotics as stated above. The cultures were allowed to grow overnight; the first ~5 hrs at 37 °C, followed by an induction period at 20 °C. C8α-MACPF was purified from lysates by immobilized metal affinity chromatography (IMAC) after which the His tag was removed by overnight incubation with TEV at room temperature. After filtering over an IMAC column to remove TEV and uncleaved C8α-MACPF, the protein was further purified by ion-exchange (Mono-Q) and size exclusion chromatography (Superdex 200). The protein was then concentrated to 12 mg/ml and dialysed against 10 mM Tris pH 7.5, 50 mM NaCl. For seleno-methionine labeling, precultures were grown as above and used to inoculate minimal medium supplemented with 0.5 % v/v glycerol, 0.2 % w/v glucose, 5 mM MgCl2, 50 mM $FeCl_3$, 20 mM $CaCl_2$, 10 mM each of $MnCl_2$ and $ZnCl_2$, 2 mM each of $CoCl_2$, $CuSO_4$ and $NiCl_2$, 1 mM vitamin B12, 50 mg/ml of each of the amino acids: A, E, F, G, H, I, K, L, P, R, S, T, and 10 mg/ml of the amino acid M, and antibiotics as stated above. After ~10 hrs at 37°C the cultures were brought to 20 °C and 0.01 % w/v lactose and 100 mg/ml Se-Met was added. The cultures were left to induce for ~14 hrs before harvesting the cells. Subsequent purification proceeded as for unlabeled protein.

Crystallization

C8α-MACPF was crystallized at 30 °C in sitting drops containing 300 nl protein and 200 nl well solution containing 1 M $LiSO_4$, 5 mM $NiCl_2$ and 100 mM Tris pH 8. Crystals were cryo-protected by adding 1.5 µl 2.1 M $LiSO_4$, 5 mM $NiCl_2$ and 100 mM Tris pH 8 directly to the drop containing the crystals. A heavy-atom derivative was obtained by soaking a crystal in a 10 µl drop containing well solution with 1 mM K_2PtCl_4 for 1 hr, followed by back-soaking in the same cryo-solution for 5 min. Crystals were harvested and immediately flash cooled in liquid N_2.

Data collection and structure solution

All data were collected at beamline ID-29 at the ESRF. Data were processed with Mosflm and CCP4 (Collaborative Computational Project 1994; Leslie 2006). The structure of C8α-MACPF was solved by a combination of multi-wavelength anomalous dispersion (MAD) using seleno-methionine substituted C8α-MACPF crystals and single-isomorphous replacement with anomalous scattering (SIRAS) of a K_2PtCl_4 derivative. Phases were calculated from the MAD data set with SOLVE (Terwilliger and Berendzen 1999) to 3 Å resolution with eight out of a possible ten selenium sites found. Anomalous difference Fourier methods were then used to identify five Pt sites in the heavy atom derivative. Phases were combined followed by density modification and phase extension to 2.5 Å resolution with

DM (Cowtan and Main 1998). This led to excellent maps in which Arp/wArp (Perrakis, Morris et al. 1999) could build a C-α trace of approximately 50 % of the molecule. The remainder was built by hand using Coot (Emsley and Cowtan 2004), making use of the anomolous maps to identify the positions of the methionines. An additional peak was visible in anomalous maps calculated from the peak data of the Se-Met substituted crystal. We identified the peak as a Ni^{2+} ion (present in the crystallization condition) on the basis of its coordination distances and the fact that Ni has a small anomalous signal at the used wavelength. The Ni ion is bound at a crystal contact site. Density for a large segment, corresponding to residues 326-387 (β3- β4 region) was very poor, most likely due to disorder. It was not possible to confidently trace the sequence in this area (parts were omitted (336-380) and one discernible helix was modeled as poly-alanine (chain B, 1-13)). Two other flexible loops (res. 159-170 and 400-412) were also not visible in the electron density and were omitted from the model. The coordinate model was refined using Refmac5 (Murshudov, Vagin et al. 1997) against native data between 40-2.5 Å resolution. TLS and restrained B-factor refinement lead to an R factor of 25.5% (Rfree 28.7 %) using 3 TLS groups. Data collection and refinement statistics are given in Table 1.

Table 1: Data collection, phasing and refinement statistics

Crystal	Native		SeMet		K_2PtCl_4
Data collection					
Space group	*I*422		*I*422		*I*422
Cell dimensions					
a, *b*, *c* (Å)	178.9, 178.9, 75.0		179.0, 179.0, 75.3		178.8, 178.8, 75.8
α, β, γ (°)	90, 90, 90		90, 90, 90		90, 90, 90
		Peak	*Inflection*	*Remote*	*Peak*
Wavelength (Å)	1.006	0.97918	0.97942	0.97564	1.07178
Resolution (Å)	40.0-2.5	40.0-3.0	40.0-3.0	40.0-3.0	40.0-3.0
R_{merge}	0.080 (0.513)	0.108 (0.569)	0.115 (0.648)	0.123 (0.776)	0.094 (0.505)
I / σI	17.3 (3.2)	21.2 (4.3)	20.4 (3.9)	19.8 (3.4)	27.1 (5.2)
Completeness (%)	100	100	100	100	99.9 (100)
Redundancy	7.1	14.0	14.0	14.1	13.7
Refinement					
Resolution (Å)	40.0-2.5				
No. reflections	20,253				
R_{work} / R_{free} (%)	25.5/28.7				
No. atoms	2461				
Mean *B*-factors (Å^2)	53.5				
R.m.s deviations					

References

Brannen, C. L. and J. M. Sodetz (2007). "Incorporation of human complement C8 into the membrane attack complex is mediated by a binding site located within the C8beta MACPF domain." Mol Immunol 44(5): 960-5.
Collaborative Computational Project, N. (1994). "The CCP4 suite: programs for protein crystallography." Acta Crystallogr D Biol Crystallogr 50(Pt 5): 760-3.
Cowtan, K. and P. Main (1998). "Miscellaneous algorithms for density modification." Acta Crystallogr D Biol Crystallogr 54(Pt 4): 487-93.
Dennert, G. and E. R. Podack (1983). "Cytolysis by H-2-specific T killer cells. Assembly of tubular complexes on target membranes." J Exp Med 157(5): 1483-95.
DiScipio, R. G. and T. E. Hugli (1985). "The architecture of complement component C9 and poly(C9)." J Biol Chem 260(27): 14802-9.
Emsley, P. and K. Cowtan (2004). "Coot: model-building tools for molecular graphics." Acta Crystallogr D Biol Crystallogr 60(Pt 12 Pt 1): 2126-32.
Esser, A. F. (1994). "The membrane attack complex of complement. Assembly, structure and cytotoxic activity." Toxicology 87(1-3): 229-47.
Gee, A. P., M. D. Boyle, et al. (1980). "Distinction between C8-mediated and C8/C9-mediated hemolysis on the basis of independent 86Rb and hemoglobin release." J Immunol 124(4): 1905-10.
Giddings, K. S., J. Zhao, et al. (2004). "Human CD59 is a receptor for the cholesterol-dependent cytolysin intermedilysin." Nat Struct Mol Biol 11(12): 1173-8.
Huang, Y., F. Qiao, et al. (2006). "Defining the CD59-C9 binding interaction." J Biol Chem 281(37): 27398-404.
Leslie, A. G. (2006). "The integration of macromolecular diffraction data." Acta Crystallogr D Biol Crystallogr 62(Pt 1): 48-57.
Lockert, D. H., K. M. Kaufman, et al. (1995). "Identity of the segment of human complement C8 recognized by complement regulatory protein CD59." J Biol Chem 270(34): 19723-8.
Muller-Eberhard, H. J. (1986). "The membrane attack complex of complement." Annu Rev Immunol 4: 503-28.
Murshudov, G. N., A. A. Vagin, et al. (1997). "Refinement of macromolecular structures by the maximum-likelihood method." Acta Crystallogr D Biol Crystallogr 53(Pt 3): 240-55.
Parker, M. W. and S. C. Feil (2005). "Pore-forming protein toxins: from structure to function." Prog Biophys Mol Biol 88(1): 91-142.
Peitsch, M. C., P. Amiguet, et al. (1990). "Localization and molecular modelling of the membrane-inserted domain of the ninth component of human complement and perforin." Mol Immunol 27(7): 589-602.
Perrakis, A., R. Morris, et al. (1999). "Automated protein model building combined with iterative structure refinement." Nat Struct Biol 6(5): 458-63.
Podack, E. R. and G. Dennert (1983). "Assembly of two types of tubules with putative cytolytic function by cloned natural killer cells." Nature 302(5907): 442-5.
Podack, E. R., H. Hengartner, et al. (1991). "A central role of perforin in cytolysis?" Annu Rev Immunol 9: 129-57.
Polekhina, G., K. S. Giddings, et al. (2005). "Insights into the action of the superfamily of cholesterol-dependent cytolysins from studies of intermedilysin." Proc Natl Acad Sci U S A 102(3): 600-5.

Rossjohn, J., S. C. Feil, et al. (1997). "Structure of a cholesterol-binding, thiol-activated cytolysin and a model of its membrane form." Cell 89(5): 685-92.
Shatursky, O., A. P. Heuck, et al. (1999). "The mechanism of membrane insertion for a cholesterol-dependent cytolysin: a novel paradigm for pore-forming toxins." Cell 99(3): 293-9.
Shepard, L. A., A. P. Heuck, et al. (1998). "Identification of a membrane-spanning domain of the thiol-activated pore-forming toxin Clostridium perfringens perfringolysin O: an alpha-helical to beta-sheet transition identified by fluorescence spectroscopy." Biochemistry 37(41): 14563-74.
Slade, D. J., B. Chiswell, et al. (2006). "Functional studies of the MACPF domain of human complement protein C8alpha reveal sites for simultaneous binding of C8beta, C8gamma, and C9." Biochemistry 45(16): 5290-6.
Sodetz, J. M. (1989). "Structure and function of C8 in the membrane attack sequence of complement." Curr Top Microbiol Immunol 140: 19-31.
Steckel, E. W., B. E. Welbaum, et al. (1983). "Evidence of direct insertion of terminal complement proteins into cell membrane bilayers during cytolysis. Labeling by a photosensitive membrane probe reveals a major role for the eighth and ninth components." J Biol Chem 258(7): 4318-24.
Studier, F. W. (2005). "Protein production by auto-induction in high density shaking cultures." Protein Expr Purif 41(1): 207-34.
Terwilliger, T. C. and J. Berendzen (1999). "Automated MAD and MIR structure solution." Acta Crystallogr D Biol Crystallogr 55(Pt 4): 849-61.
Tilley, S. J., E. V. Orlova, et al. (2005). "Structural basis of pore formation by the bacterial toxin pneumolysin." Cell 121(2): 247-56.
Tilley, S. J. and H. R. Saibil (2006). "The mechanism of pore formation by bacterial toxins." Curr Opin Struct Biol 16(2): 230-6.
Tschopp, J. (1984). "Ultrastructure of the membrane attack complex of complement. Heterogeneity of the complex caused by different degree of C9 polymerization." J Biol Chem 259(12): 7857-63.
Tschopp, J., H. J. Muller-Eberhard, et al. (1982). "Formation of transmembrane tubules by spontaneous polymerization of the hydrophilic complement protein C9." Nature 298(5874): 534-8.
Tweten, R. K. (2005). "Cholesterol-dependent cytolysins, a family of versatile pore-forming toxins." Infect Immun 73(10): 6199-209.
Voskoboinik, I., M. C. Thia, et al. (2005). "Calcium-dependent plasma membrane binding and cell lysis by perforin are mediated through its C2 domain: A critical role for aspartate residues 429, 435, 483, and 485 but not 491." J Biol Chem 280(9): 8426-34.
Walport, M. J. (2001). "Complement. First of two parts." N Engl J Med 344(14): 1058-66.
Walport, M. J. (2001). "Complement. Second of two parts." N Engl J Med 344(15): 1140-4.
Wurzner, R., A. Orren, et al. (1992). "Inherited deficiencies of the terminal components of human complement." Immunodefic Rev 3(2): 123-47.

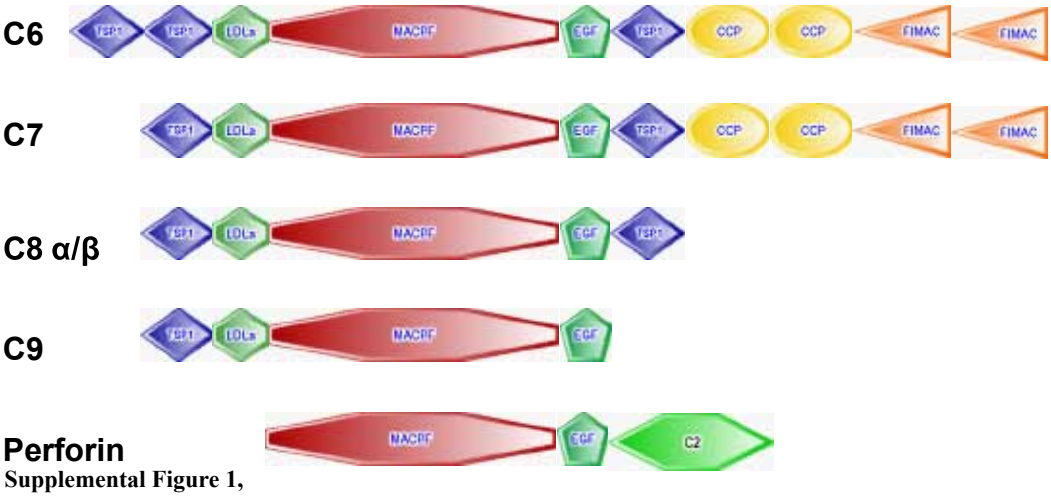

Supplemental Figure 1,

Domain organization of MACPF proteins.

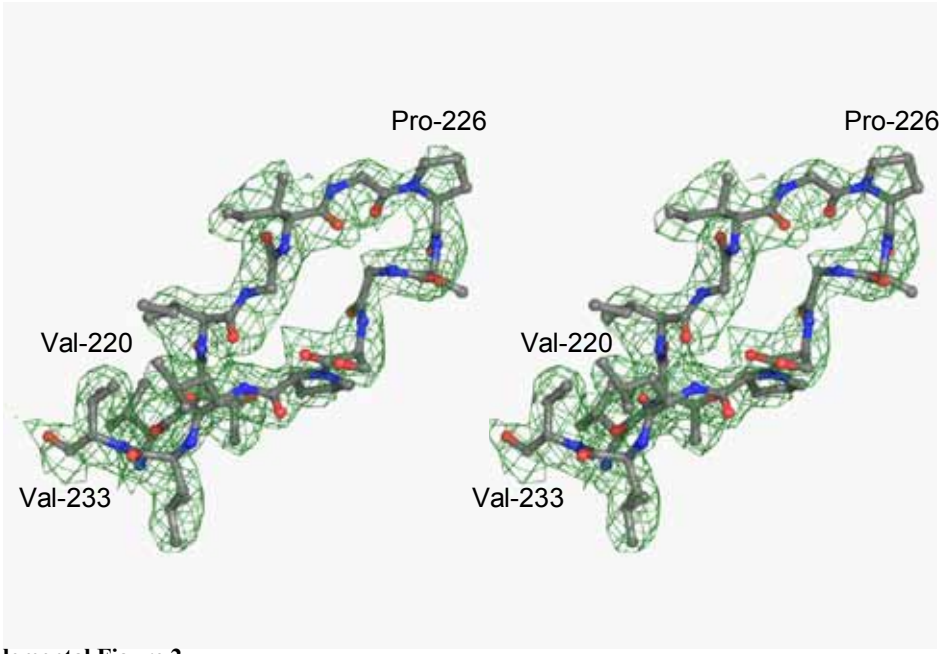

Supplemental Figure 2,

Electron density of C8α-MACPF. Shown in stereo presentation is the $2mF_o$-DF_c,φ_c map contoured at 1-σ level for the β-hairpin region in β1-β2 (res. 220-233).

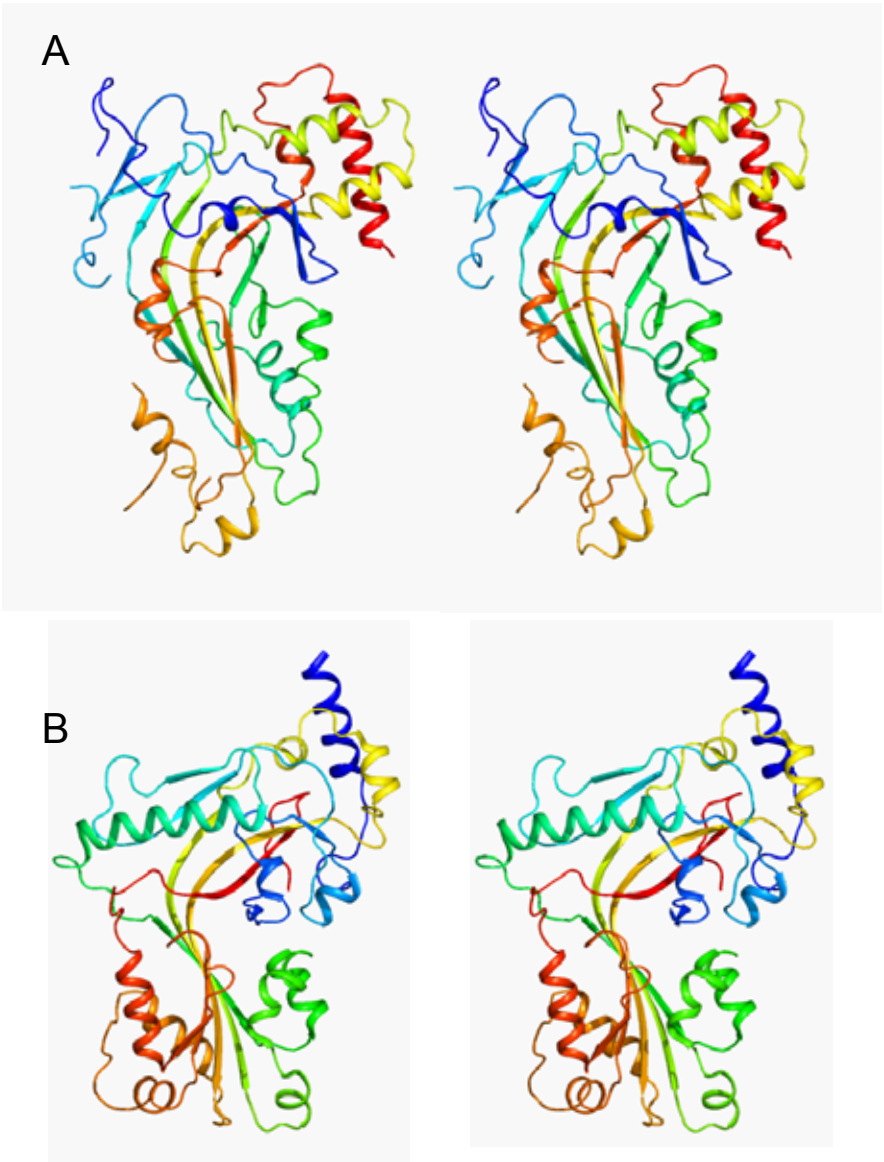

Supplemental Figure 3,

Comparison of the fold of C8α-MACPF and intermedilysin.
(**A**) Cα trace of C8α-MACPF (res. 103-462) coloured from N to C-terminus (blue to red), in stereo representation.
(**B**) Cα trace of intermedilysin domains d1 and d3 (pdb file 1s3r) coloured from N to C-terminus (blue to red). Domains d2 and d4 are omitted. Orientation and colouring as in **A**.

Supplemental Figure 4A,

Sequence alignment of the MACPF domain of C8α.
Sequence identity is indicated by red backgrounds. Sequence similarity is indicated by red letters. Blue boxes indicate region of sequence identity and similarity.

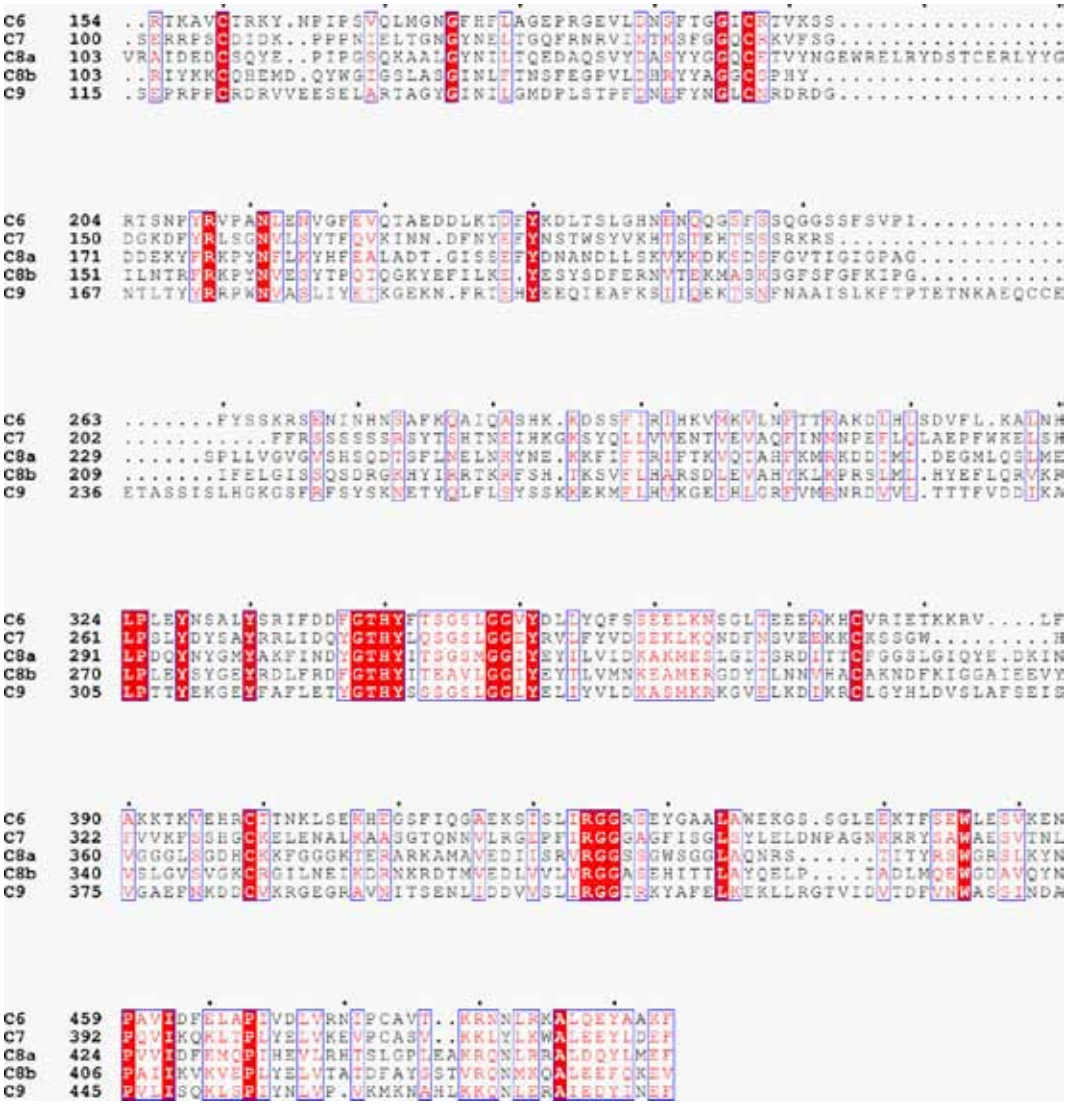

Supplemental Figure 4B,

Sequence alignment of the MACPF domains of C6, C7, C8α, C8β and C9.
Sequence identity is indicated by red backgrounds. Sequence similarity is indicated by red letters. Blue boxes indicate region of sequence identity and similarity.

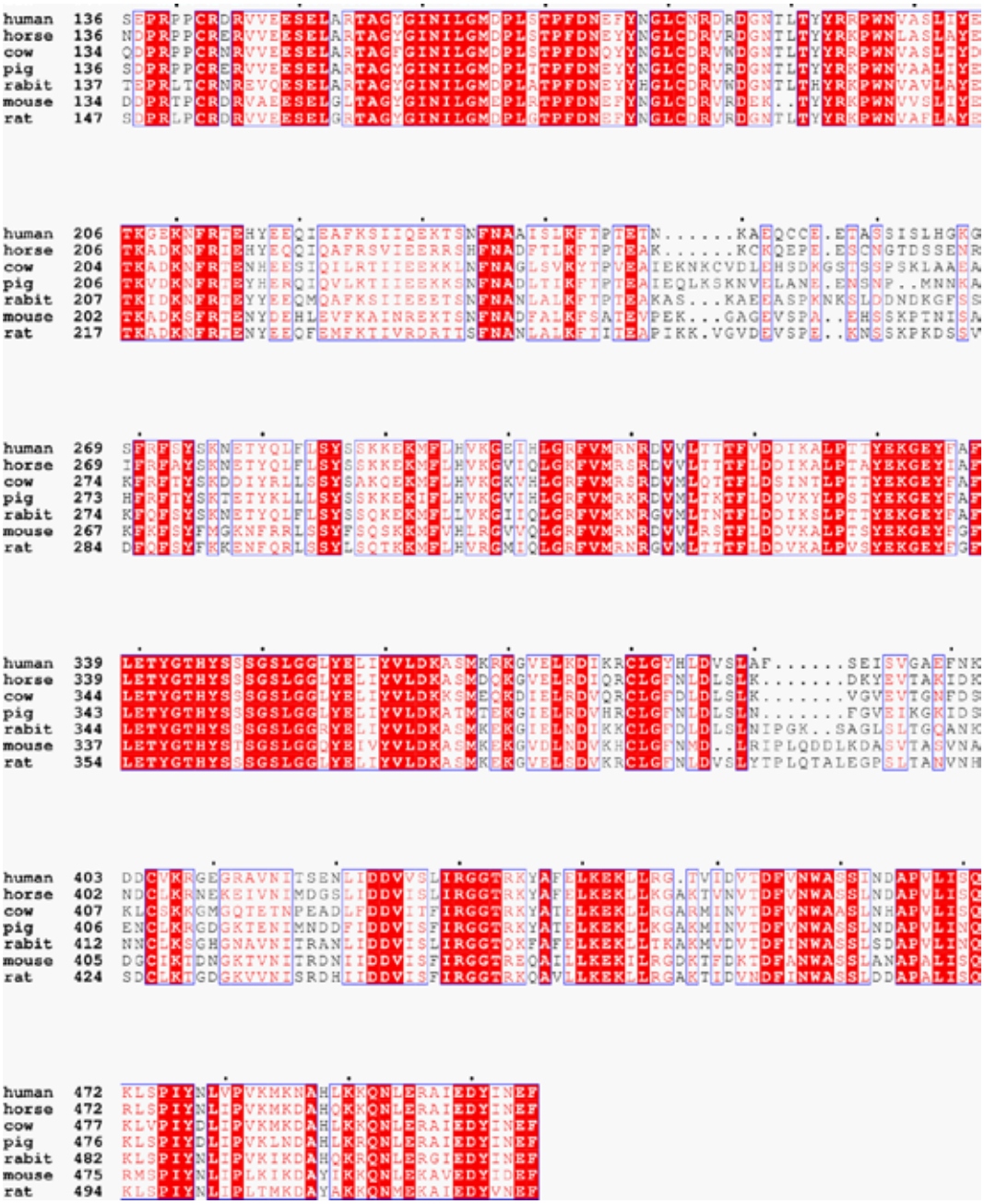

Supplemental Figure 4C,

Sequence alignment of the MACPF domain of C9.
Sequence identity is indicated by red backgrounds. Sequence similarity is indicated by red letters. Blue boxes indicate region of sequence identity and similarity.

Supplemental Figure 4D,

Sequence alignment of the MACPF domain of perforin.
Sequence identity is indicated by red backgrounds. Sequence similarity is indicated by red letters. Blue boxes indicate region of sequence identity and similarity.

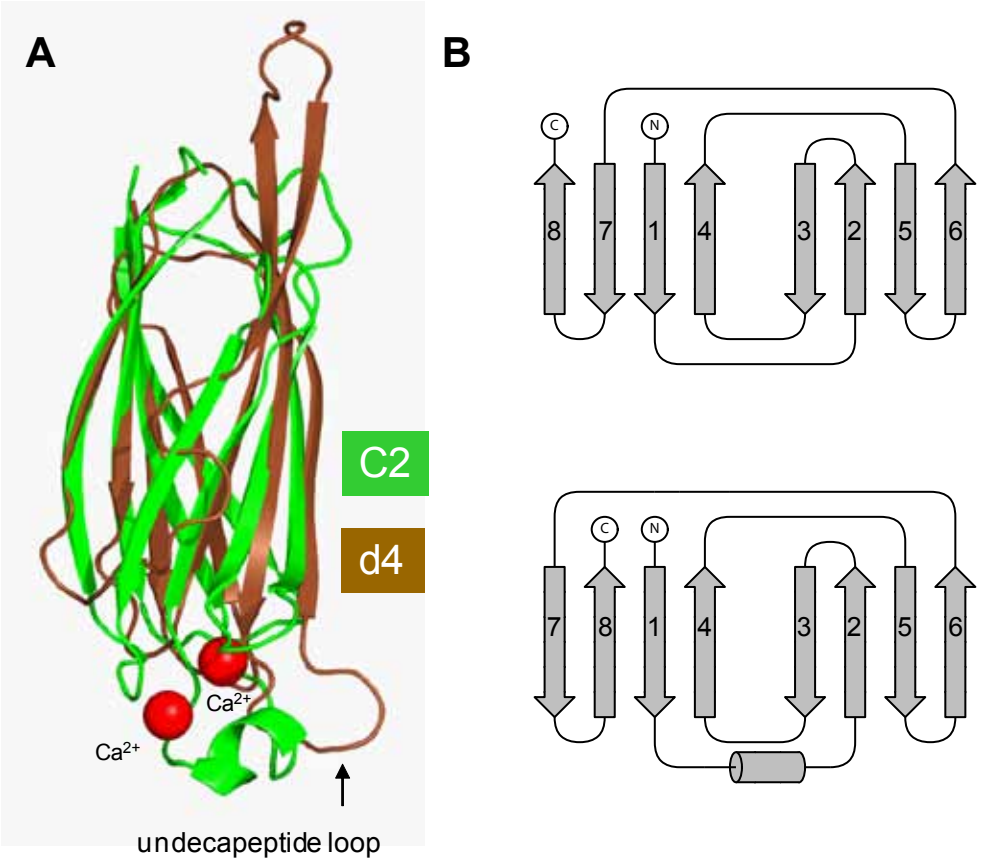

Supplemental Figure 5,

Comparison of the fold of domain d4 of intermedilysin and the C2 domain of cytosolic phospholipase A2.

(A) Cα representation of intermedilysin domain d4 (brown; pdb code 1s3r) and phospholipase 2A domain C2 (green; pdb code 1bci). Depicted in red are the two calcium ions bound by the C2 domain. Calcium ions mediate membrane binding of the C2 domain in phospholipase 2A and perforin. The highly conserved undecapeptide loop is responsible for membrane binding in CDCs.

(B) Fold diagram of a d4 domain (top) and a C2 (bottom).

Chapter 3

Insight into Initiation of Membrane Attack Complex Assembly

Michael A. Hadders[1], Clement Blanchet, Dmitri K. Svergun, Michael K. Pangburn and Piet Gros[1]

[1]Crystal and Structural Chemistry, Bijvoet Center for Biomolecular Research, Department of Chemistry, Faculty of Science, Utrecht University, Padualaan 8, 3584 CH, Utrecht, Netherlands

[2]Medical Microbiology, Eijkman Winkler Insitute, University Medical Center Utrecht, Heidelberglaan 100, 3584 CX, Utrecht, The Netherlands

Manuscript in preparation

Abstract

The membrane attack complex (MAC) of the complement system is able to directly kill Gram-negative bacteria by forming pores that disrupt the lipid bilayer. However, under pathological conditions the MAC can also target host tissue, thereby aggravating disease. To gain insight into the molecular assembly of this large protein complex we crystallized and solved the structure of the first assembly intermediate comprising the proteins C5b and C6. The structure reveals extensive conformational changes that take place upon C5 activation and highlights important differences when compared to homologous C3b. While the domain rearrangements that take place are similar, the swinging down and out of the C5d domain stops prematurely, adopting a unique intermediate conformation. The structure of C6 is the first of a full-length complement MACPF member and reveals the overall organization of its ten domains. The core of C6 is formed by a compact arrangement of five domains arranged in a left handed "superhelix". The N-terminal TSP domain is flexible while the four C-terminal domains are connected to the core via a flexible linker. This linker, together with the two C-terminal CCP domains, is essential for the interaction with C5b, but also function in stabilizing the observed conformation of the C5d domain. Solution scattering of isolated C6 constructs shows that indeed the core of forms a compact arrangement whilethe full-length protein adopts an extended conformation, with a partially disordered C-terminal region.

Introduction

The complement system forms one of the first lines of defense and is able to kill invading Gram-negative bacteria. Killing is mediated by the terminal pathway of complement which, upon activation, results in the buildup of a large protein assembly on target cells termed the membrane attack complex (MAC). The MAC consists of five soluble plasma proteins named C5 to C9 (Esser, 1994; Muller-Eberhard, 1986). Upon assembly these proteins rearrange into a transmembrane pore thereby causing lysis and target cell death. The terminal pathway is activated when complement component C5 is specifically cleaved between Arg751 and Leu752. This cleavage is mediated by enzyme complexes termed C5 convertases and results in the release of a small anaphylotoxin, called C5a (~10 kDa) and a large subunit, C5b (~180 kDa) (Pangburn and Rawal, 2002). C5a binds to and activates the C5a receptor (C5aR), a G-protein coupled receptor (GPCR) expressed by various immune effector cells, thereby eliciting a strong chemotactic and pro-inflammatory response (Guo and Ward, 2005; Haas and van Strijp, 2007). The conversion of C5 to C5b initiates MAC formation. The formation of C5b is thought to be accompanied by large conformational changes that expose a previously cryptic binding site (Cooper and Muller-Eberhard, 1970). This conformation of C5b has a short half-life that permits C6 binding. This is followed by the sequential binding of complement components C7, C8 and C9 (Podack et al., 1978a). This sequential buildup can be separated into several discrete functional steps. Initially C6 binds to C5b, thereby stabilizing the active conformation of C5b and forming a platform for further MAC assembly (Podack et al., 1978b). Binding of C7 to the C5b6 complex induces a change in C7 that renders the newly formed C5b7 lipophilic and results in a concomitant binding to membranes (Preissner et al., 1985). This is followed by binding of C8 which is the first protein to actually insert into the lipid bilayer (Hu et al., 1981; Steckel et al., 1983). The membrane inserted C5b8 complex then functions as a receptor for C9, thereby catalyzing C9 membrane insertion and oligomerization. In this process multiple C9 molecules are able to form large ring shaped pores with a single pore containing up to eighteen copies of C9 and mea-

suring an internal diameter of ~100 Å (Tschopp, 1984; Tschopp et al., 1984; Tschopp et al., 1985).

C5 belongs to the α_2-macroglobulin (α_2M) family of proteins but unlike the homologous complement components C3 and C4, it lacks the hallmark thioester (Armstrong and Quigley, 1999). In recent years several crystal structures of C3 and its activation and degradation products C3b, C3c and C3d have resulted in a wealth of information on the activation mechanism of this family of proteins (Fredslund et al., 2006; Janssen et al., 2006; Janssen et al., 2005; Nagar et al., 1998; Nishida et al., 2006; Wiesmann et al., 2006). These structures revealed that in C3 the reactive thioester is shielded from water in a hydrophobic pocket and that the conversion of C3 to C3b involves large conformational changes which reorient the thioester containing domain (TED) such that the thioester becomes fully exposed and ready to react with surrounding nucleophiles. Recently, the structure of C5 was solved, revealing that, despite the absence of a thioester, the thioester region, like the rest of the protein, is structurally conserved compared to C3 (Fredslund et al., 2008). It is however unclear whether the large rearrangements seen in C3 activation also take place in the C5 to C5b conversion.

C6, together with C7, C8 and C9, belongs to the membrane attack complex/perforin (MACPF) family of proteins. C6 consists of ten domain. Going from the N- to the C-terminus C6 consists of: two thrombospondin type 1 repeats (TSP1), a low density lipoprotein receptor class A domain (LDLa), a membrane attack complex/perforin (MACPF) domain, a epidermal growth factor-like (EGF) domain, a third TSP1 domain, two complement control protein (CCP) modules and two factor I/membrane attack complex (FIMAC) domains. We and others have previously shown that the central MACPF domain that defines this protein family structurally resembles the pore forming domain of cholesterol dependent cytolysins (CDCs), pore forming toxins secreted by Gram-positive bacteria (Hadders et al., 2007; Rosado et al., 2007; Slade et al., 2008). Based on this structural and functional similarity and conserved sequence features we proposed a model of how these domains mediate membrane insertion and pore formation in complement components C8 and C9. However, the role of the MACPF domain remains unclear in other non-pore forming, non-penetrating MACPF members such as C6 and C7. Moreover, nothing is known about the overall architecture of the multi-domain MACPF family members.

Here we present the crystal structure of the C5b6 complex. The structure reveals the activated state of C5 and shows how it differs from that of homologue C3, adopting an intermediate conformation that is stabilized by C6. C6 has a partially extended conformation and seems to function in keeping C5b in a binding competent state to create a hybrid binding platform for C7.

Results

Structure solution of C5b6

For structural studies we purified the C5b6 complex from activated, C7 depleted plasma. A serendipitous observation led to an initial crystallization hit. We found that C5b6 precipitated, even at low concentrations in a physiological buffer. Closer examination however showed that the precipitate was micro-crystalline. Optimization ultimately led to crystals with maximal dimensions of 800 x 80 x 20 µm. These crystals were very sensitive to radiation and yielded anisotropic diffraction to at best 3.5 Å resolution (d=4.2, 3.8 and 3.5 Å in the a*, b* and c* direction, respectively). Phases were determined by molecular replacement (MR). While C5b was readily solved using domains derived from C5 (PDB 3CU7), C6 required extensive trials using a series of homology models, some truncated (for details see materials and methods). Solvent flattened maps (using 71% solvent) guided placement of several C6 domains as they revealed which parts differed from the search models. In the end, all domains could be placed by MR with the exception of the N-terminal TSP1 domain and the C-terminal FIMAC domains (**Figure 1**). While the final electron density maps show TSP1 is largely disordered density for the two C-terminal FIMAC is clearly visible. The density also suggests that the structure differs considerably from the available search models explaining the failure of the MR attempts. Due to the limited resolution we were not able to reliably trace these domains and left them, together with the N-terminal TSP domain, out of the final model which was refined to an R_{work} and R_{free} of 25.09% and 28.56% respectively.

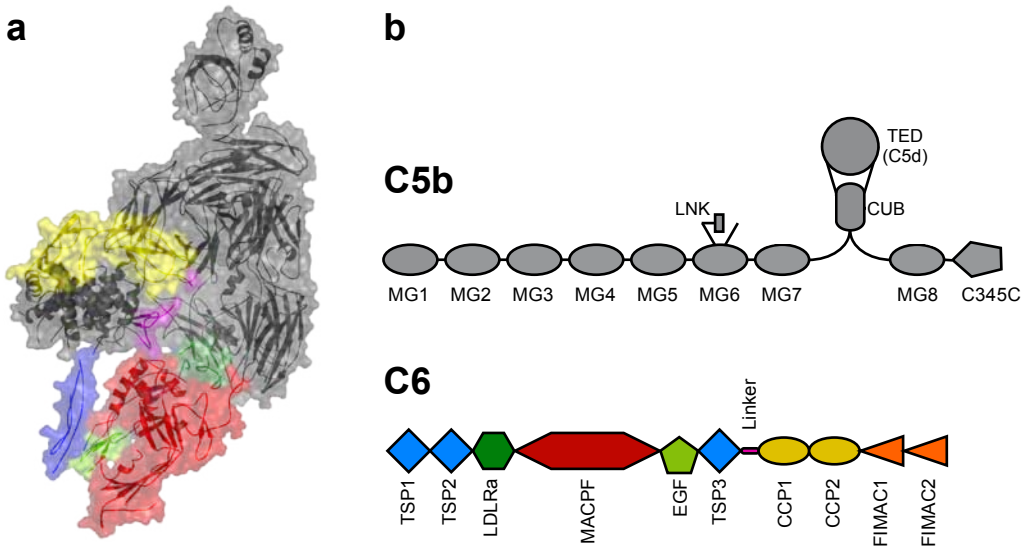

Figure 1 The structure of the C5b6 complex. (**a**) The structure of C5b6 in cartoon representation with transparent surface. C5b is colored in grey while C6 is colored according to the different domains as shown schematically in (**b**) schematic representation of the domain organization of C5b and C6.

The conformation of C5b

C5 activation to C5b is though to involve large conformational changes that expose previously cryptic binding sites as has been thoroughly established for the C3 to C3b transition (Janssen et al., 2006; Janssen et al., 2005; Nishida et al., 2006). C5 consists of eight macroglobulin (MG) domains (MG1-MG8), a domain (CUB), a thioester containing domain (TED/C5d; the residues forming the thioester are not conserved in C5), the C-terminal C345C domain, the anaphylotoxin, also known as C5a, and an extended linker region. These domains are arranged in two chains called the β-chain (residues 1-655) and the α-chain (residues 660-1658). In C5 (and C3), domains MG1-MG6 of the β-chain are arranged in a ring-like structure. We compared the conformation of C5b from the C5b6

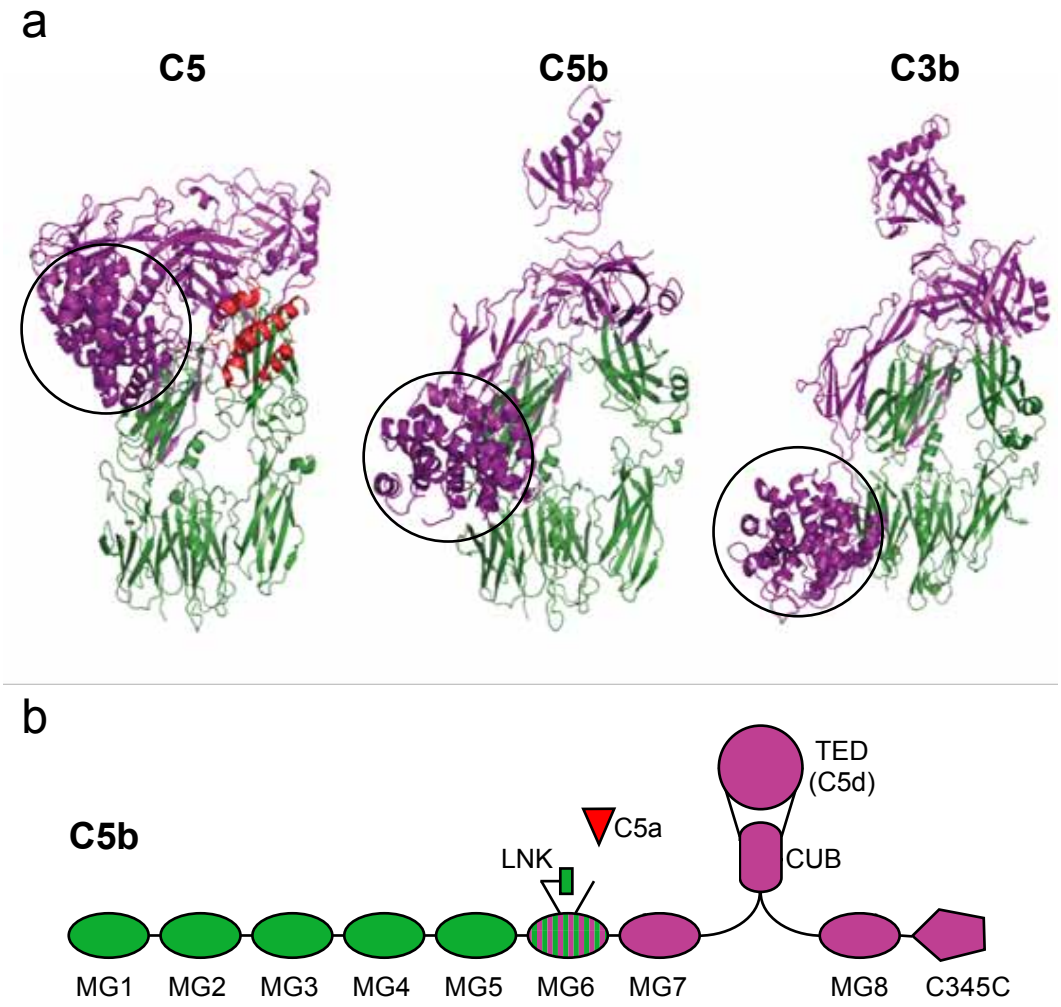

Figure 2 A comparison between C5, C5b and C3b. (**a**) The structures of C5, C5b and C3b with the β-chain colored in green and the α-chain colored in purple. The TED is encircled to highlight the movement of the domain. (**b**) Schematic representation of the domain organization of C5b.

complex with that of C5 (PDB: 3CU7) (Fredslund et al., 2008) by superimposing MG1 to MG6. This comparison reveals only minor changes in this segment, the most notable being a rotation of the MG3 domain. This movement is most likely linked to the removal of the anaphylotoxin (discussed below). The α-chain on the other hand has undergone a dramatic rearrangement which is initiated by the proteolytic removal of C5a at the N-terminus of the α-chain. In C5, the anaphylotoxin packs in between MG3 and MG8 and its release would leave a large space. In C5b this results in the coming together of domains MG3 and MG8. The MG8 domain swings around 19Å while rotating 57° to largely take up the space previously occupied by C5a. This movement breaks the MG8-TED interface which is structurally highly conserved in the α_2M family (Fredslund et al., 2008). The interface plays an important role in protecting the reactive thioester from water and forms a restraint on the position of TED. While the TED of C5 does not contain a thioester, the structure of C5 has shown that the MG8-TED interface and interdomain orientation is remarkably similar (Fredslund et al., 2008). When MG8 moves and the MG8-TED interface is broken it likely releases its restraint on the position of TED. This allows TED to swivel down 45 Å while rotating over 132° along with the adjacent CUB and MG7 domains which move togehther as a single rigid body (**Figure 2a**).

We compared the conformation of C5b to that of homologous C3b (PDB: 2IO7) (Janssen et al., 2006), again by superimposing the β-chain. No major domain rearrangements were observed in this region. It was however immediately apparent that the α-chain has adopted a different conformation (**Figure 2a**). In C5b MG8 occupies a different position compared to C3b. In C3b, MG8 swings around and back over 23 Å to form an extensive interface with domains MG3 and MG7. In C5b however, MG8 points outwards more, forming a much smaller interface with MG3 and MG7 and now largely occupying the space left by C5a. The most striking difference however is the observed position of the TED. In the C3 to C3b transition the TED moves down and out over 66Å with the residues linking the TED to the CUB domain almost fully extended. This positions the TED next to MG1 with its reactive thioester fully exposed pointing "downwards". In the C5b6 structure the TED is positioned next to MG2 having moved down only 44 Å wile rotating over 132°. The domain has not yet made the full transition as observed in C3b. Although C5b was superimposed onto the β-chain of C3b the rigid MG7-CUB segments superimpose revealing that this segment has made the full transition and the only difference is the stalling of the TED (**Figure 2a**). This forms a possible explanation for the metastable C6 binding site in C5b (Cooper and Muller-Eberhard, 1970). In the currently observed conformation the TED only interacts with a small region of C5b on the "top" of the MG1 domain (residues 95-96) which is likely not sufficient to maintain its observed orientation, which instead is stabilized by the CCP1 domain of C6. In the absence of C6, and with nothing to stabilize the observed conformation, the TED might reach the orientation observed in C3b, which would require a further rotation and downward translation over 98° and 28 Å respectively. The C3b-like conformation would clash with C6 fitting with the notion that binding is only compatible with the conformation we observe.

The conformation of C5d

The activation of C3 to C3b results in large conformational changes that serve, amongst others, to fully expose the reactive thioester in the TED so that it may react with target surfaces (Fredslund et al., 2006; Janssen et al., 2006; Janssen et al., 2005; Nishida et al., 2006; Wiesmann et al., 2006). The changes observed are however not restricted to global domain rearrangements. C3-TED itself undergoes substantial conformational changes to reorient the thioester into a much more reactive acyl-imidazole intermediate. These changes are largely restricted to the N-terminal part of

the TED (963-996) and involve a stretching out of this region including the melting of helix 1. Although C5 does not have a thioester it was previously observed that the corresponding region does adopt a similar conformation (Fredslund et al., 2008). Comparison of the TED of C5 with that of C5b shows that this domain undergoes a conformational change similar to that seen in C3 (**Figure 3a,b**). This shows that the presence of the thioester is not a prerequisite for both the conformation of TEDs as well as their conformational changes observed during activation. There are difference however like the residues corresponding to those of the C3 thioester (1007 and 1010). In C5b the segment in which these residues (1001-1011) are located are disordered (**Figure 3a,b**), likely reflecting the loss of function and a concomitant loss of restraint on structure.

The overall conformation of C6

The structure of C6 is the first of a full-length MACPF protein and reveals the overall architecture of its ten domains (**Figure 4a**). The protein is built around the central MACPF domain with three N-terminal and six C-terminal domains. The core is formed by five domains which start at the second TSP domain and extend to the third, last TSP domain, together forming a left-handed "superhelix" with maximum overall dimensions of 60 x 80 x 40 Å (**Figure 4**). The N-terminal TSP1 domain points "downwards" and is flexible, with density only visible in the "upper" N-terminal region. This domain is unique to C6 and conserved but does not seem to be involved in the interaction with C5b. To address a potential role for the N-terminal TSP1 domain downstream in MAC formation, constructs lacking this domain must be tested for activity in hemolytic assays. The most striking feature of C6 is the C-terminal region which comprises the two CCP and FIMAC domains which extend from the

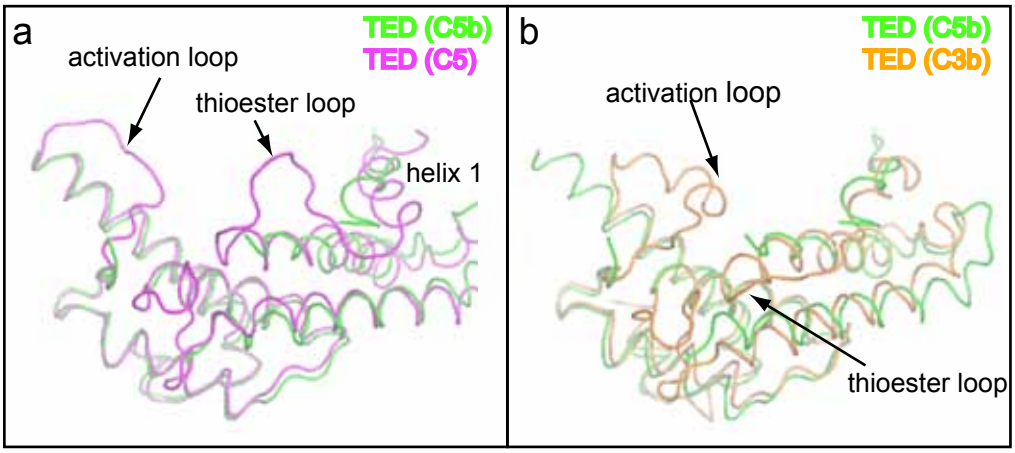

Figure 3 A comparison of the C5b TED with C5 and C3b. (**a**) superimposing the TED of C5b (green) with that of C5 (magenta). Highlighted are the N-terminal helix 1, the loop that contains the thioester in C3 and the loop that contains the catalytic histidine in C3 (**b**) superimposing the TED of C5b (green) with that of C3b (orange). Highlighted are the activation- and the thioester loop of C3b. The comparisons reveal that the N-terminal region of C5b-TED undergoes a similar structural rearrangement as that of C3b with the exception that the loop containing the thioester residues is disordered.

"top" of the TSP3 domain through a 29 residue long linker. The CCP domains and linker are intimately associated with C5b and largely bridge the TED with the remainder of C5b. This likely stabilizes the observed conformation of the TED as discussed above but also that of C6. With the long TSP3-CCP1 linker it seems unlikely C6 is able to retain the observed conformation in solution. The C-terminal domains may adopt an extended disordered conformation due to their putative flexible association to the C6 core. Alternatively, these domains may fold back and associate with the core of C6 to form an overall compact structure. To discriminate between these possibilities we performed solution X-ray scattering experiments on full-length $C6^{1-911}$ and a truncated construct comprising the core region ($C6^{60-603}$). The data show that while the core is indeed compact, full-length C6 is has a much more extended conformation (**Figure 4b,c**). This is in excellent agreement with previous negative stain electron microscopy data on C6 and C7 which revealed an extended conformation with dimensions of 66 x 144 Å and 59 x 43 x 151 Å respectively (DiScipio et al., 1988; DiScipio and Hugli, 1989).

The C5b-C6 interface

The C5b-C6 interaction has been described as being essentially irreversible. Accordingly, we observe an extensive interface between C5b and C6, involving over 150 residues and burying a total surface area of ~4000 Å2. The major interactions are formed by C5b-TED and CUB and the CCP domains and TSP3-CCP1 linker of C6 with smaller contributions by the MG1, MG2 and MG4 domains of C5b and the TSP2, TSP3 and LDLr domains of C6 (**Figure 5a**). Several of the observed interactions confirm previous studies on C6 binding. A role for the C6 TSP3 domain has previously been proposed based on the loss of an epitope of a monoclonal antibody upon complex formation with C5b

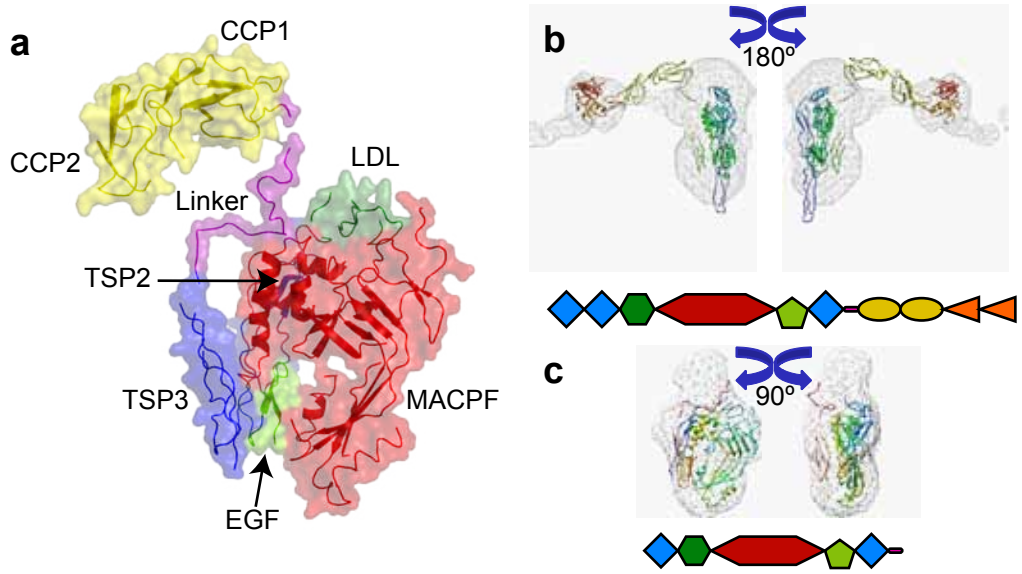

Figure 4 Structure of C6 in solution. (**a**) The structure of C6 (colored by domain; surface representation) in the complex with C5b (not depicted). The structure suggests the C-terminal four domains may be flexibly attached in solution. (**b**) The structure of full-length C6 with the C-terminal FIMAC domains and the N-terminal TSP1 domain modelled and fit into an envelope calculated from an ab-initio model based on small angle x-ray scattering. (**c**) Same as (**b**) but for the C6 'core'. Underneath is a schematic representation of the domain architecture of the constructs used.

(Wurzner et al., 1995) while other studies showed the C5b binding site is located in the four C-terminal domains (DiScipio et al., 1999; Haefliger et al., 1989). The TSP3 domain interaction with C5b is small and poorly resolved in our structure, essentially involving only the loops in the "upper" part of TSP3 and the C-terminal linker, both making contact with C5b-TED. The CCP domains on the other hand make extensive contacts, involving ~30% of their residues while losing over ~14% of their solvent exposed surface area to C5b-TED, CUB and MG2. The CCP1 domain is wedged in between the TED and CUB, forming a bridge between C5d and the β-chain of C5b. This interaction most likely stabilizes the observed position of C5d. The "bottom" side of CCP1 interacts with TED and involves strand β-2 while the adjacent site that interacts with CUB and MG2 involves strands β-3 and β-4. Both sites contain several highly to strictly conserved residues indicative of the importance in C6 function.

The TSP3-CCP1 linker comprises 29 residues (592-620). The connection with TSP3 is disordered but clear density emerges at the "top" of the domain where the linker winds through a crevasse on the surface of TED formed by residues 991-996 and 1276-1281. The linker then kinks right, ~90° where it reassociates with the MACPF domain through a disulfide formed by Cys602 and Cys478 in the MACPF domain. It then kinks again, ~90° and runs alongside an extended surface loop formed by C5b residues 1218-1226 which forms a β-hairpin that forms a cradle which accommodates the linker (**Figure 5b**). The linker then turns, again roughly 90° with a disordered segment, before con-

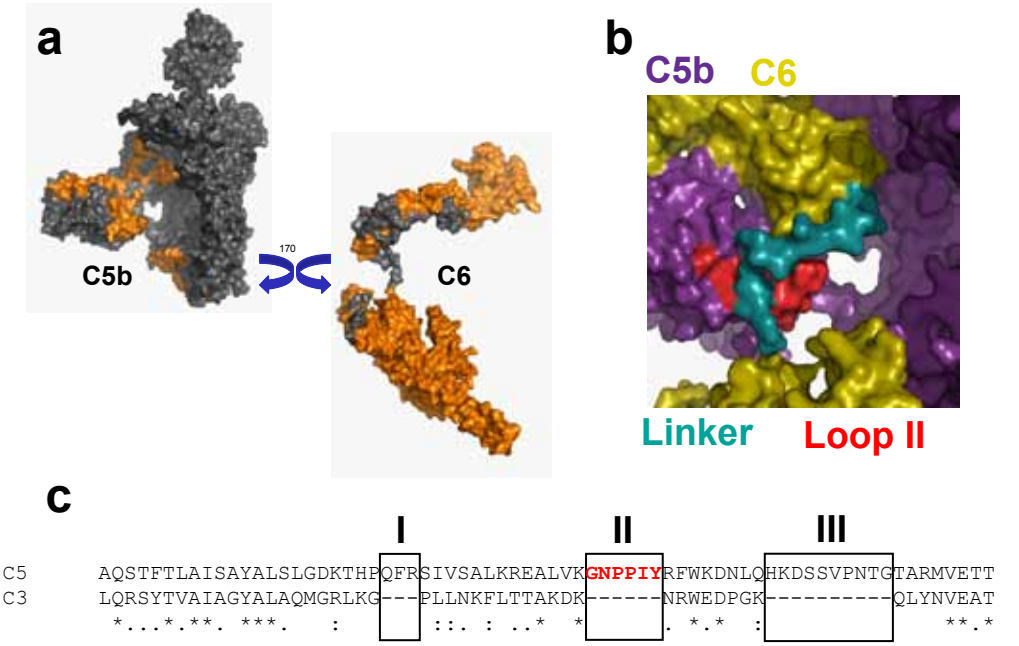

Figure 5 The C5b-C6 interface. (**a**) A surface representation of C5b (grey) and C6 (orange) peeled apart. On C5b the imprint of C6 is shown in orange while on C6 the C5b imprint is colored grey. (**b**) Closeup of the interface showing the interaction of the TSP3-CCP1 linker of C6 (cyan) with a surface loop of C5b-TED (red). (**c**) Sequence alignment between C5 and C3 showing the three insertions in C5. The second insertion, highlighted in red, interacts with C6.

necting to the CCP1 domain. Several residues in this linker are strictly conserved including S593, M595, D605 and E611 which are all located in parts of the linker that are involved in the interaction with the TED. C6 shares 31% sequence identity with C7. However, with the exception of the cysteine that bridges the linker to the MACPF domain ($C6^{602}$ and $C7^{538}$), the linker regions are not homologous. Initial results that make use of a chimeric construct in which a part of the C6 TSP3-CCP1 linker (residues 603-625) was replaced with the corresponding segment in C7 (residues 539-549) showed no hemolytic activity (data not shown) underscoring the portential functional importance of this region. A structure guided alignment of C5-TED shows that the loop formed by residues 1218-1226 that interacts with the linker is one of three insertions, two of which interact with C6 (**Figure 5b,c**). Residues 1200-1203 form the first insertion and are buried at the TED-CCP1 interface. The second insertion is the above mentioned loop formed by residues 1218-1226 which interact with the TSP2-CCP1 linker while the third insertion comprises residues 1231-1239 which are disordered and do not seem to play a role in binding to C6. The first two insertions are highly conserved fitting with their putative functional role in binding to C6 while the third, disordered insertion that does not interact with C6, shows very poor sequence conservation. This suggests no functional role for this segment although it cannot be excluded that this loop has a function downstream of C6 binding. Future mutational analysis will have to clarify the importance of these residues in the C5b-C6 interaction.

C6 binds to C5 in circulation in a reversible manner and this interaction is thought to be mediated by the C6-FIMACs and C345C. The C-terminal FIMAC domains of both C6 and C7 have indeed been shown to bind to the C345C domain of C5 (Thai and Ogata, 2003, 2004). In C5b6 however we see no interaction, confirming previous studies that indicate the C345C domain in C5b6 is free and accessible to binding either C6 or C7 (Thai and Ogata, 2005). DiScipio et al. assessed the role of the FIMAC domains by using a recombinant C6 construct that lacks the FIMAC domains and showed this construct retains 60-70% activity when C5 is activated by the alternative pathway C5 convertase, opposed to only 4-6% when activated by the classical pathway (DiScipio et al., 1999). This difference was due to the increased stability of nascent C5b and revealed a role for the FIMAC domains in the initial recruitment of C6 to C5. Although C5b does not interact with the C6 FIMAC domains, we do observe an interaction between the C-terminal FIMAC domain and the C345C domain of a symmetry related copy of C5b. Although we were not able to trace the FIMAC domains in our structure, the electron density suggests it is the C-terminal FIMAC domain that is involved in binding to the C345C domain. Further studies using specific point mutants and deletions of the C-terminal FIMAC domain will have to be performed to clarify the biological relevance of the observed contact.

Role of the MACPF domain and TMHs

Previous studies by us and others have established that MACPF domains are structurally similar to pore forming CDCs (Hadders et al., 2007; Rosado et al., 2007; Slade et al., 2008). Like CDCs, MACPF domains have a central kinked four-stranded β-sheet with two large loops that fold back, one on each side of the sheet. In CDCs these regions are termed TMH1 and 2 (for trans membrane hairpin) since, upon membrane insertion these segments rearrange from a helical conformation into transmembrane β-hairpins (Shatursky et al., 1999) (**Figure 6b**). In the membrane inserted pores the extended outer strands pair up with neighboring copies to form a large transmembrane β-barrel (Ramachandran et al., 2004; Shatursky et al., 1999). The putative membrane inserting TMH regions in C9 and the α-chain of C8 harbor sequence characteristics compatible with membrane insertion. However,the situation is less clear in C6, C7 and the β-chain of C8. While these proteins do not insert

into the membrane, C7 binding to C5b6 does expose a lipophilic site and also induces an increase in the amount of β-sheet which can also be induced by detergents (Preissner et al., 1985). Although this would fit with the CDC model of TMH refolding into extended β-hairpin structures this has not been demonstrated. The question thus remains if the MACPF fold serves only as a structural scaffold or that the unfolding of the TMH regions is a more general activation mechanism for this family of proteins beyond pore formation and membrane insertion. This would imply that C6 binding to C5b may cause the unfolding of the TMH regions which could then function in binding to subsequent MAC components. The C6 MACPF domain is very similar to that of C8α with the exception of a slight twisting of the central β-sheet (**Figure 6a**). The TMH regions are largely disordered with the exception of the loops and first helical segments emerging from the central strands. The regions point "upwards" and are clearly not compatible with the fully extended β-hairpins that have been demonstrated in CDCs and proposed for the MACPF proteins C8α and C9. This implies that in C6 either these regions do not function through a mechanism of refolding into an extended conformation or have no specific function and instead are a relic of retrograde evolution. Further biochemical studies will have to be performed to address the question of a specific function of the TMH regions in C6 and other MACPF members and if these functions involve an unfolding as seen in the CDCs.

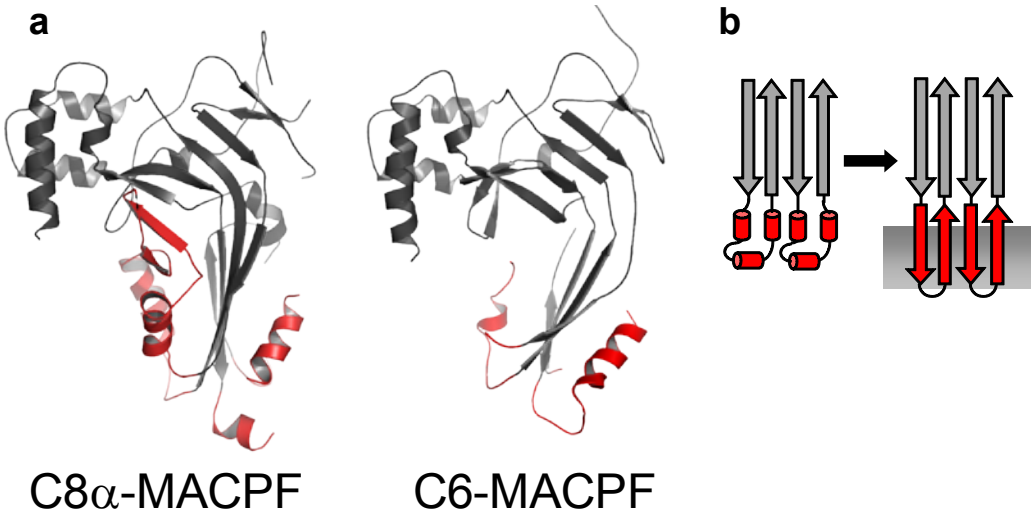

Figure 6 A comparison of the C6 MACPF structure with that of C8α (**a**) The structures of C8α and C6 MACPF domains colored in grey with their TMH regions highlighted in red. The structure of C6 shows that the TMH regions, although largely disordered, are most likely not fully extended as proposed for CDCs (**b**) A achematic model for how CDCs, and by analogy MACPF proteins, function. by unfolding the TMH regins intto two lextende β-hairpins that in the case of CDCs and C9 insert into the membrane.

Discussion

Formation of the membrane attack complex plays an important role in the killing of invading Gram-negative bacteria. It also contributes to host tissue damage in a range of diseases including ischemia/reperfusion, hyper acute rejection of transplanted organs and paroxysmal nocturnal hemoglobinuria (PNH) (Morgan, 1999). Eculizumab, an antibody that blocks C5 activation and thus MAC formation, has shown excellent results in PNH patients, reducing the need for blood transfusions during episodes of hemolysis (Hillmen et al., 2006). This treatment has now been approved by the FDA and its succes has also spawned a new interest into other potential applications of eculizumab and several succesful applications have been reported for diseases including atypical hemolytic-uremic syndrome, cold agglutinin disease and catastrophic antiphospholipid antibody syndrome (Lonze et al., ; Nurnberger et al., 2009; Roth et al., 2009). These studies clearly validate the MAC as a potential drug target. However, despite decades of intense investigation, many biochemical and structural details of MAC assembly are still largely unknown. A more detailed understanding of the molecular mechanism of MAC assembly is therefore warranted.

Here we present the crystal structure of C5b6, the first assembly intermediate of the MAC. Although crystals diffracted anisotropically to only modest resolution we were able to solve the structure. Moreover, while details at the amino acid level were not visible we could clearly distinguish the overall domain architecture. This allowed us to study the rearrangements that take place upon C5 activation to C5b which was largely similar to homologous C3b but with a markedly different position of TED. We observed that TED, despite lacking the hallmark thioester, undergoes the same structural rearrangements associated with thioester activation in C3b suggesting that in the α_2M family the thioester is not a prerequisite for either the conformation of TED as the conformational changes observed upon TED activation. The structure is also the first of a full-length MACPF protein, revealing the overall domain architecture of C6. This was confirmed by solution scattering experiments which showed C6 consists of a compact core (TSP2-LDLa-MACPF-EGF-TSP3) that is shared by all MACPF members in the complement system and an extended C-terminal region (CCP1-CCP2-FIMAC1-FIMAC2) unique to C6 and C7. Our solution scattering data show that this region is flexibly attached to the C6 core via a long unstructured linker situated between the TSP3 and CCP1 domains. This linker also plays an important role in the binding to C5b and together with the CCP domains account for more than 80% of the buried surface area at the C5b-C6 interface, essentially wrapping around three sides of C5b TED. The CCP domains have previously been shown to be essential for the interaction with C5b and using functional studies on recombinant C6 mutants, we were able to confirm a similarly important role for the linker in binding to C5b.

The structure, together with the functional data greatly improve our understanding of the membrane attack complex. However the structure also raises several questions, the most important perhaps concerning the role of the MACPF domains and more specifically the function of the TMH regions. In sequence alignments these regions stand out, showing remarkably poor sequence conservation in all members of the MACPF family. In the C5b6 structure we do not observe the TMH regions adopting a fully extended conformation as was previously proposed for the activated form of C8α and C9 (Hadders et al., 2007). In these two proteins the sequence characteristics of the TMH regions fits with the function of the protein: in C8α they are hydrophobic, facilitating initial membrane insertion whereas in C9 they are amphipathic with alternating hydrophobic and hydrophilic residues pointing towards the inside of the MAC pore and the membrane respectively.

In these segments, allthough the sequence identity is low, the similarity is high as transmembrane segments typically only require conservation of physical properties, i.e. hydrophobicity. The situation becomes less clear for C6, C7 and C8β. Again, the sequence conservation in the TMH regions is very poor, but in contrast to C8α and C9, the TMH regions lack any clear motifs. If the TMH regions would play a role in protein-protein interactions one would expect a higher degree of sequence conservation. An alternative explanation is that these regions are merely vestigial remnants of evolution. This scenario would have started with an ancestral, functional pore forming gene akin to C9. Several gene duplication events could have then added extra functionality in the form of regulation (i.e. C7 for membrane binding and C8 for membrane perturbation) and with the addition of C6, ultimately lead to coupling with the complement system and C5. In the duplications the MACPF would have lost the specific functions related to membrane insertion and pore formation, instead functioning as a scaffold for the adjacent ancillary domains.

Clearly more biochemical work must be done to delineate the function of these regions. The structure of C5b6 as well as those of previous MAC components C5 and C8α will aid in guiding these experiments. Together these results promise an exciting future for the MAC field.

Materials and Methods

C5b6 isolation and purification

Serum C5b6 was isolated from activated C7-depleted human serum. Fresh human serum at 4°C was made 10 mM in EDTA and 0.5 M in NaCl and passed consecutively through lysine-Sepharose and anti-C7 Sepharose columns; each was equilibrated with VB-EDTA and 0.5 M NaCl. The resulting C7- and plasminogen depleted serum was made 15 mM in $MgCl_2$, and 3 mM in $CaCl_2$, diluted 3-fold with VB, and incubated with zymosan at 37°C for 60 min with shaking. The activated serum was centrifuged, and the zymosan pellet was extracted with VB-EDTA and 2 M NaCl. After centrifugation, the extract was diluted 10-fold with VB and combined with the activated serum supernatant. Protease inhibitors were added to give the pool final concentrations of 10 mM Na2EDTA, 0.5 mM PMSF, and 5 mM benzamidine. The pool was then passed through a 15-ml lysine-Sepharose column equilibrated with VBS-EDTA. After the column was washed, C5b6 was eluted with a linear gradient from 0.145- to 0.7 M NaCl in VB-EDTA. Fractions with significant C5b6 activity were pooled, and the pool was supplemented with protease inhibitors (see above), dialyzed against 60 mM NaCl and 10 mM sodium phosphate, pH 7.6, and loaded onto a HPLC Protein-Pak DEAE 8HR column. The column was eluted with a linear 0.06- to 0.5M NaCl gradient. Fractions containing C5b6 activity eluted as a distinct peak and were pooled, concentrated to 0.7 mg/ml and dialysed against 10 mM Hepes pH 7.2, 120 mM NaCl and 0.02% NaN_3.

C6 expression and purification

All C6 constructs were cloned into pABC349 which contains the replication origin OriP and introduces a cystatin S signal peptide followed by a His6-tag. Constructs were transiently transfected into suspension cultures of N-acetylglucoaminyltransferase I deficient HEK293 cells that stably express Epstein-Barr virus nuclear antigen I. Medium was harvested six days post-transfection by centrifugation and concentrated ~10-fold by ultrafiltration followed by diafiltration against 25 mM Hepes/NaOH pH 7.8, 500 mM NaCl and 20 mM imidazole both using a 30 kDa cut-off filter (Quixstand hollow fiber; GE Healthcare). The proteins were purified by batch binding to Ni Sepharose™ 6 Fast Flow (GE Healthcare). After 30 minutes the beads were packed into a column and washed extensively with diafiltration buffer with 30 mM imidazole followed by a one step elution in diafiltration buffer with 250 mM imidazole. Fractions containing the C6 construct were pooled, concentrated and further purified by size exclusion chromatography using a Superdex™ 200 10/300 column equilibrated in 20 mM Hepes/NaOH pH 7.4 and 150 mM NaCl. Fractions containing the C6 construct were pooled, concentrated and flash frozen in liquid N_2. All proteins were stored at -80°C before use.

Crystallization and data collection

The C5b6 complex was crystallized by vapour diffusion of hanging drops consisting of 2.5 µl protein (0.7 mg/ml) mixed with 0.5 µl 1M Hepes/NaOH pH 7.8. Drops were allowed to equilibrate at 18°C over a resevoir solution consisting of 300 µl 0.1M Hepes/NaOH pH 7.8 and 250 mM NaCl. Crystals grew to maximum dimensions of 800 x 80 x 20 µm in ~3-4 weeks and were cryoprotected by brief incubation in a drop containing resevoir solution supplemented with 30% ethylene glycol, followed by flash freezing in liquid N_2. The crystals were very sensitive to radiation and typically showed anisotropic diffraction to at best 4.5-5.5 Å resolution. From a single crystal we were ultimately able to

collect a dataset showing anisotropic diffraction to 3.5 Å resolution (a*=4.2 , b*=3.8 , c*=3.5 Å) at ESRF beamline ID29. The dataset consists of seven wedges of 15° that were collected along the length of the crystal using 1° oscillations. The diffraction data was integrated and scaled using XDS and XSCALE. The crystals belong to space group $I2_12_12_1$ with unit-cell parameters a=154.22, b=230.75, c=269.98 Å and contain one complex of C5b6 in the asymmetric unit. For data statistics see **Table 1**.

Structure solution and refinement

The phases were determined by molecular replacement using the program PHASER. Expectedly, no solution could be found using the the known structure of C5 (PDB code: 3CU7) indicating substantial conformational changes had taken place. Separating the coordinates into TED (986-1307), the β-chain (1-673) and the MG8 (1374-1512), MG7 (822-931), CUB (932-985,1308-1368) and C345C domains (1530-1676) however led to unambigous solutions. Initial attemps at locating the separate domains of C6 using various models failed. Density modification using 71% solvent with the program PARROT clearly revealed residual electron density, indicating that C6 was present in the crystals. Moreover. The density guided the choice of how to adapt certain MR models or which models to use. After extensive trials we were able to locate a homology model of the MACPF domain based on C8α-MACPF (PDB code: 2RD7) lacking the TMH regions, the second and third thrombospondin (TSP) domains (PDB codes:1VEX and 1LSL), the two complement control protein (CCP) domains PDB codes: 2QZD and 2OK5, the epidermal growth factor (EGF) domain (PDB code: 1F7E) and the low-density lipoprotein receptor (LDLr) domain (PDB code: 2FCW). The models were then improved by iterative cycles of manual rebuilding using the program COOT and refinement using the program Buster.

Small angle X-ray scattering

Synchrotron X-ray scattering data was collected from three concentrations of plasma purified full-length C6 (0.35, 1.45 and 2.15 mg/ml) and recombinant truncated $C6^{60-611}$ (1.45, 2.74 and 4.0 mg/ml) at the EMBL beamline X33 using the Pilatus 500K detector. All samples were in 20 mM Hepes/NaOH pH 7.4, 250 mM NaCl and 1% glycerol. To ensure no radiation damage occurred, four succesive 30 second exposures were collected and compared, which showed no changes. All data was processed with PRIMUS. Molecular masses were calculated by normalization against a reference of bovine serum albumin. The solution scattering curves were calculated with CRYSOL and ab initio models were calculated by DAMMIN. Structures were fit into envelopes using the program Chimera.

Table 1 Data collection and refinement statistics

	Crystal 1
Data collection	
Space group	
Cell dimensions	
a, *b*, *c* (Å)	154.22, 230.75, 269.98
α, β, γ (°)	90, 90, 90
Resolution (Å)	50.0- 3.9 (4.00-3.90) *#
R_{sym} or R_{merge}	0.115 (0.809)
$I / \sigma I$	8.4 (1.7)
Completeness (%)	95.8 (97.1)
Redundancy	3.1 (2.9)
Refinement	
Resolution (Å)	50.0-3.5
No. reflections	59023
R_{work} / R_{free}	25.09/28.56
No. atoms	
Protein	15399
B-factors	
Protein	150.81
R.m.s. deviations	
Bond lengths (Å)	0.010
Bond angles (°)	1.39

*Values in parentheses are for highest-resolution shell.
#Data statistics are given to 3.9 Å resolution. Beyond this they become meaningless due to the very strong anisotropy of the data. The 3.5 Å resolution limit that was used for refinement was based upon a $F/\sigma F$ cut-off of 3.0.

References

Armstrong, P.B., and Quigley, J.P. (1999). Alpha2-macroglobulin: an evolutionarily conserved arm of the innate immune system. Dev Comp Immunol 23, 375-390.
Cooper, N.R., and Muller-Eberhard, H.J. (1970). The reaction mechanism of human C5 in immune hemolysis. J Exp Med 132, 775-793.
DiScipio, R.G., Chakravarti, D.N., Muller-Eberhard, H.J., and Fey, G.H. (1988). The structure of human complement component C7 and the C5b-7 complex. J Biol Chem 263, 549-560.
DiScipio, R.G., and Hugli, T.E. (1989). The molecular architecture of human complement component C6. J Biol Chem 264, 16197-16206.
DiScipio, R.G., Linton, S.M., and Rushmere, N.K. (1999). Function of the factor I modules (FIMS) of human complement component C6. J Biol Chem 274, 31811-31818.
Esser, A.F. (1994). The membrane attack complex of complement. Assembly, structure and cytotoxic activity. Toxicology 87, 229-247.
Fredslund, F., Jenner, L., Husted, L.B., Nyborg, J., Andersen, G.R., and Sottrup-Jensen, L. (2006). The structure of bovine complement component 3 reveals the basis for thioester function. J Mol Biol 361, 115-127.
Fredslund, F., Laursen, N.S., Roversi, P., Jenner, L., Oliveira, C.L., Pedersen, J.S., Nunn, M.A., Lea, S.M., Discipio, R., Sottrup-Jensen, L., et al. (2008). Structure of and influence of a tick complement inhibitor on human complement component 5. Nat Immunol 9, 753-760.
Guo, R.F., and Ward, P.A. (2005). Role of C5a in inflammatory responses. Annu Rev Immunol 23, 821-852.
Haas, P.J., and van Strijp, J. (2007). Anaphylatoxins: their role in bacterial infection and inflammation. Immunol Res 37, 161-175.
Hadders, M.A., Beringer, D.X., and Gros, P. (2007). Structure of C8alpha-MACPF reveals mechanism of membrane attack in complement immune defense. Science 317, 1552-1554.
Haefliger, J.A., Tschopp, J., Vial, N., and Jenne, D.E. (1989). Complete primary structure and functional characterization of the sixth component of the human complement system. Identification of the C5b-binding domain in complement C6. J Biol Chem 264, 18041-18051.
Hillmen, P., Young, N.S., Schubert, J., Brodsky, R.A., Socie, G., Muus, P., Roth, A., Szer, J., Elebute, M.O., Nakamura, R., et al. (2006). The complement inhibitor eculizumab in paroxysmal nocturnal hemoglobinuria. N Engl J Med 355, 1233-1243.
Hu, V.W., Esser, A.F., Podack, E.R., and Wisnieski, B.J. (1981). The membrane attack mechanism of complement: photolabeling reveals insertion of terminal proteins into target membrane. J Immunol 127, 380-386.
Janssen, B.J., Christodoulidou, A., McCarthy, A., Lambris, J.D., and Gros, P. (2006). Structure of C3b reveals conformational changes that underlie complement activity. Nature 444, 213-216.
Janssen, B.J., Huizinga, E.G., Raaijmakers, H.C., Roos, A., Daha, M.R., Nilsson-Ekdahl, K., Nilsson, B., and Gros, P. (2005). Structures of complement component C3 provide insights into the function and evolution of immunity. Nature 437, 505-511.
Lonze, B.E., Singer, A.L., and Montgomery, R.A. Eculizumab and renal transplantation in a patient with CAPS. N Engl J Med 362, 1744-1745.
Morgan, B.P. (1999). Regulation of the complement membrane attack pathway. Crit Rev Immunol 19, 173-198.
Muller-Eberhard, H.J. (1986). The membrane attack complex of complement. Annu Rev Immunol 4, 503-528.

Nagar, B., Jones, R.G., Diefenbach, R.J., Isenman, D.E., and Rini, J.M. (1998). X-ray crystal structure of C3d: a C3 fragment and ligand for complement receptor 2. Science 280, 1277-1281.
Nishida, N., Walz, T., and Springer, T.A. (2006). Structural transitions of complement component C3 and its activation products. Proc Natl Acad Sci U S A 103, 19737-19742.
Nurnberger, J., Philipp, T., Witzke, O., Opazo Saez, A., Vester, U., Baba, H.A., Kribben, A., Zimmerhackl, L.B., Janecke, A.R., Nagel, M., et al. (2009). Eculizumab for atypical hemolytic-uremic syndrome. N Engl J Med 360, 542-544.
Pangburn, M.K., and Rawal, N. (2002). Structure and function of complement C5 convertase enzymes. Biochem Soc Trans 30, 1006-1010.
Podack, E.R., Biesecker, G., Kolb, W.P., and Muller-Eberhard, H.J. (1978a). The C5b-6 complex: reaction with C7, C8, C9. J Immunol 121, 484-490.
Podack, E.R., Kolb, W.P., and Muller-Eberhard, H.J. (1978b). The C5b-6 complex: formation, isolation, and inhibition of its activity by lipoprotein and the S-protein of human serum. J Immunol 120, 1841-1848.
Preissner, K.T., Podack, E.R., and Muller-Eberhard, H.J. (1985). The membrane attack complex of complement: relation of C7 to the metastable membrane binding site of the intermediate complex C5b-7. J Immunol 135, 445-451.
Ramachandran, R., Tweten, R.K., and Johnson, A.E. (2004). Membrane-dependent conformational changes initiate cholesterol-dependent cytolysin oligomerization and intersubunit beta-strand alignment. Nat Struct Mol Biol 11, 697-705.
Rosado, C.J., Buckle, A.M., Law, R.H., Butcher, R.E., Kan, W.T., Bird, C.H., Ung, K., Browne, K.A., Baran, K., Bashtannyk-Puhalovich, T.A., et al. (2007). A common fold mediates vertebrate defense and bacterial attack. Science 317, 1548-1551.
Roth, A., Huttmann, A., Rother, R.P., Duhrsen, U., and Philipp, T. (2009). Long-term efficacy of the complement inhibitor eculizumab in cold agglutinin disease. Blood 113, 3885-3886.
Shatursky, O., Heuck, A.P., Shepard, L.A., Rossjohn, J., Parker, M.W., Johnson, A.E., and Tweten, R.K. (1999). The mechanism of membrane insertion for a cholesterol-dependent cytolysin: a novel paradigm for pore-forming toxins. Cell 99, 293-299.
Slade, D.J., Lovelace, L.L., Chruszcz, M., Minor, W., Lebioda, L., and Sodetz, J.M. (2008). Crystal structure of the MACPF domain of human complement protein C8 alpha in complex with the C8 gamma subunit. J Mol Biol 379, 331-342.
Steckel, E.W., Welbaum, B.E., and Sodetz, J.M. (1983). Evidence of direct insertion of terminal complement proteins into cell membrane bilayers during cytolysis. Labeling by a photosensitive membrane probe reveals a major role for the eighth and ninth components. J Biol Chem 258, 4318-4324.
Thai, C.T., and Ogata, R.T. (2003). Expression and characterization of the C345C/NTR domains of complement components C3 and C5. J Immunol 171, 6565-6573.
Thai, C.T., and Ogata, R.T. (2004). Complement components C5 and C7: recombinant factor I modules of C7 bind to the C345C domain of C5. J Immunol 173, 4547-4552.
Thai, C.T., and Ogata, R.T. (2005). Recombinant C345C and factor I modules of complement components C5 and C7 inhibit C7 incorporation into the complement membrane attack complex. J Immunol 174, 6227-6232.
Tschopp, J. (1984). Ultrastructure of the membrane attack complex of complement. Heterogeneity of the complex caused by different degree of C9 polymerization. J Biol Chem 259, 7857-7863.
Tschopp, J., Engel, A., and Podack, E.R. (1984). Molecular weight of poly(C9). 12 to 18 C9 molecules form the transmembrane channel of complement. J Biol Chem 259, 1922-1928.

Tschopp, J., Podack, E.R., and Muller-Eberhard, H.J. (1985). The membrane attack complex of complement: C5b-8 complex as accelerator of C9 polymerization. J Immunol 134, 495-499.
Wiesmann, C., Katschke, K.J., Yin, J., Helmy, K.Y., Steffek, M., Fairbrother, W.J., McCallum, S.A., Embuscado, L., DeForge, L., Hass, P.E., et al. (2006). Structure of C3b in complex with CRIg gives insights into regulation of complement activation. Nature 444, 217-220.
Wurzner, R., Mewar, D., Fernie, B.A., Hobart, M.J., and Lachmann, P.J. (1995). Importance of the third thrombospondin repeat of C6 for terminal complement complex assembly. Immunology 85, 214-219.

Chapter 4

Structural basis of phagocytosis inhibition by *S. aureus* FLIPr-like in complex with FcγRIIa

Michael A. Hadders[1], Piet C. Aerts[2], Nico de Mol[3], Piet Gros[1], Jos A. van Strijp[2], and Carla C.J. de Haas[2]

[1]Crystal and Structural Chemistry, Bijvoet Center for Biomolecular Research, Department of Chemistry, Faculty of Science, Utrecht University, Padualaan 8, 3584 CH, Utrecht, Netherlands

[2]Medical Microbiology, Eijkman Winkler Insitute, University Medical Center Utrecht, Heidelberglaan 100, 3584 CX, Utrecht, The Netherlands

[3]Department of Medicinal Chemistry and Chemical Biology, Utrecht Institute for Pharmaceutical Sciences, Utrecht, The Netherlands

manuscript in preparation

Abstract

Staphylococcus aureus **can cause several diseases ranging from minor skin infections to potentially fatal sepsis. To facilitate infection,** *S. aureus* **secretes a whole range of proteins that modulate specific steps of the host immune response, including the chemotaxis of phagocytic cells towards sites of infection. Staphylococcal formyl peptide receptor-like 1 inhibitory protein (FLIPr) and FLIPr-like are two proteins that can inhibit chemotaxis towards bacteria-derived N-formylated peptides and phenol soluble modulins. Recently, we discovered that FLIPr and FLIPr-like also bind to FcγRs and thereby inhibit subsequent phagocytosis by neutrophils. Here we present the crystal structure of FLIPr-like in complex with the extracellular segment of FcγRIIa. The structure reveals FLIPr-like adopts a fold similar to staphylococcal super antigen like proteins and binds to domain two of FcγRIIa. The binding site completely overlaps with that of IgG, giving a straightforward mechanism for FcγR inhibition. The structure, together with functional binding studies, forms a starting blueprint for the rational design of isoform specific FcγR inhibitors that may have therapeutic implications in autoimmune and inflammatory disorders.**

Introduction

Staphylococcus aureus is a Gram-positive pathogen and a major cause of wound and nosocomial infections in humans (Lowy, 1998). Its pathology is linked to its arsenal of immune evasive molecules (Chavakis et al., 2007). One of the most important non-specific immune reactions of the host is phagocytosis, a process in which bacteria are internalized and destroyed by phagocytes. Once bacteria infect the host they are quickly opsonised with complement component C3b and specific antibodies. Neutrophils, which are the first phagocytes arriving at the site of infection, express complement receptor 3 (CR3) and Fc receptors for immunoglobulin G (IgG) (FcγR) which mediate recognition and efficient phagocytosis of opsonised bacteria. *S. aureus* expresses several proteins which are able to interfere with this recognition by neutrophils. The staphylococcal complement inhibitors (SCIN), extracellular fibrinogen binding protein (Efb) and extracellular complement binding protein (Ecb) bind C3 convertases on the bacterial surface, thereby inhibiting C3b deposition (Jongerius et al., 2007). Staphylococcal superantigen-like protein 7 (SSL7) inhibits C5a-induced phagocytosis of *S. aureus* through binding to and inhibition of the cleavage of C5 (Bestebroer et al.). Staphylokinase removes C3b and IgG from the bacterial surface by cleavage (Rooijakkers et al., 2005), whereas protein A, SSL10 and S. aureus binder of IgG (Sbi) bind the Fc fragment of IgG, thereby preventing recognition of IgG-opsonized bacteria by neutrophil FcγR's (Chavakis et al., 2007; Jongerius et al., 2007; Patel et al.). Recently, two novel inhibitors of neutrophil phagocytosis were described by our group, FLIPr and FLIPr-like. These proteins were initially described as inhibitors of the FPR-like 1 receptor (FPRL1), hence their name FPRL1-Inhibitory Protein (Prat et al., 2006; Prat et al., 2009). However, we found that FLIPr and FLIPr-like also bind to FcγR's (Stemerding et al.). FLIPr and FLIPr-like share 73% sequence identity and are located on an immune evasion cluster that also encodes for Efb, Ecb, and two SCIN homologs SCIN-B and SCIN-C (Jongerius et al., 2007).

In humans, three major classes of FcγR's exist: FcγRI (CD64), FcγRII (CD32) and FcγRIII (CD16). FcγRI represents a high affinity receptor, capable of binding monomeric human IgG1, IgG3, and IgG4. FcγRII and FcγRIII are low affinity receptors, interacting only with IgG in a complexed form. Both receptors exist as two isoforms, A and B. Human neutrophils constitutively express the transmembrane FcγRIIa and the GPI-anchored FcγRIIIb. FcγRIIIb is much less efficient in initiating

phagocytosis when compared to FcγRIIa, but cross-linking of FcγRIIIb was shown to enhance the FcγRIIa function (Anderson et al., 1990; Pricop and Salmon, 2002; Salmon et al., 1995). FLIPr was found to bind mainly to FcγRII, whereas FLIPr-like binds all FcγR's, except for FcγRIIIb. Both proteins showed efficient inhibition of FcγR-mediated phagocytosis of S. aureus by human neutrophils. Additionally, FLIPr-like showed complete inhibition of the FcγR-mediated Arthus reaction in a mouse model (Stemerding et al.). Here we report the crystal structure of the IgG receptor FcγRIIa in complex with FLIPr-like. The FLIPr-like bindingsite is located on domain 2 of FcγRIIa and almost fully overlaps with the bindingsite of the IgG Fc fragment. This exludes simultaneous binding and reveals a clear explanation for how FLIPr-like inhibits FcγR signalling. Analysis of point mutants of FLIPr-like and FcγRIIa confirm this binding site and explain the lack of binding of FLIPr-like to FcγRIIIb. Fc receptors play a major role in the immune defense against pathogens but also in inflammatory disorders (Nakamura et al., 2008; Takai, 2002). Interference of immune complex binding to FcγRs by FLIPr and FLIPr-like may result in novel therapies against autoimmune and inflammatory diseases.

Results

Production and characterisation of FLIPr-like (8-104)

FLIPr-like was expressed with an N-terminal histidine tag for efficient isolation. Removal of the histidine tag with enterokinase resulted in an extra cleavage between amino acid 7 and 8 of FLIPr-like, as described earlier by Prat et al. We were able to separate FLIPr-like and FLIPr-like (8-104) using different pH buffers for elution from the nickel column. Concentration of FLIPr-like for crystallography above 3 to 4 mg/ml resulted in precipitation and loss of the protein. In contrast, FLIPr-like (8-104) could easily be concentrated to 7 mg/ml without loss of protein. Both FLIPr-like and FLIPr-like (8-104) were equally active in their inhibitory capacity on IgG-mediated phagocytosis (**figure 1a**). Therefore, FLIPr-like (8-104) was used for crystallography.

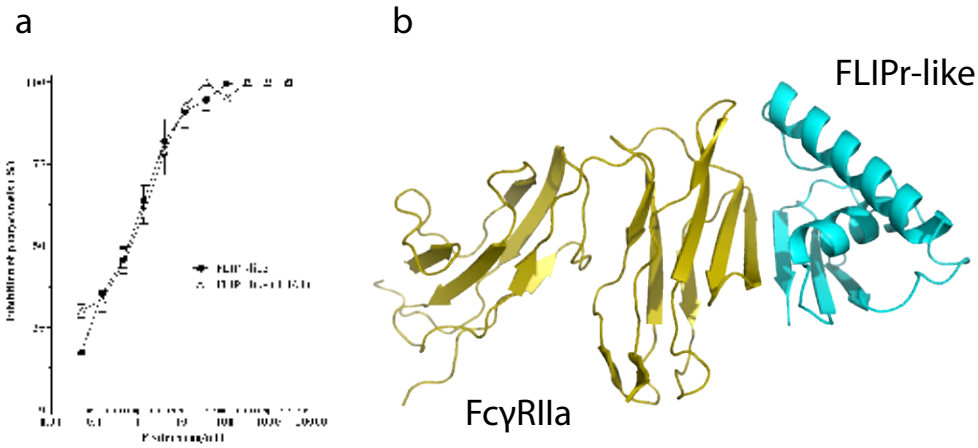

Figure 1 (**a**) Phagocytosis inhibition assay using neutrophils pre-incubated with various concentrations of FLIPr-like or FLIPr-like (8-104) before exposure to serum and FITC labelled *S. aureus*. The amount of FITC positive neutrophils were counted using flow cytometry. (**b**) The crystal structure of FLIPr-like in complex with FcγRIIa at 1.75 A resolution. A cartoon representation showing FLIPr-like colored in cyan and FcγRIIa colored in olive.

Overall structure

Using FLIPr-like (8-104), mixed in an equimolar ratio with FcγRIIa (1-174; HR), we were able to obtain crystals in two different spacegroups. The best crystals diffracted to 1.75 Å and 2.6 Å respectively and phases were obtained by molecular replacement using the structure of FcγRIIa (PDB code: 1FCG; see Materials and Methods). Both crystal forms are essentially identical with a root-mean-square-deviation (RMSD) of 0.72 Å in atomic position of all backbone atoms. Therefore we will only refer to the high resolution crystal form 1 in the remainder of the text. FLIPr-like and FcγRIIa form a 1:1 complex in the crystallographic asymmetric unit. The structure reveals that FLIPr-like binds exclusively to domain 2 of FcγRIIa (**figure 1b**). The protein aligns with the two Ig domains of FcγRIIa to form an overall extended structure measuring in maximum dimensions 85 x 40 x 40 Å. Comparison of FcγRIIa from the complex with isolated FcγRIIa (PDB code: 1FCG) shows the same heart shaped arrangement of the two Ig domains with an interdomain angle of approximately 66° (Maxwell et al., 1999). The binding of FLIPr-like does not induce significant changes in FcγRIIa which has a RMSD of all backbone atoms of 0.63 Å compared to free FcγRIIa.

Structure of FLIPr-like

FLIPr-like consists of a three stranded anti-parallel β-sheet that packs against two N-terminal α-helices that lay on top of each other in a perpendicular fashion (**figure 2a,c**). The N-terminal 15 residues extending from the first α-helix were not visible in the electron density, most likely due to disorder. A comparison of FLIP-like with the PDB using the DALI server at the EBI (Holm and Rosenstrom) revealed FLIPr-like resembles the C-terminal β-grasp domain of S. aureus superantigen-like proteins SSL11 (PDB code: 2RDH), SSL5 (previously known as SET3; PDB code: 1M4V) and SSL7 (previously known as SET1; PDB code: 1V1O) and CHIPS (PDB code: 1XEE) and the staphylococcal superantigen TSST-1 (PDB code: 2IJ0) (Al-Shangiti et al., 2004; Arcus et al., 2002; Chung et al., 2007; Haas et al., 2005; Moza et al., 2007). The β-grasp fold consists of a five stranded β-sheet packed against an N-terminal α-helix. However, comparison with the superantigen-like family shows FLIPr-like differs from the canonical β-grasp fold. In SSL11, SSL5 and SSL7, the region proximal (N-terminal) to the α-helix folds back, forming an extend anti-parallel β-hairpin that aligns with strand β-3 in a parallel fashion (**figure 2c**). In FLIPr-like this region forms the second α-helix that lays over the domain, perpendicular to helix α-1. Furthermore, the α-2 helix (12 versus 17 residues in SSL11) and the loop that connects the α-2 helix with the β-1 strand (4 versus 10 residues in SSL11) are much shorter in FLIPr-like. A comparison with CHIPS shows it differs from both FLIPr-like and the SSL's. The C-terminus has an extra extension that folds back to form a unique fourth β-strand which aligns anti-parallel to strand β-3 (**figure 2b,c**)whereas the N-terminal region, that forms the proximal helix in FLIPr-like and the β-hairpin in the SSL's, was shown to be disordered and therefore excluded from the construct used to determine the structure.

FcγR-FLIPr-like interface

The structure of the FLIPr-like-FcγRIIa complex reveals FLIPr-like binds solely to domain 2 of FcγRIIa with complex formation resulting in a total buried surface area of ~1200Å^2 (**figure 1b**). The binding site is centered around an anti-parallel β-sheet formed between FLIPr-like residues 99-103 and FcγRIIa residues 130-134 and results in the formation of an extended seven stranded β-sheet. This interaction is further stabilized by several hydrophobic contacts and a salt bridge that

involve the insertion of a single residue of FcγRIIa into two coresponding pockets on the FLIPr-like surface (figure 3a). The hydrophobic interactions involve F132 of FcγRIIa which inserts into a hydrophobic pocket formed by FLIPr-like residues Y40, M55, I98, I101, and W103 (**figure 3b**) whereas the elecrostatic interaction is formed by FcγRIIa residue K120 which protrudes into the second pocket on FLIPr-like formed by residues 33-40 and forms a salt bridge with D34 (**figure 3c**).

Functional and biophysical characterization of the FcγRIIa-FLIPr-like interaction

To gain insight into the nature of the FLIPr-like-FcγRIIa interaction we analysed the binding of several FLIPr-like variants and FLIPr to FcγRIIa using isothermal titration calorimetry (ITC**)**. FLIPr-like, FLIPr-like (8-104) and FLIPr-like (16-104) all displayed a similar high affinity 1:1 binding to FcγRIIa with a dissociation constant of 30 nM (**Table 1**). FLIPr binds with a slightly higher affinity of 14 nM and this correlates with the corresponding values

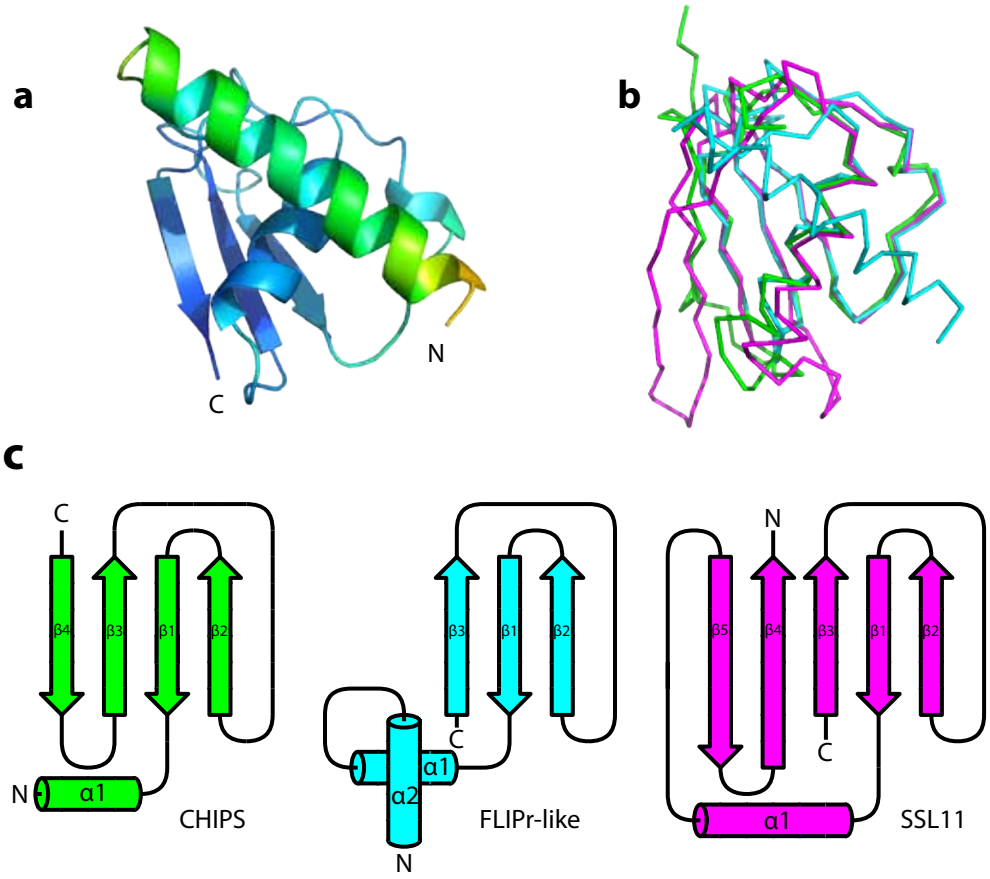

Figure 2 The crystal structure of FLIPr-like from the complex with FcγRIIa at 1.75 A resolution. (**a**) cartoon representation colored according to refined B-factors. (**b**) A ribbon representation of FLIPr-like (cyan) superimposed on SSL11 (magenta) and CHIPS (green). (**c**) Topology diagrams comparing FLIPr-like (cyan) with SSL11 (magenta) and CHIPS (green).

for ΔG of binding: -10.0 kcal/mol for FLIPr-like versus -11.0 kcal/mol for FLIPr. The thermodynamic parameters of binding differ however. FLIPr binding displays a strong enthalpic contribution of -15.3 kcal/mol but this is compensated by a more unfavorable effect in entropy of -4.5 kcal/mol while FLIPr-like binding is dominated by enthalpy, with a ΔH of -10.2 kcal/mol.

We then investigated the binding of several point mutants of FLIPr-like which, based on the structure, were thought to be important for binding to FcγRIIa. The mutations made were D34A, H39A, Y40A, N59A and W103A (**Table 1**). These mutants were tested, both in a functional assay that assesses the role of phagocytosis inhibition and for binding using ITC. The N59A mutant showed a binding affinity comparable to wild type FLIPr-like whereas the H39A mutation actually showed an increased affinity. It is of interest to note that neither of these residues are conserved between FLIPr-like and FLIPr. In FLIPr, position 39 is occupied by a proline and indeed shows binding comparable to FLIPr-likeH39A. The imidazole ring of the histidine side-chain stacks against that of H134 of FcγRIIa but this interaction apparently has a negative contribution to overall binding. We have previously seen that the FcγRIIa H134R polymorphism binds less strong to both FLIPr and FLIPr-like indicating that the presence of too much bulk at this position on the interface negatively influences the FcγRIIa interaction with FLIPr and FLIPr-like.

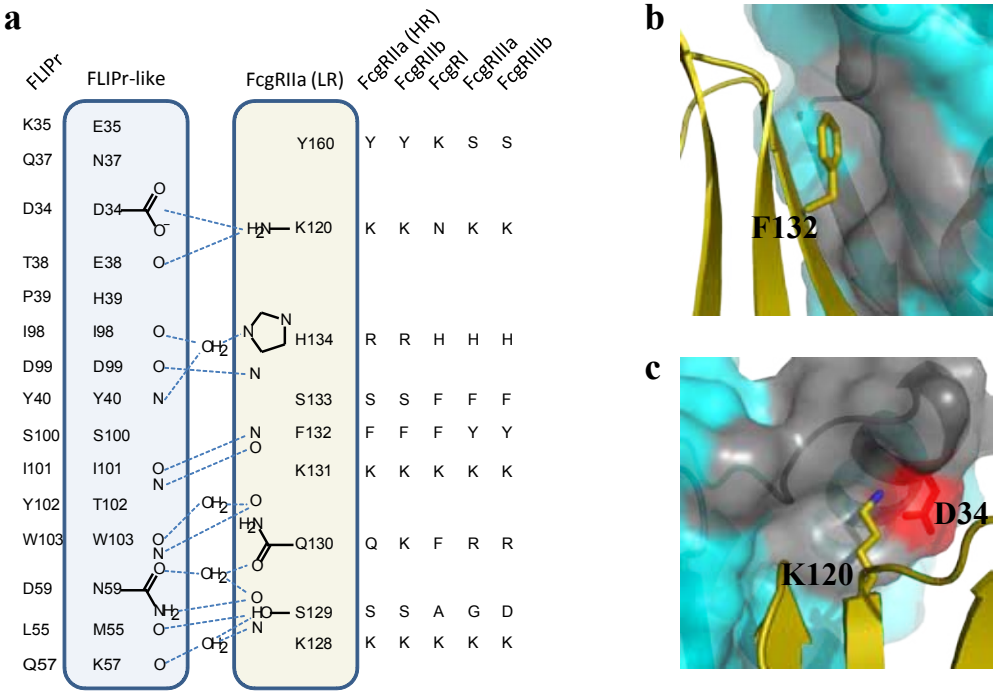

Figure 3 The FcγRIIa-FLIPr-like interface (**a**) Table of interactions between FLIPr-like and FcγRIIa with the corresponding residues in FLIPr and the other FcγRs listedlisted on the left and right respectively (**b**) FcγRIIa residue F132 protrudes into a hydrophobic pocket (colored grey) on the FLIPr-like surface (**c**) FcγRIIa residue K120 sticks into a negatively charged pocket (colored grey) on the FLIPr-like surface with the electronegative patch, caused by FLIPr-like residue D34, in red

The D34A,Y40A and W103A mutations had a much more pronounced effect on FLIPr-like binding. Residue D34 is located in a pocket (**figure 3c**) on the FLIPr-like surface and forms a salt bridge with K120 of FcγRIIa which protrudes into this pocket. Mutation of D34 to alanine reduced the binding affinity almost 10 fold. Y40 and W103 are two of the residues involved in the formation of a hydrophobic pocket on the FLIPr-like surface which accomodates F132 of FcγRIIa (**figure 3b**). The Y40A mutation resulted in a 100 fold decrease in binding affinity while binding of the W103A mutant

Table 1

		Kd (nM)	SEM
FLIPr	FcγRIIa	13.5	4.2
FLIPr-like	FcγRIIa	35.1	7.5
FLIPr-like (8-104)	FcγRIIa	24.0	8.9
His-FLIPr-like (16-104)	FcγRIIa	29.3	10.9
His-FLIPr-like (16-104)-D34A	FcγRIIa	131.8	33.3
His-FLIPr-like (16-104)-H39A	FcγRIIa	10.2	3.6
His-FLIPr-like (16-104)-Y40A	FcγRIIa	1080.0	385
His-FLIPr-like (16-104)-N59A	FcγRIIa	20.6	9.3
His-FLIPr-like (16-104)-W103A	FcγRIIa	9280	6760

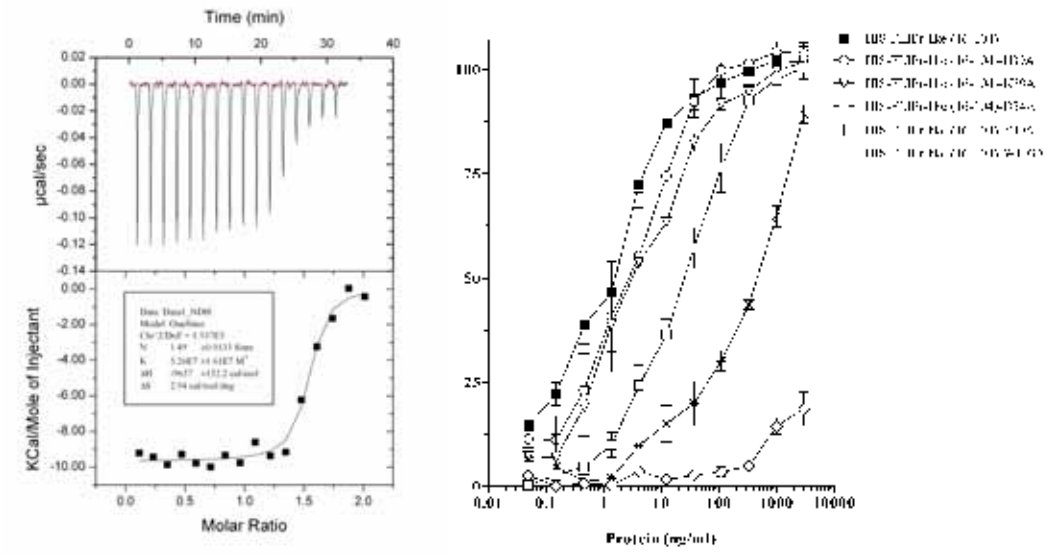

Figure 4 Functional analysis of FLIPr-like mutants. (**a**) representative ITC experiment with FLIPr-like (8-104) in the cell and FcγRIIa in the syringe. (**b**) Phagocytosis inhibition assay using neutrophils pre-incubated with various concentrations of FLIPr-like or mutants before exposure to serum and FITC labelled *S. aureus*. The amount of FITC positive neutrophils were counted using flow cytometry.

was not measurable. The binding data was confirmed by the phagocytosis inhibition assay (**figure 4**) and taken together clearly support the binding interface determined from the crystal structure.

FLIPr-like does not bind to FcγRIIIb

While FLIPr binds to FcγRII only, FLIPr-like binds to all Fcγ receptors with the notable exception of the non-signalling receptor FcγRIIIb. FcγRIIIb differs in only five residues from the extracellular segment of FcγRIIIa, which does bind to FLIPr-like, namely S20R, N66D, D131G, H142Y and V159F. When mapping these residues to FcγRIIa only one overlaps with the FLIPr-like binding site, D131, which corresponds to residue 129 in FcγRIIa (**figure 5a**). An examination of the other amino acids present at this position in the other FcγR's reveals this position is occupied by alanine (FcγRI), serine (FcγRIIa and FcγRIIb) and glycine (FcγRIIIa) (**figure 3a**). To adress the role of this residue in the binding of FLIPr-like we mutated the equivalent position (129) in FcγRIIa to those found in the other FcγR's and studied their binding using ITC (**Table 2**). Indeed, mutating S129 in FcγRIIa to alanine and glycine, as found in FcγRI and FcγRIIIa was well tolerated with only minor effects on the binding affinity. The introduction of an aspartate however resulted in a complete loss of binding to FcγRIIa. The electrostatic potential on the FLIPr-like surface that makes contact with residue 129 of FcγRIIa is neutral to slighly negative (**figure 5b**). The presence of an aspartate at position 129 adds both bulk and a negative charge and would cause an unfavorable interaction combined with electrostatic repulsion, explaining the effect on binding.

Table 2

		Kd (nM)	SEM
FLIPr-like (8-104)	FcγRIIa	33.3	14.1
FLIPr-like (8-104)	FcγRIIa-S129D	16082.5	11290.7
FLIPr-like (8-104)	FcγRIIa-S129A	71.6	3.7
FLIPr-like (8-104)	FcγRIIa-S129G	16.7	4.4

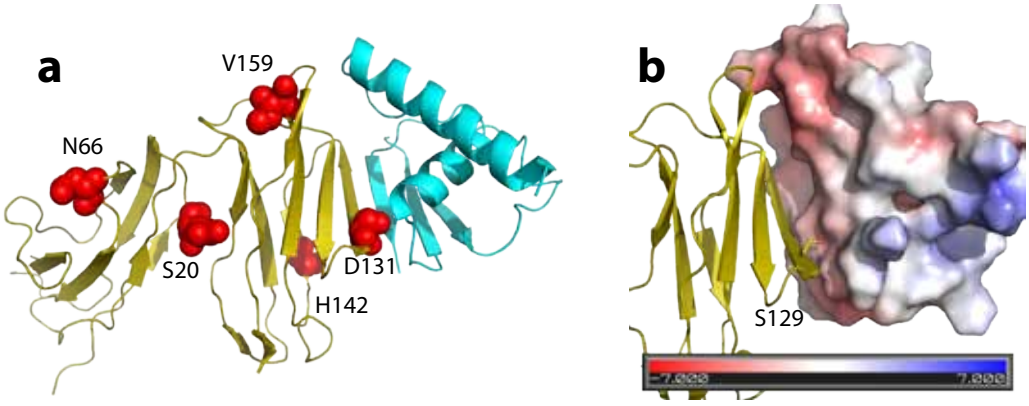

Figure 5 The FcγRIIa-FLIPr-like interface (**a**) differences between FcγIIIb and FcγIIIa mapped in red on the structure of Fcγ RIIa-FLIPr-like (**b**) Electrostatic surface potential of FLIPr-like at the interface where contact is made with residue 129

Inhibition of Fc binding

FLIPr-like binds to FcγRs and thereby interferes with immune complex signaling. This is most likely due to blocking of the IgG Fc binding site on the receptors. The interaction between FcγRs and the IgG Fc region involves both receptor domains. They interact with both Cγ2 domains of the Fc fragment. The Cγ2A domain of the Fc fragment binds to a discontinous region consisting of residues 88-90, 113-117 and 158-161 whereas the bindingsite for the Cγ2B domain comprises residues 119-122 and 129-135 and is solely located on receptor domain 2 (Sondermann et al., 2000). We compared the FLIPr-like-FcγRIIa complex with the structure of soluble FcγRIIIb bound to an IgG1-Fc fragment (pdb code: 1E4K) (Sondermann et al., 2000). Although no structure is available for the complex of FcγRIIa with an Fc fragment this receptor is thought to bind to Fc fragments in the same way as FcγRIIIb. We therefore mapped the FcγRIIIb residues involved in Fc binding onto the corresponding residues in FcγRIIa and compared them with those involved in binding to FLIPr-like. The FLIPr-like binding site comprises residues 120, 128-129, 130-134 and 157-159 and with the exception of residue 157, fully overlaps with the Fc bindingsite on domain 2. Indeed, superimposing FcγRIIIb from the FcγRIIIb-IgG1-Fc fragment complex with FcγRIIa from the FLIPr-like-FcγRIIa complex results in large overlap of FLIPr-like and the Fc fragment and excludes simultaneous binding (**figure 6a,b**).

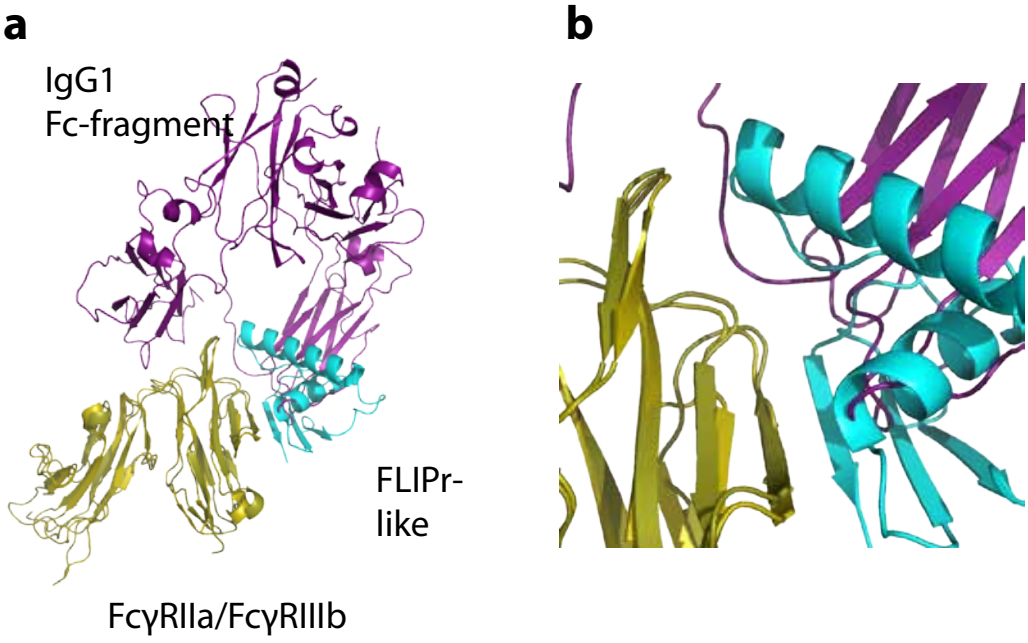

Figure 6 A comparison of the Fcγ RIIa-FLIPr-like structure with that of Fcγ RIIIb-Fc (**a**) superimposing Fcγ RIIa of the Fcγ RIIa-FLIPr-like complex onto Fcγ RIIIb from the Fcγ RIIIb-Fc complex (**b**) closeup of the interface showing the clash between FLIPr-like and the Fc fragment.

Discussion

Upon infection with bacteria the host must respond immediately to keep the infection at bay and exposure of bacteria to plasma typically results in rapid phagocytosis of the invading cells. Phagocytosis relies on direct interaction between phagocytes and opsonins on the bacterial surface. Pathogenic bacteria, like *S. aureus*, secrete a whole range of immune modulating factors that can interfere with these responses (Bestebroer et al., ; Chavakis et al., 2007; Jongerius et al., 2007; Patel et al.). We have recently identified two homologous proteins, FLIPr and FLIPr-like, that bind to Fcγ receptors, thereby potently inhibiting FcγR mediated phagocytosis (Stemerding et al.). Here we present the crystal structure of FLIPr-like bound to the IgG receptor FcγRIIa, the receptor that mediates neutrophil phagocytosis of IgG opsonized S. aureus. The structure reveals that FLIPr-like adopts a fold similar to the β-grasp domain of SSLs and CHIPS. There are however notable differences that shape FLIPr-like to create a unique surface that accommodates FcγR binding. These include a shorter α-2 helix, a shorter loop that connects the α-2 helix with the β-1 strand and a free, exposed β-3 strand. This strand forms the center of the interaction to FcγRIIa and the FLIPr-like binding footprint almost fully overlaps with the IgG binding site, clearly explaining the mechanism of inhibition.

We have also characterized the interaction of FLIPr and FLIPr-like with FcγRIIa using ITC. FLIPr and FLIPr-like both bind with high affinity to FcγRIIa but although the proteins share 73% sequence identity they show a different binding profile to FcγRs. While FLIPr binds only to FcγRIIa and FcγRIIb, FLIPr-like binds to all FcγRs with the exception of FcγRIIIb. We have clarified the lack of binding to FcγRIIIb due to the presence of an aspartate at position 126 (129 in FcγRIIa) but why FLIPr, in contrast to FLIPr-like, does not bind to FcγRI and FcγRIIIa is less obvious. The main difference these receptors share is a phenylalanine at position 130 (S133 in FcγRIIa). The adjacent tyrosine in FLIPr at position 103 (T102 in FLIPr-like) may result in a lack of space at the interface, leading to disruption of binding.

Although FLIPr and FLIPr-like both bind with high affinity to FcγRIIa and have similar values for the ΔG of binding we noticed that the thermodynamic parameters differ strongly. Compared to FLIPr-like, FLIPr binding to FcγRIIa shows a much stronger contribution of enthalpy but this is compensated by a rather unfavorable entropy. This unfavorable entropy of FLIPr binding may be explained by the slightly less hydrophobic surface at the FcγR binding interface. Alternatively, the binding of FLIPr may display a better fit, i.e. surface complimentarily, resulting in a reduction of degrees of freedom. The more favorable enthalpy, typically due to more hydrogen bonds formed, is not directly apparent when comparing the FLIPr sequence in the context of the FLIPr-like-FcγRIIa structure. These effects probably involve more subtle differences that require the structural characterization of the FLIPr-FcγRIIa complex. The FLIPr and FLIPr-like mediated inhibition of phagocytosis provides a strong advantage for invading *S. aureus*. These proteins also block signaling through FPRL1 by the major chemotactic compounds fMLP and phenol soluble modulins (Kretschmer et al., ; Prat et al., 2006; Prat et al., 2009) and the combination of these two functions underscores the potential importance of FLIPr and FLIPr-like in staphylococcal virulence. Our structure reveals that the β-grasp fold forms an extremely versatile platform for protein-protein interactions and not only aids in our understanding of staphylococcal virulence but also forms a starting blue-print for the design of specific inhibitors against the different FcγRs that may have therapeutic potential.

Materials and Methods

Cloning and expression of human FcγRIIa

The extracellular ligand binding domain of the human FcγRIIa (residues 1-174: QAAAP....VQV), with a histidine at position 134, was subcloned into the pRSET vector using the NdeI and EcoRI restriction sites. The protein was expressed in inclusion bodies in *E. coli* BL21(DE3), after induction with 1 mM IPTG at an OD_{660} of 0.6 for 18 h at 37°C. After harvesting the bacteria, the inclusion bodies were isolated using CelLytic B lysis buffer (Sigma) supplemented with EDTA-free protease inhibitor cocktail tablets (Roche Diagnostics), 200 µg/ml lysozyme and 25 µg/ml DNase and RNase, according to the manufacturer's description. Inclusion bodies were then washed with 0.5% LDAO (lauryl dimethyldodecylamine N-oxide; Fluka) using a dounce homogenizer. The inclusion bodies were dissolved to a protein concentration of 10 mg/ml in 6 M guanidine, 50 mM Tris, 100 mM 2-mercaptoethanol, pH 10.0 for 30 min at room temperature. The insoluble matter were removed by centrifugation at 20.000**g*. FcγRIIa was then refolded by rapid dilution of 1 ml protein solution (dropwise with stirring) into 100 ml of a refolding buffer consisting of 0.1 M Tris, 0.5 M L-arginine, 150 mM NaCl, 5 mM reduced glutathione, 0.5 mM oxidized glutathione, 0.1 mM PMSF and 0.02% NaN_3 (pH 10.0) for 24 h at 4°C. Then the pH of the refolding buffer was gradually lowered as follows: pH 9.0 for 16 h, pH 8.8 for 8 h, pH 8.6 for 16 h, pH 8.4 for 8 h, pH 8.2 for 16 h, and pH8.0 for 8 h. The buffer was subsequently exchanged for 0.075 M Tris (pH 8.0) using the Proflux M12 system (Amicon). The protein solution was then applied to a human IgG HiTRAP-NHS column and eluted by 0.1 M glycine, 0.5 M NaCl (pH 2.7). The eluate was immediately neutralized with 1 M Tris/HCl pH 10. The FcγRIIa containing solution was concentrated and applied to a gelfiltration Superdex-75 GL10/300 column equilibrated with 10 mM Hepes, 50 mM NaCl (pH 7.4). The fractions containing FcγRIIa were pooled and concentrated to 14 mg/ml for crystallization studies. Histidine-tagged human FcγRIIa was expressed for mutagenesis studies on amino acid 129, as described above, with a few exceptions. For cloning, a modified pRSET vector, in which the original NdeI-BamH1 part was replaced by a NdeI-BamHI part consisting of only 6 histidine residues, was used. The same extracellular ligand binding domain of the human FcγRIIa as described above was cloned into the BamHI and NotI restriction sites. This resulted in an expressed FcγRIIa, containing an extra MHHHHHHGS at the N-terminus and 3 alanines at the C-terminal end of the protein. For mutagenesis of amino acid 129, overlap extension PCR was used.

Cloning and expression of FLIPr-like

N-terminal histidine tagged FLIPr-like was expressed and isolated from Rosetta Gami(DE3)pLysS *E. coli* as described before. For removal of the histidine tag, the protein was digested with enterokinase, which resulted in an additional cleavage site after amino acid 7 of FLIPr-like. After enterokinase cleavage, the HIS-tag, but also FLIPr-like and FLIPr-like (8-104) were bound to the nickel column at pH 7.8. A phosphate buffer pH 6.0 eluted FLIPr-like (8-104), enabling separation of FLIPr-like and FLIPr-like (8-104). FLIPr-like (8-104) was then concentrated and applied to a gelfiltration Superdex-75 GL10/300 column equilibrated with 10 mM Hepes, 50 mM NaCl (pH 7.4). The fractions containing FLIPr-like (8-104) were pooled and concentrated to 7 mg/ml for crystallization studies. HIS- FLIPr-like (16-104) single mutants were cloned, expressed and isolated from Rosetta Gami(DE3)pLysS E. coli using Nickel chromatography, as described for HIS-tagged FLIPr-like.

Human neutrophil isolation

Fresh whole blood was obtained from healthy volunteers, heparinized and mixed with an equal volume of phosphate-buffered saline (PBS). This was centrifuged through step gradients of Histopaque (ρ=1.077, Sigma, St Louis, MO) and Ficoll-paque (ρ=1.119, Amersham, Chalfont St Giles, UK) and neutrophils were aspirated from the buffy coat between the Ficoll and Histopaque layers. Cells were washed in RPMI-1640 medium, containing 10 mM HEPES, 25 mM glutamine and 0.05% (v/v) human serum albumin (RPMI/0.05% HSA), and resuspended in water. After a 30 s osmotic shock to lyse contaminating red blood cells, 10×PBS was added and the cells were again washed in RPMI/0.05% HSA. Neutrophils were adjusted to 5 × 106 cells/mL in RPMI/0.05% HSA. This procedure typically yielded >97% neutrophils with >95% viability, as determined by trypan blue exclusion. All reagents used in neutrophil isolation were certified endotoxin-free.

Phagocytosis assay

Staphylococcus aureus, strain NCTC 8325, was grown to stationary phase, washed twice in PBS, and labeled with 100 μg/ml fluorescein isothiocyanate (FITC) in sodiumcarbonate buffer, pH 9.6 for 1 h at 37°C with shaking. Cells were washed three times in PBS, adjusted to 5 × 108 CFU/ml in RPMI/0.05% HSA and stored frozen at −20°C. Bacteria were thawed on ice and diluted to 5 × 107 CFU/ml in RPMI/0.05% HSA. Neutrophils (15 μl) 4x106/ml were preincubated with a concentration range of FLIPr-like or mutants (10 μl) for 10 min at 37°C, while shaking. Then 5% pooled human serum (10 μl), heat-inactivated for 30 min at 56°C, was added together with FITC-labeled bacteria (15 μl) 4x107/ml. This reaction mixture was vigorously shaken for 15 min at 37°C. The final bacteria : neutrophil ratio was 10 : 1. Reactions were stopped by addition of 100 μl ice-cold 1% (w/v) paraformaldehyde in PBS. The percentage of neutrophils bearing FITC-labeled bacteria (% phagocytosis) was determined by flow cytometric analysis of 10000 cells with manual gating using a flow cytometer (FACSCalibur, Becton Dickinson, Franklin Lanes, NJ). All experiments were repeated a minimum of three times using the neutrophils of different donors.

Isothermal Titration Calorimetry and Kd determinations

Heats of interaction were measured at 25 ºC with an iTC200 automated system (GE Healthcare – Microcal). The protein and ligands were in phosphate buffered saline. The cell was filled with 200 μL of FLIPr-like or FLIPr-like mutants in concentrations ranging from 5 to 10 μM. The FcγRIIa ligands in a concentration range from 50 to 100 μM were generally injected in 16 steps of 2.5 μL. Experiments were performed in triplicate. Heats of dilution were assayed from endpoint signals after saturation of binding. The corrected data were fitted with a single site binding model with floating values for stoichiometry, binding constant (KA), and enthalpy change (ΔH), using the Microcal – Origin software delivered with the iTC200 system.

Crystallization and structure determination

Purified FLIPr-like (~7 mg/ml) and FcγRIIa (~14 mg/ml), both in 10 mM Hepes pH 7.4, 50 mM NaCl, were mixed 1:1 and used directly for crystallization trials. Initially, rod-like crystals (crystal form 2) were obtained at 18 °C by sitting drop vapour diffusion. Drops consisted of 0.25 ul protein mixed with 0.25 ul resevoir solution (0.9 M ammonium sulphate, 0.1 M lithium sulphate, 0.1 M citric acid

pH 4.0) and the crystals were cryoprotected by adding 2 µl of 2.3 M lithium sulphate, 0.5 M ammonium sulphate and 0.1 M citric acid pH 4.0 directly to the crystallization drop. Crystals were allowed to equillibrate for several minutes before harvesting and flash freezing in liquid N_2. Crystals belonged to spacegroup $P6_1$ and diffracted to 2.6 Å (Table 1) at ESRF beamline ID14-EH4. Phases were obtained by molecular replacement using the program Phaser with the known structure of FcγRIIa (PDB accession code, 1FCG) (Maxwell et al., 1999). These phases were then supplied to ARP/wARP (Langer et al., 2008) which was able to build a poly-glycine model of FLIPr-like. The resulting maps were of excellent quality and allowed for straightforward sequence assignment of FLIPr-like. The model was then improved by itterative modelbuilding and refinement to a final Rwork / Rfree of 19.0% / 22.0% using the programs Coot (Emsley et al.) and Buster (Bricogne et al. 2009) respectively. Another crystal form (crystal form 1) was later obtained at 4 °C by vapour diffusion of hanging drops consisting of 1 ul protein mixed with 1 µl resevoir solution (17% PEG 1500, 0.1 M Hepes pH 7.4). These crystals were cryoprotected by briefly soaking in a drop containing 20% (w/v) PEG 1500, 0.1 M Hepes pH 7.4 and 25% (v/v) glycerol followed by flash freezing in liquid N_2. Crystals diffracted to 1.75 Å (Table 1) at ESRF beamline ID29 and belonged to spacegroup C2. The structure was solved by molecular replacement, again using the known structure of FcγRIIa (PDB accession code, 1FCG) (Maxwell et al., 1999) and the structure of FLIPr-like as obtained in crystal form 2. The structure was refined with Buster (Bricogne et al. 2009) to an Rwork / Rfree of 19.0% / 20.5%.

Table 1 Data collection and refinement statistics

	Crystal 1	Crystal 2
Data collection		
Space group	C2	$P6_1$
Cell dimensions		
a, *b*, *c* (Å)	169.57, 39.72, 46.68	132.79, 132.79, 72.02
α, β, γ (°)	90.00, 101.62, 90.00	90.00, 90.00, 120.00
Resolution (Å)	40.00-1.75 (1.84-1.75)*	50.00-2.6 (2.74-2.60)*
R_{merge}	0.048 (0.548)	0.090 (0.759)
$I / \sigma I$	14.9 (2.4)	15.7 (2.6)
Completeness (%)	99.6 (100)	99.9 (99.9)
Redundancy	4.0 (4.1)	7.4 (7.5)
Refinement		
Resolution (Å)	40-1.75	
No. reflections	30,940	
R_{work} / R_{free}	19.0 / 20.5	
No. atoms	2,187	
Protein	2,057	
Ligand/ion	130	
Water	106	
B-factors		
Protein	34.2	
Ligand/ion	38.1	
Water	39.3	
R.m.s. deviations		
Bond lengths (Å)	0.011	
Bond angles (°)	1.130	

*Values in parentheses are for highest-resolution shell.

References

Al-Shangiti, A.M., Naylor, C.E., Nair, S.P., Briggs, D.C., Henderson, B., and Chain, B.M. (2004). Structural relationships and cellular tropism of staphylococcal superantigen-like proteins. Infect Immun 72, 4261-4270.
Anderson, C.L., Shen, L., Eicher, D.M., Wewers, M.D., and Gill, J.K. (1990). Phagocytosis mediated by three distinct Fc gamma receptor classes on human leukocytes. J Exp Med 171, 1333-1345.
Arcus, V.L., Langley, R., Proft, T., Fraser, J.D., and Baker, E.N. (2002). The Three-dimensional structure of a superantigen-like protein, SET3, from a pathogenicity island of the Staphylococcus aureus genome. J Biol Chem 277, 32274-32281.
Bestebroer, J., Aerts, P.C., Rooijakkers, S.H., Pandey, M.K., Kohl, J., van Strijp, J.A., and de Haas, C.J. Functional basis for complement evasion by staphylococcal superantigen-like 7. Cell Microbiol.
Chavakis, T., Preissner, K.T., and Herrmann, M. (2007). The anti-inflammatory activities of Staphylococcus aureus. Trends Immunol 28, 408-418.
Chung, M.C., Wines, B.D., Baker, H., Langley, R.J., Baker, E.N., and Fraser, J.D. (2007). The crystal structure of staphylococcal superantigen-like protein 11 in complex with sialyl Lewis X reveals the mechanism for cell binding and immune inhibition. Mol Microbiol 66, 1342-1355.
Emsley, P., Lohkamp, B., Scott, W.G., and Cowtan, K. Features and development of Coot. Acta Crystallogr D Biol Crystallogr 66, 486-501.
Haas, P.J., de Haas, C.J., Poppelier, M.J., van Kessel, K.P., van Strijp, J.A., Dijkstra, K., Scheek, R.M., Fan, H., Kruijtzer, J.A., Liskamp, R.M., et al. (2005). The structure of the C5a receptor-blocking domain of chemotaxis inhibitory protein of Staphylococcus aureus is related to a group of immune evasive molecules. J Mol Biol 353, 859-872.
Holm, L., and Rosenstrom, P. Dali server: conservation mapping in 3D. Nucleic Acids Res 38 Suppl, W545-549.
Jongerius, I., Kohl, J., Pandey, M.K., Ruyken, M., van Kessel, K.P., van Strijp, J.A., and Rooijakkers, S.H. (2007). Staphylococcal complement evasion by various convertase-blocking molecules. J Exp Med 204, 2461-2471.
Kretschmer, D., Gleske, A.K., Rautenberg, M., Wang, R., Koberle, M., Bohn, E., Schoneberg, T., Rabiet, M.J., Boulay, F., Klebanoff, S.J., et al. Human formyl peptide receptor 2 senses highly pathogenic Staphylococcus aureus. Cell Host Microbe 7, 463-473.
Langer, G., Cohen, S.X., Lamzin, V.S., and Perrakis, A. (2008). Automated macromolecular model building for X-ray crystallography using ARP/wARP version 7. Nat Protoc 3, 1171-1179.
Lowy, F.D. (1998). Staphylococcus aureus infections. N Engl J Med 339, 520-532.
Maxwell, K.F., Powell, M.S., Hulett, M.D., Barton, P.A., McKenzie, I.F., Garrett, T.P., and Hogarth, P.M. (1999). Crystal structure of the human leukocyte Fc receptor, Fc gammaRIIa. Nat Struct Biol 6, 437-442.
Moza, B., Varma, A.K., Buonpane, R.A., Zhu, P., Herfst, C.A., Nicholson, M.J., Wilbuer, A.K., Seth, N.P., Wucherpfennig, K.W., McCormick, J.K., et al. (2007). Structural basis of T-cell specificity and activation by the bacterial superantigen TSST-1. EMBO J 26, 1187-1197.
Nakamura, A., Kubo, T., and Takai, T. (2008). Fc receptor targeting in the treatment of allergy, autoimmune diseases and cancer. Adv Exp Med Biol 640, 220-233.
Patel, D., Wines, B.D., Langley, R.J., and Fraser, J.D. Specificity of staphylococcal superantigen-like protein 10 toward the human IgG1 Fc domain. J Immunol 184, 6283-6292.

Prat, C., Bestebroer, J., de Haas, C.J., van Strijp, J.A., and van Kessel, K.P. (2006). A new staphylococcal anti-inflammatory protein that antagonizes the formyl peptide receptor-like 1. J Immunol 177, 8017-8026.
Prat, C., Haas, P.J., Bestebroer, J., de Haas, C.J., van Strijp, J.A., and van Kessel, K.P. (2009). A homolog of formyl peptide receptor-like 1 (FPRL1) inhibitor from Staphylococcus aureus (FPRL1 inhibitory protein) that inhibits FPRL1 and FPR. J Immunol 183, 6569-6578.
Pricop, L., and Salmon, J.E. (2002). Redox regulation of Fcgamma receptor-mediated phagocytosis: implications for host defense and tissue injury. Antioxid Redox Signal 4, 85-95.
Rooijakkers, S.H., van Wamel, W.J., Ruyken, M., van Kessel, K.P., and van Strijp, J.A. (2005). Anti-opsonic properties of staphylokinase. Microbes Infect 7, 476-484.
Salmon, J.E., Millard, S.S., Brogle, N.L., and Kimberly, R.P. (1995). Fc gamma receptor IIIb enhances Fc gamma receptor IIa function in an oxidant-dependent and allele-sensitive manner. J Clin Invest 95, 2877-2885.
Sondermann, P., Huber, R., Oosthuizen, V., and Jacob, U. (2000). The 3.2-A crystal structure of the human IgG1 Fc fragment-Fc gammaRIII complex. Nature 406, 267-273.
Takai, T. (2002). Roles of Fc receptors in autoimmunity. Nat Rev Immunol 2, 580-592.

Chapter 5

General Discussion

Michael A. Hadders

The human body is continuously at battle with the microorganisms encountered in our daily environment. The responses to such encounters have been shaped by millions of years of co-evolution, both from the host as the microbial point of view. The human immune system is elaborate and seemingly redundant with numerous mechanisms to fight infections. And yet for almost every step, pathogens have acquired the capabilities to block it (chapter 4). Intriguingly, as we have shown in Chapter 2 and 3, the host and bacterial pathogens even make use of architecturally similar structures (yet disparate at the sequence level) as a means to the same end, i.e. membrane attack through the formation of lytic pores.

The complement system

In humans, invasion of microorganisms triggers a rapid immune response. Amongst the first barriers the pathogen encounters is the complement system. This includes over thirty plasma and membrane associated proteins. Several microbial cues can activate the complement system which in turn results in the start of an intricate proteolytic cascade that activates various effector mechanisms. This response is rapid and highly localized to pathogenic surfaces, typically allowing the efficient killing and clearance of invading microorganisms. The system is also tightly regulated to prevent damage of surrounding host tissue. However, certain disease states can shift this balance and ultimately lead to uncontrolled complement activation that harms the host.

The membrane attack complex

One of the major effectors of the complement system is the membrane attack complex (MAC). The MAC consists of five soluble plasma proteins named C5 to C9 (Esser, 1994; Muller-Eberhard, 1986). These proteins assemble together to form large lytic pores that can kill Gram-negative bacteria but also host cells in cases of aberrant complement regulation. The formation of the MAC is initiated when the peptide bond between Arg751 and Leu752 of C5 is cleaved. Since C5 is the final substrate of the proteolytic complement cascade, MAC formation is also referred to as the terminal pathway of complement. The cleavage of C5 has two consequences: first, it results in the release of C5a, a small anaphylotoxin that is chemotactic for neutrophils and induces a powerful pro-inflammatory response. And second, it generates C5b which initiates formation of the MAC on the target surface.

C5 belongs to the alpha 2-macroglobulin (α_2M) family of proteins and its activation to C5b is thought to be accompanied by large conformational changes that create new binding sites for the MACPF proteins C6 to C9 (Cooper and Muller-Eberhard, 1970). These proteins share a similar modular architecture and, starting with C6, they bind in an obligate sequential manner with each protein adding additional functionality. The initial binding of C6 stabilizes a metastable conformation of C5b and, together with C5b, likely plays a role in the formation of a hybrid binding site for C7 (Podack et al., 1978a; Podack et al., 1978b). The binding of C7 induces conformational changes that expose a lipophilic binding site. This site is located in C7 and results in docking of C5b67 on membrane surfaces (Preissner et al., 1985). The C5b67 complex docked on the membrane then forms a receptor for C8, a heterotrimer composed of two non-covalently associated MACPF chains called C8α and C8β and a lipocalin called C8γ that is attached to C8α through a disulfide bond (Sodetz, 1989). C8 binding to C5b67 is mediated by its β-chain and involves the C8β-MACPF domain which is thought to interact with C5b and C7 (Monahan and Sodetz, 1981; Monahan et al., 1983; Stewart et al., 1987). The binding of C8 to C5b67 results in membrane insertion of a segment of C8α located in the MACPF domain.

While this membrane insertion results in mild hemolysis when C5b8 is assembled on erythrocytes it is not sufficient for bactericidal activity when assembled on bacteria (Hu et al., 1981; Ishida et al., 1982; Monahan and Sodetz, 1980; Steckel et al., 1983; Tschopp and Podack, 1981). This requires the "killer" molecule of the MAC, C9 (Joiner et al., 1985). Membrane bound (inserted) C5b8 forms a binding platform for C9. The binding site is located in the MACPF domain of C8α and induces membrane insertion and oligomerization of C9. This results in bactericidal pores that contain up to 18 copies of C9 and have an internal diameter of 100Å (Tschopp et al., 1984; Tschopp et al., 1985).

While several decades of work have provided us with a reasonably detailed picture of the biochemistry regarding the assembly of the MAC, the structural data is limited to negative stain electron microscopy images. In this thesis we describe the first high resolution crystal structures of two MAC components: the MACPF domain of C8α and the C5b6 complex. These structures allow us for the first time to discuss the wealth of biochemical data in the context of structures.

Conformational changes and binding sites in C5

Large conformational changes are a common theme in the activation of proteins belonging to the α_2M family (Armstrong and Quigley, 1999; Dodds and Law, 1998). These changes have two functions: 1) to expose the reactive thioester and 2) to expose previously cryptic binding sites. Since C5 has no thioester, the putative changes that occur upon activation to C5b likely liberate the binding sites for downstream MAC proteins, and so initiate MAC formation. Recently, crystal structures have been solved for several α_2M family members including C3, the insect thioester containing protein 1 (TEP1) and C5 (Baxter et al., 2007; Fredslund et al., 2006; Fredslund et al., 2008; Janssen et al., 2005). These structures reveal a common domain architecture that include 8 macroglobulin domains (MG), a 'complement C1r/C1s, UEGF, BMP1' domain (CUB), a thioester containing domain (TED), a C-terminal C345C domain, an anaphylotoxin domain, and an extended linker region. The domains are arranged in two chains (α and β) since the proteins are proteolytically processed prior to secretion. The structures of the C3 activation and degradation products C3b, C3c and C3d have also been solved and reveal the domain rearrangements that take place upon activation of these proteins (Janssen et al., 2006; Janssen et al., 2005; Nagar et al., 1998; Nishida et al., 2006; Wiesmann et al., 2006). In C3b this involves a displacement of MG8 and a swinging down and out of the TED and the attached CUB and MG7 domains. As a consequence the thioester is translocated over a distance of more than 85Å. These changes are initiated upon proteolytic removal of C3a from the N-terminus of the α-chain. The newly formed N-terminus (α'NT) is subsequently translocated through the ring formed by MG1-4 of the β-chain, ending on the opposite side of the protein. The α'NT is critical for the interaction of C3b with many of its binding partners (Rooijakkers et al., 2009; Wu et al., 2009).

The structure of C5b6 reveals that many of the domain rearrangements previously observed in the C3 to C3b transition are similar in the conversion of C5 to C5b. This includes the swinging down of the MG7 and CUB domains and the translocation of the α'NT through the ring formed by the β-chain (chapter 3). There are major differences however in the position of the TED and MG8 domain. In C3b the TED swings down over a distance of 80 Å to align next to the MG1 domain at the "bottom" of C3b (Janssen et al., 2006). In C5b the domain is stalled at an intermediate position at the height of the MG2 domain having translocated only 60 Å. The purpose of the domain rearrangements that occur upon C5 activation is to shape the C5b surface to create a binding site for downstream MACPF members. This is precisely what is observed for the TED, which in its new position

forms the major interaction site for C6 in C5b. This conformation also provides an explanation for the labile conformation of C5b. The half-life of newly formed C5b with respect to the C6 binding capability, is only ~2 minutes (Cooper and Muller-Eberhard, 1970). After that, C5b decays irreversibly to an inactive conformation that is unable to bind C6. The observed transitory conformation of the TED in C5b6 is largely stabilized by C6 and has only one minor contact with MG2 in C5b. In the absence of C6 this interaction is most likely not enough to stabilize the TED which would then shift down to adopt a C3b-like conformation that would clash with C6 in its observed position.

The activation of C3 to C3b is mediated by the proteolytic removal of C3a. This results in a newly formed N-terminus for the α-chain called the α'NT. The conformational changes that accompany C3 activation result in the relocation of the α'NT to the opposite side of the protein by passing through the β-ring where it becomes associated with the MG7 domain (Janssen et al., 2006). The region contains several highly conserved acidic residues which are important for the interaction with several proteins including complement receptors CR1 and 3, factor H, and factor B (Janssen et al., 2006; Wu et al., 2009). In C5b however, the α'NT does not seem to be involved in binding, at least not in the case of C6 (chapter 3). Accordingly, the corresponding residues in C5b (752-769) show poor sequence conservation and are not visible in the C5b6 structure, most likely due to disorder. We cannot however rule out a potential role in the interaction with the downstream MACPF members C7 and C8 in view of the fact that both are known to contain a C5b binding site (discussed below). Instead the major C6 binding site in C5b is formed by the TED and CUB domains. The CCP1 domain of C6 is wedged in between the two, putatively stabilizing the observed conformation of TED. While the surface of TED that interacts with CCP1 is exposed in C5 the site in the CUB domain is hidden at an interface formed with the TED. The observed domain rearrangements are thus required to liberate the observed binding site.

When compared to C3b the MG8 domain of C5b is positioned differently. Instead of swiveling back to tightly associate with MG3 and MG7 it sticks out to largely occupy the space left by C5a. This results in a unique surface that may be important for binding to other proteins. However, MG8 does not interact with C6. Perhaps the unique position of MG8 observed in C5b reflects a specific role in the binding of the downstream MACPF proteins C7 or C8. Both C7 and C8 have been shown to interact with C5b in the C5b7 and C5b8 complexes respectively. In C7 the major binding site for C5b6 has been shown to reside in the C-terminal region consisting of two FIMAC and two CCP domains (DiScipio et al., 1988). The FIMAC domains interact with the C345C domain of C5b (Thai and Ogata, 2004, 2005). Accordingly, cross-linking experiments have shown that C7 mainly interacts with the α chain of C5b (DiScipio, 1992). The C345C domain is flexibly attached to MG8 making it difficult to predict its orientation in the C5b7 complex and thus the orientation of the CCP. Since the cross-linking data suggests a major role for the α-chain in binding to C7, the groove between the adjacent MG8 and CUB domains and CCP1 of C6 may be an attractive candidate. Placement of C7 on the other sides of C5b would place the C7 core in close proximity of the β-chain of C5b which is not supported by the cross-linking experiments. The suggested site would also put the C7 core with the central MACPF domain next to that of C6, perhaps allowing them to pair up strand to strand as proposed for C9 oligomerization (discussed below). C8 has been shown to bind both C5 and the active conformation of C5b (as in C5b6) but not the inactive form that is unable to bind to C6. In C8 the C5/C5b binding site is located in the β-chain (Monahan and Sodetz, 1980, 1981; Monahan et al., 1983). More recently this site was mapped to the MACPF domain which also contains the primary binding site for the α-chain of C8 (Bran-

nen and Sodetz, 2007). Cross-linking experiments using only C8β showed the major sites of interaction were on C5b and to a lesser extent C6. When C8 was used with the cross-linking agent present solely on the β-subunit, interactions could be seen with C5b, C6 and C7 (Stewart et al., 1987). These studies however did not discriminate between binding to the α- and/or the β-chain of C5b. The observation that C8 has an affinity for C5 and active C5b, but not decayed C5b is also difficult to explain. If we assume inactive C5b adopts a conformation similar to C3b, the major difference would be the position of the TED. However, the position of the TED is also one of the major differences between C5 and active C5b making it unlikely the TED forms the major binding determinant for C8. The interaction between C8 and C5 was determined at sub-physiological ionic strength and increasing the salt concentration strongly reduced the observed binding (Stewart et al., 1987). Furthermore, using a different assay at physiological ionic strength, DiScipio was not able to detect C8 binding to C5 (DiScipio, 1992). Taken together, these data suggest that the observed binding of C8 to C5 is most likely not the same as the binding of C8 to active C5b. Clearly, the newly available structural data raise many questions. Further biochemical experiments guided by the C5b6 structure should give a more precise picture of the C7 and C8 binding sites.

The thioester, a structural role?

One of the hallmark features of the α_2M family of proteins is the presence of a reactive thioester which is used to covalently link to target surfaces (Dodds and Law, 1998). The structures of C3 and TEP1 have revealed that the thioester, which is located in the TED, is buried in a hydrophobic interface formed together with MG8 (Baxter et al., 2007; Fredslund et al., 2006; Janssen et al., 2005). This interface protects the thioester from premature hydrolysis and is highly conserved between α_2M family members. C5 does not contain the thioester that otherwise defines this family of proteins. Accordingly, the highly conserved residues forming the hydrophobic patch that protects the thioester are not conserved in C5, instead being replaced by more hydrophilic residues. Interestingly, the structure of C5 revealed that despite this lack of sequence conservation the interface remains structurally similar (Fredslund et al., 2008). This suggests the thioester is not necessary for the conformation of α_2M members. In the C3 to C3b transition, removal of C3a results in the breaking of the MG8-TED interface. This exposes the thioester region to the solvent but also results in a conformational change in the N-terminal region of TED. As a consequence the loop consisting of residues 1102-1117 rearranges to bring the catalytic His1104 closer to the thioester to form a highly reactive acyl-imidazole intermediate that can then react with surrounding nucleophiles. In the structure of C5b6 (**chapter 3**) we observe the same rearrangements in the N-terminal region of TED, again despite the absence of the thioester. The loop that contains the actual residues corresponding to those that form the thioester is however disordered as is the activation loop that contains the catalytic His1104 in C3 (Pro1126 in C5). This data suggests that in α_2M members the thioester does not determine the global domain arrangement or rearrangements. This fits with the observation that C3 mutants that are unable to form a thioester retain C3 like properties i.e. the mutants can act as substrates for classical pathway convertases (Isaac et al., 1998; Isaac and Isenman, 1992). This is also seen for bovine α_2M and ovomacroglobulin (Dangott et al., 1983; Feldman and Pizzo, 1984). Conversely, C4 that contains mutations that preclude the formation of the thioester do not retain a native C4-like conformation and are no longer susceptible to cleavage by C1s (Isaac et al., 1998). This was also observed for two mutants of human α_2M, also unable to form a thioester (Gettins et al., 1994; Van Rompaey et al., 1995). Taken together the data suggest that the thioester does not determine the native conformation of α_2M members but may play a role in stabilization of the pro-

teins. In some members the native conformation is inherently more stable allowing them to tolerate the absence of the thioester. The ultimate trigger for activation is however peptide bond cleavage, i.e. the removal of the anaphylotoxins in C3, C4 and C5 or the cleavage of the bait region in α_2M. Summarizing, C5 makes use of the same global domain rearrangements observed in homologous C3 and most likely in other α_2M members. It differs though in the details like the conformation of the "active" state of C5b and the binding sites used to interact with downstream MACPF members, at least in the case of C6. These differences cannot be attributed to the absence of the thioester as even within the TED, many of the observed conformational changes are similar to those in C3b.

The structure of the MACPF domain

The critical effectors of the MAC are the MACPF proteins C6, C7, C8 and C9. It is the α-chain of C8 that initially penetrates the membrane and C9 that forms the ultimate cytolytic pore. In both C8α and C9 the segments that are important for membrane insertion have been mapped to the central MACPF domain. Despite the functional importance of the MACPF domains it wasn't until 2006 the recombinant expression of this domain was reported (Slade et al., 2006). The paper reported on the expression of the C8α MACPF domain and showed for the first time these domains actually form independently folded structural entities. This work was followed shortly thereafter by a report describing the recombinant production of the C8β MACPF domain (Brannen and Sodetz, 2007). Together, the work reveals the presence of a total of 6 protein interaction sites in the two domains. The C8β MACPF domain mediates the binding to the C5b7 complex and to C8α while the MACPF domain of C8α, next to inserting into the membrane, binds to C8β, C8γ, C9 and CD59. Importantly, both the C8α- and the C8β MACPF domains can function independently, in the absence of their N- and C-terminal ancillary domains, to form a hemolytic C5b9 complex. These studies have paved the way for the first structure determination of a MACPF domain, that of C8α.

The structure of the C8α MACPF domain (**chapter 2**) has revealed the MACPF domain structurally resembles the pore-forming domain of cholesterol dependent cytolysins (CDCs) (Hadders et al., 2007; Rosado et al., 2007; Slade et al., 2008). The proteins lack sequence identity. However, the common function of cytolytic pore formation provides a framework for the understanding of MACPF function. CDCs consist of four domains referred to as d1 to d4. The d4 domain mediates the initial membrane attachment while d2 forms a linker to domains d1 and d3. These domains (d1 and d3) form the structural units that contains the membrane inserting segments and form the actual pore. This is also the part of the protein which resembles the MACPF domain. The heart of the d1/d3 segment consists of a kinked four-stranded β-sheet. Two helical loops protrude from the "bottom" of the outer strands of this sheet and point upwards, one loop located on each side of the sheet.

The biochemical and structural details of how CDCs transform from their secreted soluble state into a membrane inserted pore have been thoroughly studied. The binding to cholesterol containing membranes causes a conformational change that exposes the edge of the previously hidden outer strand of the central β-sheet (Heuck et al., 2000; Ramachandran et al., 2002; Ramachandran et al., 2004). This permits the alignment of the outer strands with neighboring CDCs, resulting in oligomerization and ultimately the formation of a large prepore (Heuck et al., 2003; Shepard et al., 2000). The two helical loops then undergo a substantial structural rearrangement, fully extending and moving down toward the membrane to form two transmembrane β-hairpins (TMH1 and TMH2) (Ramachandran et al., 2005; Shatursky et al., 1999; Shepard et al., 1998; Shepard et al., 2000). This rearrangement results

in a vertical collapse of the pore and the concerted penetration of the membrane by the TMHs (Czajkowsky et al., 2004). These membrane inserting regions do not contain large stretches of hydrophobic amino acids. Instead the TMHs are amphipathic with alternating polar and apolar residues. When the TMHs form they align in register, with the hydrophilic residues facing the interior of the pore and the hydrophobic residues pointing towards the membrane. Only then does the prepore become sufficiently hydrophobic to penetrate the membrane and form a large transmembrane β-barrel.

The TMH regions

The structure of the C8α-MACPF domain has revealed a striking similarity to the d1 and d3 domains of CDCs suggesting a similar mechanism of action. While there are marked differences in topology for the upper half of the domain, the MACPF domain shares with the CDCs a similar central kinked β-sheet, including the two protruding loops that form the membrane inserting TMHs in CDCs. These loops in MACPF domains differ however and are roughly twice as long with the central segment at the end already forming a β-hairpin. The CDC model of pore formation implies the full unfolding of the these loops to form extended β-hairpins that partake in the formation of a large β-barrel pore. The fact that these regions are twice as long in MACPF proteins, including C9, fits well with the observed height of the MAC in electron micrographs (DiScipio and Hugli, 1985; Tschopp, 1984b). Moreover, upon oligomerization of C9 an increase in the amount of β-sheet is observed which correlates with the formation of a β-barrel pore (Tschopp et al., 1982).

Sequence analysis of the central segments of the loop region in the different MACPF members (the region that forms the putative β-hairpin and which we will now refer to as TMHs) suggests a functional role in C8α and C9. In C8α the β-hairpin regions are largely hydrophobic corresponding with the fact that C8α is the first protein in the MAC to insert into the membrane while in C9 they display a strong consensus of alternating hydrophobic and hydrophilic residues which fits with the role of C9 as the pore forming protein of the MAC. In contrast to the CDCs, the presence of limiting amounts of C9 results in the formation of incomplete pores. Pores containing as little as three molecules of C9 for every one C5b8 complex already display full hemolytic and bactericidal activity. Moreover, when C9 is added to C5b8 on membranes at 0°C the binding is reversible showing that pore formation by C9 is a gradual process in contrast to CDCs which first need to form an oligomeric prepore before becoming sufficiently hydrophobic to insert into the membrane in a single orchestrated punch. During MAC formation, C8α instead takes up this role in mediating the initial membrane perturbation which then facilitates the insertion and polymerization of C9. The CDC model of TMH unfolding also forms a clear explanation for the CD59 mediated protection of host cells. The sites in C8α and C9 that interact with CD59 have been mapped to the TMH2 region of the respective MACPF domains (Farkas et al., 2002; Huang et al., 2006; Husler et al., 1995; Lehto and Meri, 1993; Lockert et al., 1995; Tomlinson et al., 1995). A simple model would suggest that C8 binding to membrane attached C5b7 induces the unfolding of C8α TMH1 and 2. However, upon unfolding, the TMH2 region would be "caught in the act" by CD59 which would prevent both membrane pertubation and the formation of the C9 binding site. Similarly, the binding of C9 to membrane inserted C5b8 would induce the unfolding of the TMH regions of C9 of which TMH2 would be caught thereby inhibiting membrane insertion and the binding of subsequent C9 molecules.

The functional role of the TMH regions in C6, C7 and C8β is less clear, at least from a sequence perspective. While the TMH regions in all MACPF domains display very low sequence con-

servation there are a couple of exceptions including some highly conserved residues and motifs. In C8β the TMH segments are largely hydrophobic and include several highly conserved residues. C8β functions mainly as an adaptor that links the initiating C5b7 complex to C9 (through C8α) and while the binding sites for C5b7 and C8α are both located in the MACPF domain the contribution of the TMH regions is unknown (Brannen and Sodetz, 2007). The presence of a few conserved residues could however point at a putative role in protein-protein interactions.

The binding of C7 to C5b6 results in a clear phenotype, i.e. the binding to a membrane surface. The C5b7 complex displays a strong preference for binding to membranes containing anionic lipids. Analogous to C9, the formation of the membrane binding site in C7 is accompanied by an increase in the amount of β-sheet (DiScipio et al., 1988; Preissner et al., 1985). This would suggest a mechanism similar to that proposed for C8α and C9 in which the TMH regions unfold to form extended β-hairpins. Intriguingly, the TMH regions in C7 are much shorter compared to the other MACPF members. Both TMH1 and TMH2 contain a central very hydrophobic cluster of 2-4 residues. In TMH1 the hydrophobic segment is flanked by positively charged residues which in turn are flanked by a stretch of serine residues. TMH2 has similar characteristics although it is less positively charged and the stretches of serines are shorter. This suggests that C7 functions in a manner similar to CDCs (and proposed for C8α and C9). Binding to C5b6 would then induce the unfolding of TMH1 and 2, perhaps guided by the attraction of the positively charged residues towards the negative charges on the membrane surface. Due to their shorter length and sequence characteristics, they would not penetrate the membrane with the exception of the central hydrophobic cluster located at the tip of the β-hairpins. Accordingly, membrane docking of C5b7 does not lead to significant membrane perturbation as noted by the lack of hemolysis of erythrocytes and the lack of labeling using membrane restricted probes (Amiguet et al., 1985; DiScipio et al., 1988; Esser et al., 1979; Hu et al., 1981; Ishida et al., 1982; Podack et al., 1981; Steckel et al., 1983).

Based on the C5b6 structure C6 seems to function in stabilizing the labile conformation of C5b. This does not involve the central MACPF domain but instead uses the C-terminal CCP domains and the TSP3-CCP1 linker. However, the MACPF domain may be involved in the binding of C7 or the other downstream MACPF proteins. The structure revealed the TMH regions are largely disordered but the fact that the initial helical segments protruding from the central two strands are clearly visible and are facing “up” strongly suggests the TMHs do not form extended “downward” facing β-hairpins. Analysis of the TMH regions shows that although their length is comparable to the rest of the MACPF members they share sequence similarity with C7, i.e. a central cluster of 2-4 hydrophobic residues surrounded by several positively charged residues. Perhaps C5b6 also plays a minor role in the initial attachment to the membrane surface. The full unfolding and extension of the TMH regions as observed for the CDCs may not be necessary. When mediating only superficial membrane attachment the TMH regions may only partially unfold and associate with the membrane in a monotopic fashion.

C9, perforin and the prepore

CDCs separate the different functional steps of pore formation like membrane attachment, membrane penetration and oligomerization into different domains of a single protein. During the assembly of the MAC the different functional steps are divided over different proteins. This adds a regulatory layer, most likely to protect host tissue by localizing the cytolytic effect on target surfaces on which complement is actually activated. However, C9 can also oligomerize in the absence

of the catalyzing C5b8 (Tschopp, 1984a; Tschopp et al., 1984). This results in the formation of ring-like structures similar to the MAC. These pores are not bactericidal though which is most likely due to futile oligomerization in solution due to the absence of a membrane targeting moiety. The pore forming protein perforin also contains a MACPF domain. Perforin is secreted by natural killer and cytotoxic T-cells and facilitates the membrane translocation of granzymes into transformed and virally infected target cells where they induce apoptosis (Voskoboinik et al., 2006). Interestingly, perforin functions alone and forms pores without the help of accessory proteins. In contrast to C9, perforin has a C-terminal C2-domain that targets the protein to membranes in a Ca^{2+} dependent manner (Voskoboinik et al., 2005). This suggests perforin perhaps functions more like CDCs and forms an initial prepore before punching through the membrane in one concerted action. This also implies perforin function must be regulated since uncontrolled exposure to perforin leads to necrotic cell death. Accordingly, perforin is stored in secretory granules prior to secretion. These granules are maintained at a low pH that prevents Ca^{2+} binding and hence membrane association and perforation. The subsequent release is very localized, taking place only at the immunological synapse formed with a target cell. Combined, these two mechanisms contribute to regulate perforin pore formation and the associated, potentially toxic effects.

The domain architecture of MACPF proteins

The structure of C5b6 has revealed the overall architecture of a full-length MACPF member and how it associates with one of its binding partners. Interestingly, it shows the functional association with C5b is mainly mediated by the C-terminal CCP domains and the TSP3-CCP1 linker which are flexibly associated with the core formed by the TSP2, LDLr, MACPF, EGF and TSP3 domains. In C7, it is the C-terminal FIMAC domains that play a crucial role in the interaction with C5b6 and, as previously noted, it is unclear if the MACPF domains (or the TMH regions therein) in C6 and C7 have any specific role apart from functioning as a scaffold for the functional C-terminal regions. In contrast, in C8 (both the α- and the β-chain) the MACPF domain is sufficient in mediating all necessary interactions and the proteins do not require their adjacent ancillary domains. The same is observed for perforin, where the C-terminal C2 domain is only necesarry for membrane binding but the pore forming and membrane inserting activity is located in the MACPF domain (Baran et al., 2009; Voskoboinik et al., 2005). These data suggest that from a evolutionary point of view a C9-like protein was most likely the first to appear. Selection would have been on the basis of functional pore formation. Later, gene duplication events might have added additional layers of regulation. Initially, function would have been retained in the MACPF domain as seen in C8. Later however, as both sequences and functions (i.e. regulation versus pore formation) diverged, the adjacent domains would gain in functional importance as observed for C6 and C7. The presence of the central MACPF domain in these proteins may still be important though in mediating self association as discussed below.

Implications of the MACPF structure on MAC assembly

The structural similarity between MACPF domain and CDCs has led to the proposal that C9 of the MAC forms pores through a mechanism of strand to strand alignment. This implies that the MACPF domain of C9 has two self association sites, one on each side of the flat face of the MACPF domain with each one being formed by one edge of the central β-sheet. In perforin this was confirmed and extended to the helical segments in the top of the MACPF domain. Specifically, these regions, located on each side of the flat face of the MACPF domain, contain a residue of

opposite charge that is critical for self interaction upon oligomerization (Baran et al., 2009). However, while these residues are highly conserved in perforin a similar motif is absent in C9. The CDC model of pore formation would also imply both edges of the central sheet of the MACPF domain to be exposed. The domain architecture of the C6 core now allows the construction of a model of C9.The adjacent domains are situated around two sides of the MACPF domain but importantly, not on the sides that form the flat faces that in CDCs and perforin self associate.

The fact that C6-C8 also have a central MACPF domain suggests that the protein-protein interactions between the various MAC components might also be mediated to an extent by MACPF-MACPF interactions analogous to the MACPF mediated oligomerization of C9. For example, it is known that the C9 binding site in C8α is located in the MACPF domain. C8α mediates the initial membrane perturbation that allows C9 binding and membrane insertion and it is tempting to envision a model in which C9 binds to C8α in a similar fashion as hypothesized for C9 self association. In theory this model of MACPF mediated self association could be extended for the other MACPF members of the MAC. An unpublished structure of C8 shows that the α and β subunit indeed associate in such a manner (J. Sodetz, personal communication) although the MACPF domains don't align perfectly. The model does have certain consequences though and would imply that C8α forms part of the actual pore. Although it is known that C8α inserts into the membrane like C9 there is no evidence to suggest this actually happens. Moreover, strand to strand association of C8α with C9 would effectively block one of the self association sites in C9. This would imply uni-directional growth of the pore which actually fits with the fact that CD59 binding to TMH2 is sufficient to block both binding of C9 to C8α as well as C9 self association. The model would however pose a problem with respect to ring closure of C9 since both edges of the initiating C8α and C9 molecules would be blocked. It must be stressed though that ring closure is not a prerequisite for the formation of a bactericidal pore since maximal activity is reached with only three copies of C9 per C5b8.

The structure elucidation of the first MACPF domain has led to great insight into the mechanism of MAC assembly. It is also clear that the structure has on its turn raised many more questions. The structure can now guide future research into the many details of MAC assembly that remain unclear and/or must be proven by more detailed biochemical experiments.

The initial immune response

Invasion of bacterial pathogens triggers a rapid immune response. Upon exposure to plasma bacteria become rapidly opsonized by antibodies like immunoglobulin G (IgG). The opsonization marks the bacteria for destruction by forming an "eat me" signal for phagocytes. Opsonization with IgG also leads to activation of the classical pathway of the complement system which on its turn unleashes various effectors including opsonization with C3b, formation of the membrane attack complex and generation of pro-inflammatory peptides like C5a that are chemotactic for leukocytes (Walport, 2001a, b). The formation of these chemotactic gradients by both immune activation products like C5a, and bacterially derived compounds like fMLP, results in the recruitment of immune effector cells (Bestebroer et al., 2009). One of the first types of cells to arrive at sites of infection are neutrophils. When invading bacteria encounter neutrophils they are engulfed in a process known as phagocytosis. Neutrophils express on their surface Fc receptors for IgG (FcγRs) and efficient phagocytosis requires the ligation to the bacterially bound opsonin IgG (Lee et al., 2003; McKenzie and Schreiber, 1998). This process plays a crucial role in the clearance of invading bacteria. Accordingly, an effective defense against opsonophagocytosis is extremely important in determining the success of bacterial pathogens.

Bacterial immune evasion

Bacteria have evolved numerous methods to evade detection by our immune system. The Gram-positive Staphylococcus aureus is a true master in this respect (Foster, 2005; Lambris et al., 2008; Serruto et al.). While the bacteria is often found as part of the skin flora it is also the most common cause of nocosomial infections. The success of S. aureus is in a large part due to the extremely versatile immune evasion strategies it possesses which are mediated by a large number of secreted proteins. Phagocytosis by neutrophils is crucial for the immune clearance of S. aureus. Accordingly, the bacteria dedicate a significant amount of energy in the production of proteins that inhibit the various steps essential for phagocytosis. These include proteins that mask their antigenic surface, inhibit chemotaxis of neutrophils, interfere with C3b deposition, mediate the proteolytic removal of opsonins and neutralize reactive oxygen species (ROS) in neutrophils. S. aureus also interferes with IgG mediated immunity by secreting several proteins that bind to the Fc portion of IgG, thereby interfering with the interaction with both C1q of the complement system and FcγRs on neutrophils.

Recently, two staphylococcal proteins have been described that inhibit formyl peptide receptor (FPR) and FPR-like 1 (FPRL1) mediated chemotaxis (Prat et al., 2006; Prat et al., 2009). The proteins were coined FPRL1 inhibitory protein (FLIPr) and FLIPr-like. During these studies it was noted that apart from binding to FPR and FPRL1 on monocytes and neutrophils, FLIPr and FLIPr-like also bound to subpopulations of lymphocytes not known to express these receptors. These studies prompted the question if FLIPr and FLIPr-like also bind to other receptors. Subsequent investigation then led to the observation that these proteins also potently inhibit phagocytosis (Stemerding et al.). This inhibition was dependent on binding of FLIPr and FLIPr-like to FcγRs which could compete for binding to IgG. The in vivo relevance of this interaction was further confirmed by the demonstration that FLIPr and FLIPr-like were able to completely block the immune-complex dependent Arthus reaction in a mouse model.

FLIPr and FLIPr-like are not the first reported bacterial inhibitors of FcγRs. In the human pathogen Streptococcus pyogenes two allelic variants have been identified that encode for cysteine proteases termed IdeS and Mac-2. Both proteins inhibit FcγR mediated phagocyosis by specifically cleaving

the heavy chain of IgG (Soderberg et al., 2008). The Mac-2 variant can however also bind to FcγRs. Specifically, binding has been demonstrated for FcγRII and FcγRIII which bind with an affinity of 5 and 70 μM respectively (Agniswamy et al., 2004). While this interaction is able to compete with binding of IgG the in vivo relevance remains unclear. Interestingly, both Mac-2 and IdeS inhibit opsonophagocytosis induced production of ROS and this inhibition is independent of their enzymatic activity towards IgG. However, the inhibition of ROS production alone, in the absence of IgG proteolysis, does not confer resistance to killing in bactericidal assays. The fact that both IdeS and Mac-2 inhibit ROS formation while only Mac-2 binds to FcγRs (with modest affinity) strongly suggests the effect is mediated by some other receptor. Moreover, the absence of a selective advantage regarding streptococcal survival questions the functional relevance of this interaction and that observed for FcγRs.

FLIPr and FLIPr-like are homologous, sharing 73% sequence identity. Interestingly, the proteins show clear differences in the binding profiles to different classes of FcγRs. While FLIPr-like binds to all FcγR classes (with the exception of FcγRIIIb), FLIPr only binds to FcγRII (Stemerding et al.). Neutrophils, which are the most abundant phagocytes in the bloodstream and the primary cells responsible for phagocytosis of S. aureus constitutively express FcγRIIa and FcγRIIIb although FcγRI expression is induced when cells are primed. FcγRIIIb is attached to the membrane through a GPI anchor and is inefficient in activating phagocytosis alone. Although it has been shown that cross linking of FcγRIIIb to FcγRIIa by immune complexes does enhance the function of FcγRIIa in initiating phagocytosis the main advantage for staphylococcal survival is most likely the inhibition of FcγRIIa (Salmon et al., 1995). Since FcγRIIa is the most widely expressed FcγR, blockage of FcγRIIa and consequently opsonophagocytosis is most likely the core function of FLIPr and FLIPr-like. The binding to other receptors, i.e. FcγRIIb for FLIPr and FcγRI and FcγRIIIa for FLIPr-like, is most likely a consequence of the similarity of the binding site on FcγRs. Obviously the inhibition of FcγRI and FcγRIIIa would offer distinct advantages for invading S. aureus. However, the real contribution to staphylococcal virulence and the differences attributed to blocking of different FcγRs would need to be studied in a relevant animal disease model.

We have clarified the lack of binding of FLIPr-like to FcγRIIIb to a single amino acid. This residue forms the only difference between non-binding FcγRIIIb and binding FcγRIIIa at the FLIPr-like interface. Why FLIPr, in contrast to FLIPr-like, does not bind to FcγRI and FcγRIIIa is less obvious. At the heart of these differences may be the strikingly different thermodynamic profiles for FLIPr and FLIPr-like binding to FcγRIIa with FLIPr binding to FcγRIIa showing a much stronger contribution of enthalpy compared to FLIPr-like. This is however compensated by a rather unfavorable entropy which ultimately results in only a slightly higher affinity. The crystal structure of the FLIPr-like complex with FcγRIIa does not readily explain these differences. Understanding these subtle effects would most likely require the high resolution structure of the FLIPr- FcγRIIa complex. Structural characterization using solution based techniques such as small angle X-ray scattering and nuclear magnetic resonance would also give valuable insight into dynamics perhaps missed in crystal structures due to crystal lattice restraints.

Apart from binding to different classes and isotypes of FcγRs, FLIPr and FLIPr-like also display variation in binding to FPR and FPRL1. While they display a comparable affinity for FPRL1, FLIPr-like is ~100 fold more potent in inhibiting FPR (Prat et al., 2006; Prat et al., 2009). The N-terminal region plays a crucial role in binding to FPR. Intriguingly, although FLIPr and FLIPr-like share

73% sequence identity, the N-terminal 26 residues are identical. Furthermore, a peptide consisting of FLIPr (and thus FLIPr-like) residues 1-6 can also inhibit FPR but is ~100 fold less potent. This suggest that the limited FPR inhibiting activity of FLIPr is located in this N-terminal segment, specifically the phenylalanine at position 2. This also implies the presence of a secondary binding site in FLIPr-like that raises the level of inhibition of the N-terminal six residues to that observed for full-length FLIPr-like. The structure of FLIPr-like now allows us to make prediction regarding this secondary FPR binding site by mapping the sequence differences with FLIPr onto the structure. Taking into account the topological restraint posed by the location of the N-terminus suggests the loop between α-2 and β-1 could be involved. This loop points in the same direction as the N-terminus of FLIPr-like. Moreover, the sequence strongly differs compared to FLIPr. It must be noted though that the N-terminal 15 residues are not visible in the structure of FLIPr-like due to disorder. This inherent flexibility might position the core of FLIPr-like in a number of alternative orientations, thereby allowing different regions to associate with a secondary site on FPR. Further studies using FLIPr-like mutants and/or chimeras will shed light on the presence and location of the putative FPR exosite.

FLIPr and FLIPr-like adopt a fold similar to the β-grasp domain that is also found in staphylococcal superantigen-like proteins (SSLs), staphylococcal superantigens and CHIPS. It is of interest to note the extreme versatility of this fold in mediating protein-protein interactions. The domain is able to bind to proteins as diverse as C5, MHC class II, T-cell receptor β-chain, various GPCRs and FcγRs but also polysaccharides such as sialyllactosamine (Fraser and Proft, 2008). The difference in the length of the N- and C-terminal regions and surface loops uniquely shape the core fold to accommodate binding to such a diverse set of ligands and one may only speculate on what other binding partners remain to be discovered.

The crystal structure of FLIPr-like bound to FcγRIIa shows that FLIPr-like binds exclusively to domain two of FcγRIIa and the binding site almost completely overlaps with that of IgG. Interestingly, although the N-terminal 15 residues of FLIPr-like are disordered the N-terminus points in roughly the same direction as the C-terminus of FcγRIIa which is where in the intact receptor the transmembrane region is located. This would orient the N-terminal region towards the membrane and thus suggests FLIPr and FLIPr-like may actually bind simultaneously to both FcγRs as well as their other targets FPR and/or FPRL1. It is of interest to note that a functional coupling has been observed between FcγRIIIb and FPR signalling in inducing chemotaxis (Kew et al., 1992). This suggests such a mechanism could provide a selective advantage. The ability of FLIPr-like to inhibit both fMLP mediated chemotaxis and immune complex mediated opsonophagocytosis suggests it may play a very important role in staphylococcal virulence. Whether simultaneous ligation has functional consequences for staphylococcal virulence will have to be assessed, again using a relevant animal disease model.

The structure of FLIPr-like, together with the unique binding to FcγRs forms a starting point for the design of class and isotype specific inhibitors for FcγRs. These may have implications in various autoimmune disorders, in modulating the responses of cytotoxic antibodies targeted against neoplastic pathologies but also function as tools in studying the individual biological roles of the different receptors. The difference in binding profile between FLIPr and FLIPr-like forms a good start in getting to understand the determinants for receptor specificity.

References

Agniswamy, J., Lei, B., Musser, J.M., and Sun, P.D. (2004). Insight of host immune evasion mediated by two variants of group a Streptococcus Mac protein. J Biol Chem 279, 52789-52796.
Amiguet, P., Brunner, J., and Tschopp, J. (1985). The membrane attack complex of complement: lipid insertion of tubular and nontubular polymerized C9. Biochemistry 24, 7328-7334.
Armstrong, P.B., and Quigley, J.P. (1999). Alpha2-macroglobulin: an evolutionarily conserved arm of the innate immune system. Dev Comp Immunol 23, 375-390.
Baran, K., Dunstone, M., Chia, J., Ciccone, A., Browne, K.A., Clarke, C.J., Lukoyanova, N., Saibil, H., Whisstock, J.C., Voskoboinik, I., et al. (2009). The molecular basis for perforin oligomerization and transmembrane pore assembly. Immunity 30, 684-695.
Baxter, R.H., Chang, C.I., Chelliah, Y., Blandin, S., Levashina, E.A., and Deisenhofer, J. (2007). Structural basis for conserved complement factor-like function in the antimalarial protein TEP1. Proc Natl Acad Sci U S A 104, 11615-11620.
Bestebroer, J., de Haas, C.J., and van Strijp, J.A. (2009). How microorganisms avoid phagocyte attraction. FEMS Microbiol Rev.
Brannen, C.L., and Sodetz, J.M. (2007). Incorporation of human complement C8 into the membrane attack complex is mediated by a binding site located within the C8beta MACPF domain. Mol Immunol 44, 960-965.
Cooper, N.R., and Muller-Eberhard, H.J. (1970). The reaction mechanism of human C5 in immune hemolysis. J Exp Med 132, 775-793.
Czajkowsky, D.M., Hotze, E.M., Shao, Z., and Tweten, R.K. (2004). Vertical collapse of a cytolysin prepore moves its transmembrane beta-hairpins to the membrane. EMBO J 23, 3206-3215.
Dangott, L.J., Puett, D., and Cunningham, L.W. (1983). Conformational changes induced in human alpha 2-macroglobulin by protease and nucleophilic modification. Biochemistry 22, 3647-3653.
DiScipio, R.G. (1992). Formation and structure of the C5b-7 complex of the lytic pathway of complement. J Biol Chem 267, 17087-17094.
DiScipio, R.G., Chakravarti, D.N., Muller-Eberhard, H.J., and Fey, G.H. (1988). The structure of human complement component C7 and the C5b-7 complex. J Biol Chem 263, 549-560.
DiScipio, R.G., and Hugli, T.E. (1985). The architecture of complement component C9 and poly(C9). J Biol Chem 260, 14802-14809.
Dodds, A.W., and Law, S.K. (1998). The phylogeny and evolution of the thioester bond-containing proteins C3, C4 and alpha 2-macroglobulin. Immunol Rev 166, 15-26.
Esser, A.F. (1994). The membrane attack complex of complement. Assembly, structure and cytotoxic activity. Toxicology 87, 229-247.
Esser, A.F., Kolb, W.P., Podack, E.R., and Muller-Eberhard, H.J. (1979). Molecular reorganization of lipid bilayers by complement: a possible mechanism for membranolysis. Proc Natl Acad Sci U S A 76, 1410-1414.
Farkas, I., Baranyi, L., Ishikawa, Y., Okada, N., Bohata, C., Budai, D., Fukuda, A., Imai, M., and Okada, H. (2002). CD59 blocks not only the insertion of C9 into MAC but inhibits ion channel formation by homologous C5b-8 as well as C5b-9. J Physiol 539, 537-545.
Feldman, S.R., and Pizzo, S.V. (1984). Comparison of the binding of chicken alpha-macroglobulin and ovomacroglobulin to the mammalian alpha 2-macroglobulin receptor. Arch Biochem Biophys 235, 267-275.
Foster, T.J. (2005). Immune evasion by staphylococci. Nat Rev Microbiol 3, 948-958.

Fraser, J.D., and Proft, T. (2008). The bacterial superantigen and superantigen-like proteins. Immunol Rev 225, 226-243.
Fredslund, F., Jenner, L., Husted, L.B., Nyborg, J., Andersen, G.R., and Sottrup-Jensen, L. (2006). The structure of bovine complement component 3 reveals the basis for thioester function. J Mol Biol 361, 115-127.
Fredslund, F., Laursen, N.S., Roversi, P., Jenner, L., Oliveira, C.L., Pedersen, J.S., Nunn, M.A., Lea, S.M., Discipio, R., Sottrup-Jensen, L., et al. (2008). Structure of and influence of a tick complement inhibitor on human complement component 5. Nat Immunol 9, 753-760.
Gettins, P.G., Boel, E., and Crews, B.C. (1994). Thiol ester role in correct folding and conformation of human alpha 2-macroglobulin. Properties of recombinant C949S variant. FEBS Lett 339, 276-280.
Hadders, M.A., Beringer, D.X., and Gros, P. (2007). Structure of C8alpha-MACPF reveals mechanism of membrane attack in complement immune defense. Science 317, 1552-1554.
Heuck, A.P., Hotze, E.M., Tweten, R.K., and Johnson, A.E. (2000). Mechanism of membrane insertion of a multimeric beta-barrel protein: perfringolysin O creates a pore using ordered and coupled conformational changes. Mol Cell 6, 1233-1242.
Heuck, A.P., Tweten, R.K., and Johnson, A.E. (2003). Assembly and topography of the prepore complex in cholesterol-dependent cytolysins. J Biol Chem 278, 31218-31225.
Hu, V.W., Esser, A.F., Podack, E.R., and Wisnieski, B.J. (1981). The membrane attack mechanism of complement: photolabeling reveals insertion of terminal proteins into target membrane. J Immunol 127, 380-386.
Huang, Y., Qiao, F., Abagyan, R., Hazard, S., and Tomlinson, S. (2006). Defining the CD59-C9 binding interaction. J Biol Chem 281, 27398-27404.
Husler, T., Lockert, D.H., Kaufman, K.M., Sodetz, J.M., and Sims, P.J. (1995). Chimeras of human complement C9 reveal the site recognized by complement regulatory protein CD59. J Biol Chem 270, 3483-3486.
Isaac, L., Aivazian, D., Taniguchi-Sidle, A., Ebanks, R.O., Farah, C.S., Florido, M.P., Pangburn, M.K., and Isenman, D.E. (1998). Native conformations of human complement components C3 and C4 show different dependencies on thioester formation. Biochem J 329 (Pt 3), 705-712.
Isaac, L., and Isenman, D.E. (1992). Structural requirements for thioester bond formation in human complement component C3. Reassessment of the role of thioester bond integrity on the conformation of C3. J Biol Chem 267, 10062-10069.
Ishida, B., Wisnieski, B.J., Lavine, C.H., and Esser, A.F. (1982). Photolabeling of a hydrophobic domain of the ninth component of human complement. J Biol Chem 257, 10551-10553.
Janssen, B.J., Christodoulidou, A., McCarthy, A., Lambris, J.D., and Gros, P. (2006). Structure of C3b reveals conformational changes that underlie complement activity. Nature 444, 213-216.
Janssen, B.J., Huizinga, E.G., Raaijmakers, H.C., Roos, A., Daha, M.R., Nilsson-Ekdahl, K., Nilsson, B., and Gros, P. (2005). Structures of complement component C3 provide insights into the function and evolution of immunity. Nature 437, 505-511.
Joiner, K.A., Schmetz, M.A., Sanders, M.E., Murray, T.G., Hammer, C.H., Dourmashkin, R., and Frank, M.M. (1985). Multimeric complement component C9 is necessary for killing of Escherichia coli J5 by terminal attack complex C5b-9. Proc Natl Acad Sci U S A 82, 4808-4812.
Kew, R.R., Grimaldi, C.M., Furie, M.B., and Fleit, H.B. (1992). Human neutrophil Fc gamma RIIIB and formyl peptide receptors are functionally linked during formyl-methionyl-leucyl-phenylalanine-induced chemotaxis. J Immunol 149, 989-997.

Lambris, J.D., Ricklin, D., and Geisbrecht, B.V. (2008). Complement evasion by human pathogens. Nat Rev Microbiol 6, 132-142.
Lee, W.L., Harrison, R.E., and Grinstein, S. (2003). Phagocytosis by neutrophils. Microbes Infect 5, 1299-1306.
Lehto, T., and Meri, S. (1993). Interactions of soluble CD59 with the terminal complement complexes. CD59 and C9 compete for a nascent epitope on C8. J Immunol 151, 4941-4949.
Lockert, D.H., Kaufman, K.M., Chang, C.P., Husler, T., Sodetz, J.M., and Sims, P.J. (1995). Identity of the segment of human complement C8 recognized by complement regulatory protein CD59. J Biol Chem 270, 19723-19728.
McKenzie, S.E., and Schreiber, A.D. (1998). Fc gamma receptors in phagocytes. Curr Opin Hematol 5, 16-21.
Monahan, J.B., and Sodetz, J.M. (1980). Binding of the eighth component of human complement to the soluble cytolytic complex is mediated by its beta subunit. J Biol Chem 255, 10579-10582.
Monahan, J.B., and Sodetz, J.M. (1981). Role of the beta subunit in interaction of the eighth component of human complement with the membrane-bound cytolytic complex. J Biol Chem 256, 3258-3262.
Monahan, J.B., Stewart, J.L., and Sodetz, J.M. (1983). Studies of the association of the eighth and ninth components of human complement within the membrane-bound cytolytic complex. J Biol Chem 258, 5056-5062.
Muller-Eberhard, H.J. (1986). The membrane attack complex of complement. Annu Rev Immunol 4, 503-528.
Nagar, B., Jones, R.G., Diefenbach, R.J., Isenman, D.E., and Rini, J.M. (1998). X-ray crystal structure of C3d: a C3 fragment and ligand for complement receptor 2. Science 280, 1277-1281.
Nishida, N., Walz, T., and Springer, T.A. (2006). Structural transitions of complement component C3 and its activation products. Proc Natl Acad Sci U S A 103, 19737-19742.
Podack, E.R., Biesecker, G., Kolb, W.P., and Muller-Eberhard, H.J. (1978a). The C5b-6 complex: reaction with C7, C8, C9. J Immunol 121, 484-490.
Podack, E.R., Kolb, W.P., and Muller-Eberhard, H.J. (1978b). The C5b-6 complex: formation, isolation, and inhibition of its activity by lipoprotein and the S-protein of human serum. J Immunol 120, 1841-1848.
Podack, E.R., Stoffel, W., Esser, A.F., and Muller-Eberhard, H.J. (1981). Membrane attack complex of complement: distribution of subunits between the hydrocarbon phase of target membranes and water. Proc Natl Acad Sci U S A 78, 4544-4548.
Prat, C., Bestebroer, J., de Haas, C.J., van Strijp, J.A., and van Kessel, K.P. (2006). A new staphylococcal anti-inflammatory protein that antagonizes the formyl peptide receptor-like 1. J Immunol 177, 8017-8026.
Prat, C., Haas, P.J., Bestebroer, J., de Haas, C.J., van Strijp, J.A., and van Kessel, K.P. (2009). A homolog of formyl peptide receptor-like 1 (FPRL1) inhibitor from Staphylococcus aureus (FPRL1 inhibitory protein) that inhibits FPRL1 and FPR. J Immunol 183, 6569-6578.
Preissner, K.T., Podack, E.R., and Muller-Eberhard, H.J. (1985). The membrane attack complex of complement: relation of C7 to the metastable membrane binding site of the intermediate complex C5b-7. J Immunol 135, 445-451.
Ramachandran, R., Heuck, A.P., Tweten, R.K., and Johnson, A.E. (2002). Structural insights into the membrane-anchoring mechanism of a cholesterol-dependent cytolysin. Nat Struct Biol 9, 823-827.

Ramachandran, R., Tweten, R.K., and Johnson, A.E. (2004). Membrane-dependent conformational changes initiate cholesterol-dependent cytolysin oligomerization and intersubunit beta-strand alignment. Nat Struct Mol Biol 11, 697-705.
Ramachandran, R., Tweten, R.K., and Johnson, A.E. (2005). The domains of a cholesterol-dependent cytolysin undergo a major FRET-detected rearrangement during pore formation. Proc Natl Acad Sci U S A 102, 7139-7144.
Rooijakkers, S.H., Wu, J., Ruyken, M., van Domselaar, R., Planken, K.L., Tzekou, A., Ricklin, D., Lambris, J.D., Janssen, B.J., van Strijp, J.A., et al. (2009). Structural and functional implications of the alternative complement pathway C3 convertase stabilized by a staphylococcal inhibitor. Nat Immunol 10, 721-727.
Rosado, C.J., Buckle, A.M., Law, R.H., Butcher, R.E., Kan, W.T., Bird, C.H., Ung, K., Browne, K.A., Baran, K., Bashtannyk-Puhalovich, T.A., et al. (2007). A common fold mediates vertebrate defense and bacterial attack. Science 317, 1548-1551.
Salmon, J.E., Millard, S.S., Brogle, N.L., and Kimberly, R.P. (1995). Fc gamma receptor IIIb enhances Fc gamma receptor IIa function in an oxidant-dependent and allele-sensitive manner. J Clin Invest 95, 2877-2885.
Serruto, D., Rappuoli, R., Scarselli, M., Gros, P., and van Strijp, J.A. Molecular mechanisms of complement evasion: learning from staphylococci and meningococci. Nat Rev Microbiol 8, 393-399.
Shatursky, O., Heuck, A.P., Shepard, L.A., Rossjohn, J., Parker, M.W., Johnson, A.E., and Tweten, R.K. (1999). The mechanism of membrane insertion for a cholesterol-dependent cytolysin: a novel paradigm for pore-forming toxins. Cell 99, 293-299.
Shepard, L.A., Heuck, A.P., Hamman, B.D., Rossjohn, J., Parker, M.W., Ryan, K.R., Johnson, A.E., and Tweten, R.K. (1998). Identification of a membrane-spanning domain of the thiol-activated pore-forming toxin Clostridium perfringens perfringolysin O: an alpha-helical to beta-sheet transition identified by fluorescence spectroscopy. Biochemistry 37, 14563-14574.
Shepard, L.A., Shatursky, O., Johnson, A.E., and Tweten, R.K. (2000). The mechanism of pore assembly for a cholesterol-dependent cytolysin: formation of a large prepore complex precedes the insertion of the transmembrane beta-hairpins. Biochemistry 39, 10284-10293.
Slade, D.J., Chiswell, B., and Sodetz, J.M. (2006). Functional studies of the MACPF domain of human complement protein C8alpha reveal sites for simultaneous binding of C8beta, C8gamma, and C9. Biochemistry 45, 5290-5296.
Slade, D.J., Lovelace, L.L., Chruszcz, M., Minor, W., Lebioda, L., and Sodetz, J.M. (2008). Crystal structure of the MACPF domain of human complement protein C8 alpha in complex with the C8 gamma subunit. J Mol Biol 379, 331-342.
Soderberg, J.J., Engstrom, P., and von Pawel-Rammingen, U. (2008). The intrinsic immunoglobulin g endopeptidase activity of streptococcal Mac-2 proteins implies a unique role for the enzymatically impaired Mac-2 protein of M28 serotype strains. Infect Immun 76, 2183-2188.
Sodetz, J.M. (1989). Structure and function of C8 in the membrane attack sequence of complement. Curr Top Microbiol Immunol 140, 19-31.
Steckel, E.W., Welbaum, B.E., and Sodetz, J.M. (1983). Evidence of direct insertion of terminal complement proteins into cell membrane bilayers during cytolysis. Labeling by a photosensitive membrane probe reveals a major role for the eighth and ninth components. J Biol Chem 258, 4318-4324.
Stewart, J.L., Kolb, W.P., and Sodetz, J.M. (1987). Evidence that C5b recognizes and mediates C8 incorporation into the cytolytic complex of complement. J Immunol 139, 1960-1964.

Thai, C.T., and Ogata, R.T. (2004). Complement components C5 and C7: recombinant factor I modules of C7 bind to the C345C domain of C5. J Immunol 173, 4547-4552.
Thai, C.T., and Ogata, R.T. (2005). Recombinant C345C and factor I modules of complement components C5 and C7 inhibit C7 incorporation into the complement membrane attack complex. J Immunol 174, 6227-6232.
Tomlinson, S., Wang, Y., Ueda, E., and Esser, A.F. (1995). Chimeric horse/human recombinant C9 proteins identify the amino acid sequence in horse C9 responsible for restriction of hemolysis. J Immunol 155, 436-444.
Tschopp, J. (1984a). Circular polymerization of the membranolytic ninth component of complement. Dependence on metal ions. J Biol Chem 259, 10569-10573.
Tschopp, J. (1984b). Ultrastructure of the membrane attack complex of complement. Heterogeneity of the complex caused by different degree of C9 polymerization. J Biol Chem 259, 7857-7863.
Tschopp, J., Engel, A., and Podack, E.R. (1984). Molecular weight of poly(C9). 12 to 18 C9 molecules form the transmembrane channel of complement. J Biol Chem 259, 1922-1928.
Tschopp, J., Muller-Eberhard, H.J., and Podack, E.R. (1982). Formation of transmembrane tubules by spontaneous polymerization of the hydrophilic complement protein C9. Nature 298, 534-538.
Tschopp, J., and Podack, E.R. (1981). Membranolysis by the ninth component of human complement. Biochem Biophys Res Commun 100, 1409-1414.
Tschopp, J., Podack, E.R., and Muller-Eberhard, H.J. (1985). The membrane attack complex of complement: C5b-8 complex as accelerator of C9 polymerization. J Immunol 134, 495-499.
Van Rompaey, L., Van den Berghe, H., and Marynen, P. (1995). Synthesis of a Cys949Tyr alpha 2-macroglobulin thiol ester mutant: co-transfection with wild-type alpha 2-macroglobulin in an episomal expression system. Biochem J 312 (Pt 1), 183-190.
Voskoboinik, I., Smyth, M.J., and Trapani, J.A. (2006). Perforin-mediated target-cell death and immune homeostasis. Nat Rev Immunol 6, 940-952.
Voskoboinik, I., Thia, M.C., Fletcher, J., Ciccone, A., Browne, K., Smyth, M.J., and Trapani, J.A. (2005). Calcium-dependent plasma membrane binding and cell lysis by perforin are mediated through its C2 domain: A critical role for aspartate residues 429, 435, 483, and 485 but not 491. J Biol Chem 280, 8426-8434.
Walport, M.J. (2001a). Complement. First of two parts. N Engl J Med 344, 1058-1066.
Walport, M.J. (2001b). Complement. Second of two parts. N Engl J Med 344, 1140-1144.
Wiesmann, C., Katschke, K.J., Yin, J., Helmy, K.Y., Steffek, M., Fairbrother, W.J., McCallum, S.A., Embuscado, L., DeForge, L., Hass, P.E., et al. (2006). Structure of C3b in complex with CRIg gives insights into regulation of complement activation. Nature 444, 217-220.
Wu, J., Wu, Y.Q., Ricklin, D., Janssen, B.J., Lambris, J.D., and Gros, P. (2009). Structure of complement fragment C3b-factor H and implications for host protection by complement regulators. Nat Immunol 10, 728-733.

Summary

Humans and pathogenic bacteria are under continuous pressure to evolve strategies that confer their survival. For humans this entails mechanisms that kill and clear invading bacteria while bacteria require similar killing of host cells or systems that mediate shielding of the bacteria from the host immune system. When bacteria breach physical barriers such as the skin and enter into the blood stream they are rapidly recognized by a.o. antibodies. This results in 1) recognition by phagocytes which internalize the bacteria in a process known as phagocytosis and 2) activates the complement system which then results in a range of effector functions including the formation of the membrane attack complex (MAC).

The MAC is a large multi-protein complex that drills holes in the membrane of targeted bacteria resulting in their death. The system is initiated when the protein C5 is cleaved into C5b after complement activation. This results in the sequential binding of four proteins called C6, C7, C8 and C9. In this process C8 is the first protein that inserts into the target membrane. It then forms a binding platform for C9 which then polymerizes to form the membrane inserted pore through which bacterial lysis takes place. The MACPF domain is central to C6-C9 and it was previously shown that the membrane inserting segments of C8 and C9 are located in this domain. However, no detailed model exists of how these proteins form pores due in part to a lack of structural information.

Bacteria on the other hand have ways of preventing the initial recognition event. *Staphylococcus aureus* is a good example as it secretes numerous proteins that target almost all branches of our immune system. Recently it was discovered that two of these proteins, called FLIPr and FLIPr-like, can inhibit phagocytosis. These proteins function by interfering with the receptors on white blood cells that recognize the antibodies bound to bacteria.

In this thesis both systems (killing of bacteria by the human immune system and immune evasion by bacteria) were studied, mainly using X-ray crystallography. This technique allows us to probe the 3-dimensional structures of proteins from which we can then infer invaluable information on how they function.

In **chapter 2** we describe the first structure of a MACPF domain, that of C8α. We show that despite a complete lack of sequence identity the MACPF domain has a striking structural similarity to cholesterol dependent cytolysins (CDCs), a group of well characterized bacterial pore-forming toxins. This includes two regions (termed TMH1 and TMH2) that in CDCs are amphipathic with alternating hydrophobic and hydrophilic residues. In CDCs these regions refold to form extended β-hairpins that form the lining of a β-barrel pore with the hydrophobic residues pointing towards the interior of the membrane and the hydrophilic ones pointing towards the solvent inside the pore. In C8α these segments are largely hydrophobic which fits with the fact that C8α does not form a pore but needs to penetrate the membrane. In C9 however the TMH regions are amphipathic fitting with its function as the pore forming protein of the MAC.

In **chapter 3** we describe the structure of the complex between C5b and C6. This complex initiates formation of the membrane attack complex. The structure reveals how the C5

to C5b conversion is accompanied by large conformational changes that shape a novel binding site for C6. The observed rearrangements differ from those previously observed for homologous C3 and seem to be stabilized by C6. The binding site for C6 lies primarily in the C5d and CUB domains. The structure also shows for the first time the overall domain arrangement of a MACPF member. C6 has a compact core and binds to C5b mainly through its CCP domains and a 29 residue linker situated in between the third TSP- and the first CCP domain. This linker renders isolated C6 flexible which was confirmed by solution scattering studies.

In **chapter 4** we describe the structure of an immune modulating protein from *S. aureus*, FLIPr-like, in complex with its target, FcγRIIa. FcγRIIa is a receptor for IgG and is essential for phagocytosis by neutrophils. The structure reveals that FLIPr-like has a fold similar to the β-grasp fold found in many staphylococcal immune modulating proteins. FLIPr-like differs though and these differences uniquely shape the proteins surface to create the binding site for FcγRIIa. FLIPr-like binds to FcγRIIa and the binding site almost fully overlaps with that of IgG, explaining how the FLIPr-like functions to inhibit phagocytosis. The structure also gives insight into the specificity of FLIPr-like for certain isoforms of FcγRs and forms a blueprint for the rational design of isoform specific inhibitors that may have therapeutic potential in fighting inflammatory disorders or autoimmune disease.

Samenvatting

Mensen en pathogene bacteriën staan onder continue evolutionaire druk om strategieën te ontwikkelen die een voordeel voor hun overleving hebben. Voor mensen houdt dit mechanismen in die binnendringende bacteriën moeten doden terwijl bacteriën menselijke cellen moeten kunnen doden of zich kunnen verstoppen voor het menselijke immuun systeem. Wanneer bacteriën de fysieke barrière van bijvoorbeeld de huid doordringen en in het bloed terecht komen worden ze snel herkend door onder andere antistoffen. Dit leidt tot 1) herkenning door witte bloed cellen die de bacteriën kunnen opnemen, een proces dat bekend staat als fagocytose, en 2) activeert het complement systeem dat resulteert in allerlei effecten zoals de formatie van het membraan aanvals complex (MAC).

Het MAC is een groot complex dat bestaat uit meerdere eiwitten en kan gaten boren in het membraan van bacteriën wat dan leidt tot hun dood door lysis. Het systeem wordt geïnitieerd als na complement activatie het eiwit C5 wordt geknipt in C5b. Dit leidt tot het sequentieel binden van vier eiwitten die C6, C7, C8 en C9 heten. Tijdens dit proces is C8 het eerste eiwit dat in het membraan steekt. Het eiwit vormt dan een platform voor het binding van het eiwit C9 dat vervolgens polymeriseert om een membraan geïnserteerde porie te vormen waardoor lysis van de bacterie plaatsvindt. Het MACPF domein vormt het hart van de eiwitten C6 tot en met C9. Eerder is al aangetoond dat de delen van C8 en C9 die in het membraan steken zich in het MACPF domein bevinden. Er bestaat echter geen gedetailleerd model van hoe deze eiwitten een porie vormen, o.a. door een gebrek aan informatie over de structuur van deze eiwitten.

Bacteriën daarentegen hebben manieren om de initiële herkenning door het menselijke immuun systeem te voorkomen. *Staphylococcus aureus* is een goed voorbeeld die vele eiwitten uitscheidt die bijna alle takken van ons immuunsysteem kan plat leggen. Recent is ontdekt dat twee van deze eiwitten, FLIPr en FLIPr-like, naast hun eerder beschreven functie als remmers van chemotaxis, ook fagocytose kunnen inhiberen. Deze eiwitten functioneren door te binden aan receptoren op witte bloed cellen die de antilichamen herkennen die aan bacteriën zijn gebonden.

In dit proefschrift wordt onderzoek beschreven naar beide systemen (het doden van bacteriën door het menselijke immuun systeem en ontduiking van het immuun systeem door bacteriën). Hiervoor werd voornamelijk gebruik gemaakt van röntgen diffractie. Deze techniek stelt ons in staat om de driedimensionale structuur van eiwitten te bepalen waaruit we vervolgens waardevolle informatie kunnen halen over het functioneren van het eiwit.

In **hoofdstuk 2** beschrijven we de eerste structuur van een MACPF domein, die van het eiwit C8α. We tonen aan dat, ook al zijn de sequenties kompleet verschillend, het MACPF domein een opvallende structurele gelijkenis vertoond met cholesterol afhankelijk cytolysins (CDC), een groep goed gekarakteriseerde bacteriële porie vormende toxinen. Zo bevatten MACPF domeinen ook twee regio's (de zogenoemde TMH1 en TMH2) die in CDCs amphipathisch zijn met afwisselend hydrofobe en hydrofiele residuen. In CDCs hervouwen deze regio's waarbij ze uitgestrekte β-haarspelden vormen. Deze vormen de voering van een β-barrel porie met de hydrofobe residuen

wijzend naar de binnenkant van het membraan en de hydrofiele wijzend naar de waterige omgeving binnen in de porie. In C8α zijn deze segmenten grotendeels hydrofoob wat past bij het feit dat C8α niet een porie vormt, maar alleen maar moet doordringen in de membraan. In C9 echter zijn de TMH regio's wel amphipathisch wat weer past bij de functie van porie vormend eiwit van de MAC.

In **hoofdstuk 3** beschrijven we de structuur van het complex tussen de eiwitten C5b en C6. Dit complex initieert de vorming van het membraan aanvals complex. De structuur laat zien hoe de overgang van C5 tot C5b gepaard gaat met grote conformationele veranderingen die leiden tot een nieuwe bindingsplaats voor C6. De veranderingen verschillen van die eerder waargenomen voor het homologe eiwit C3 en deze verschillende conformatie lijkt te worden gestabiliseerd door C6. De bindingsplek voor C6 ligt voornamelijk in het C5d en het CUB domein. De structuur laat ook voor het eerst de algemene schikking van alle domeinen zien van MACPF eiwit. C6 heeft een compacte kern en bindt aan C5b voornamelijk via de CCP domeinen en een verbindingsstuk van 29 residuen lang die het derde TSP- en het eerste CCP domein met elkaar verbindt. Deze linker maakt het geïsoleerde C6 in oplossing flexibel hetgeen werd bevestigd door röntgen verstrooiing studies in oplossing.

In **hoofdstuk 4** beschrijven we de structuur van een immuun modulerend eiwit van *S. aureus,* FLIPR-like, in complex met zijn doelwit, FcγRIIa. FcγRIIa is een receptor voor antilichamen van het type IgG en is essentieel voor fagocytose door neutrofielen. Uit de structuur blijkt dat de vouwing van FLIPR-like vergelijkbaar is met een β-grasp domein die voorkomt bij veel immuun modulerende eiwitten van *S. aureus*. FLIPR-like kent echter subtiele verschillen en al deze verschillen zorgen voor een unieke vorm van het oppervlak die de bindingsplaats voor FcγRIIa creëren. FLIPR-like bindt aan FcγRIIa en de bindingsplaats overlapt bijna volledig met die van IgG. Dit maakt duidelijk hoe FLIPR-like zijn functie als remmer van fagocytose uitvoert. De structuur geeft ook inzicht in de specifieke voorkeur van FLIPR-like voor bepaalde isovormen van FcγRs en vormt een blauwdruk voor het rationele ontwerpen van isovorm specifieke remmers die therapeutisch potentieel kunnen hebben voor de bestrijding van inflammatoire aandoeningen of auto-immuunziekte.

Dankwoord

En dan het dankwoord. Het slot stuk van je boekje en tevens het enige stuk die daadwerkelijk door mensen gelezen wordt. De gewoonte wil dat je begint met het bedanken van je promoter en dan het lijstje afwerkt waarbij je eindigt met je geliefde. Ik houd niet zo van conventies dus ik gooi het lekker om.

Lieve Suus, ik zal niet altijd makkelijk zijn geweest de laatste tijd en me dikwijls aan mijn huishoudelijke taken hebben ontrokken onder het mom van "werken aan mijn proefschrift. Daarnaast heb ik je ook nog eens naar Engeland gesleurd om verder te werken aan mijn carrière. Dat je nog bij me bent moet haast wel betekenen dat het goed zit en daar twijfel ik dan ook geen seconde aan. Nog maar 9 maanden en je mag weer naar huis ;-). De basis ligt natuurlijk bij je familie. Papa en mama ik zou hier natuurlijk nooit staan zonder jullie onvoorwaardelijke steun en goede zorgen (en goede genen natuurlijk). Ik waardeer dat eindeloos veel meer dan jullie je realiseren en dan ik vaak duidelijk maak. Ruben en Martijn, helaas kunnen jullie er niet bij zijn op mijn promotie. Gelukkig is het een en ander samengevat in dit boekje die zijn weg naar Down Under wel zal vinden. Ook de surrogaat (lees schoon) familie speelt een belangrijke rol. Ries en Lia + zwagers en schoonzussen, bedankt voor al jullie gastvrijheid en gezelligheid en goede zorgen.

Afleiding buiten het werk houdt de geest fris en staat garant voor inspiratie en nieuwe ideeën eenmaal terug op het lab. Veel van die afleiding heb ik gevonden bij de Stichting, ook wel bekend als STB. De verhalen zijn veel en groots en waarschijnlijk niet geschikt voor dit medium. Arjan, Ben, Hendrik, Hidde, Jeroen, Luuk, Richard en Toine, (en aanhang) Bedankt! Gewoon vol houden die tweede vrijdag van de maand en ik probeer zo snel mogelijk er weer eens bij te zijn. Ook de oude collega's van de Mc mogen niet ongenoemd blijven. Rob, Joep en Vinnie, ooit ga ik een keer geld winnen in een casino. Bedankt!

Collega's, daar heb ik veel van gehad. Aangezien ik wat langer dan gemiddeld in het lab van Kristal en Structuurchemie heb rondgelopen (ach, 6 ½ jaar zijn zo om) zijn er toch aardig wat mensen die er mede voor gezorgd hebben dat ik het zo naar mijn zin heb gehad op mijn werk. Op een universiteit is het toch een komen en gaan van mensen maar allemaal hebben ze een invloed gehad op mijn tijd in Utrecht.

Bert en Fin, collega's van het eerste uur die mij hebben verwelkomt op de vakgroep en al snel daarbuiten. Er volgden vele hoogtepunten: duiken in zeeland, (apres) skiën in Alpe d'Huez (Hej, waar is Bert nu weer aan het dansen), Lunteren, motor rijden in Duitsland (Ouch), en talloze avonden Fightclubs (ook met Lucio) met veels te uitgebreide chinees buffet. Mannen bedankt! Eric, bij jou begon mijn loopbaan als structuurbioloog. Ik heb in het eerste jaar dat ik stage bij jou liep, maar ook in de ruim vijf jaar daarna ontzettend veel van je geleerd. Bedankt! Toine, onontbeerlijk computer advies. Ik knikte wel maar begreep het vaak niet. Arie, spil van het lab. Als iedereen nu eens op tijd bestelde en zijn rommel opruimde….. Loes,voor echte diepgang in de (kristallografische) theorie. Martin, voor het aankondigen van de koffiepauze en een verfrissende Nederlandse kijk op allerlei zaken. Wieger, Roland en Niels (later Lucio), bedankt voor alle cellen en verfrissende gesprekken die eens niet over kristallografie gingen. Harma, succes met TI, Els, jij ook en geen zorgen, de resultaten komen vanzelf. Jin, almost finished now and record holder most structures

solved by a PhD. Federico, the Italian …. No I won't go there. Amazing tiramisu and off to very productive start, keep it up! Pramod, the indian baby naming ceremonie was very interesting! Peng and Ramesh, the asian future of the complement group, good luck! Tom thanks for rekindling my "passion" for cycling. Your absence has had an almost immediate effect on my mileage. Xinyi, Qinghong (no chicken feet for me), Lucy (niet weg te slaan uit het Kruyt gebouw), Hans (does Santa really exist?), Hugo (nu weer in hetzelfde gebouw, knutsel je op het LMB ook alles zelf in elkaar?), Huub, Ton, Marjan, Eddie, Marian, Aaike, Christoph, voor alle hulp en gezelligheid, bedankt.

Mijn paranimfen Dennis en Arjen. Dankzij jullie was het de laatste jaren altijd een plezier om naar het werk te gaan. Gesprekken varieerden van chromatogrammen tot mooie phenotypes, en konden binnen een zin wisselen. Dennis, jouw bijdrage aan dit proefschrift is evident (zie hoofdstuk 2) maar belangrijker nog waren je goede ideeen buiten het werk (chocolade ijs maken met vloeibaar stikstof). Arjen, zonder twijfel de slimste persoon op het lab en altijd bereid om te helpen. Ik zal je sinterklaas surprise nooit vergeten….. De afmattende squash partijen, tripjes naar Gent (vast komen te zitten in Antwerpen), en de tequila eyeball zijn maar een zeer beperkt aantal van de vele hoogtepunten waarbij jullie betrokken waren.

Ook heb ik het genoegen gekend om meerdere Master studenten te mogen begeleiden die allen een bijdrage hebben geleverd zij het soms niet zo zichtbaar in dit boekje. Dennis (zie Hoofdstuk 2 en boven), Bram en Roel, bedankt! Daarnaast heb ik K&S meerdere jaren mogen vertegenwoordigen voor het Bijvoet met als hoogtepunten (voor mij tenminste) de organisatie van de pubquiz tijdens de Bijvoet symposia. Het uitwisselen van gezelligheid en ideeën met collega AIO's van het Bijvoet op de AIO avonden was altijd leuk (eten op kosten van). Alle collega's binnen het Bijvoet center bedankt voor alle gezelligheid en discussies!

Jos en Carla, ik begon mijn promotie onderzoek met het wilde idee om met jullie samen te werken aan een nogal gewaagd project. De realiteit was hard en het project werd niet voort gezet. Echter, tijdens een tweede poging was het wel raak! Ik heb onze samenwerking altijd als heel prettig ervaren. En nu snel die paper de deur uit! ;-)

En dan ten slotte Piet. Dit alles was natuurlijk niet mogelijk geweest zonder jou en het lab dat jij hebt neergezet. Ik ben dan ook blij dat je mij alweer bijna zes jaar geleden in dienst wilde nemen. Ik weet dat een vorige AIO jou flink op de kast heeft gejaagd met opmerkingen over de geschonken vrijheid maar ook ik neig naar die gedachte. Vat dat alsjeblieft niet verkeerd op! Jij hebt mij alle kansen gegeven mij te ontwikkelen als wetenschapper. De laatste jaren zullen voor jou persoonlijk niet makkelijk zijn geweest maar ik vind het het bewonderenswaardig hoe je hier naar buiten toe mee omgaat. Maar er waren natuurlijk ook hoogtepunten (Spinoza prijs) en ik ben trots dat ik daar toch een minieme bijdrage aan heb mogen leveren.

Michael

Curriculum Vitae

Michiel Arjan Hadders werd geboren op 31 juli 1979 te Jubail, Saoedi Arabië. Hij behaalde zijn VWO diploma in 1998 aan het Cals college in Nieuwegein. In 1999 begon hij met de studie biologie aan de Universiteit Utrecht. Hierbij werden twee afstudeerstages gelopen, beiden in Utrecht. De eerste vond plaats bij de vakgroep Moleculaire Microbiologie (faculteit biologie). Hier werd het transport mechanisme van bacteriele autotransporters onderzocht onder begeleiding van Dr. Peter van Ulsen en Prof. Dr. Jan Tommassen. De tweede stage werd gelopen bij de vakgroep Kristal en Structuur Chemie (faculteit scheikunde). Hier werd onder begeleiding van Dr. Eric Huizinga onderzoek verricht aan het eiwit von Willebrand Factor dat betrokken is bij adhesie van bloed plaatjes. Na het behalen van zijn diploma in Februari 2005 begon hij als AIO bij de vakgroep Kristal- en Structuurchemie aan de Universiteit Utrecht waar het in dit proefschrift beschreven onderzoek werd verricht onder begeleiding van Prof. Dr. Piet Gros. Sinds juni 2010 is hij werkzaam in de groep van Dr. Roger Williams aan het Laboratory of Molecular Biology in Cambridge, UK waar hij de rol van het ESCRT systeem in celdeling onderzoekt.

List of Publications

Hadders MA, Blanchet C, Svergun, DI, Pangburn MK, Gros P Structural insights into the first step of MAC formation. *Manuscript in preparation*

Hadders MA, Aerts PC, de Mol N, Gros P, van Strijp JAG, de Haas CJC Structural basis for evasion of FcγRIIA-mediated phagocytosis by FLIPr-like of *Staphylococcus aureus*. *Manuscript in preparation*

van Wijk R, Huizinga EG, van Wesel AC, van Oirschot BA, **Hadders MA**, van Solinge WW (2009) Fifteen novel mutations in PKLR associated with pyruvate kinase (PK) deficiency: structural implications of amino acid substitutions in PK. *Hum Mutat*. 30:446-53.

Rehmann H, Arias-Palomo E, **Hadders MA**, Schwede F, Llorca O, Bos JL (2008) Structure of Epac2 in complex with a cyclic AMP analogue and RAP1B. *Nature*. 455:124-7

Hadders MA, Beringer DX, Gros P (2007) Structure of C8α-MACPF reveals mechanism of membrane attack in complement immune defense. *Science*. 317:1552-4

Staelens S, **Hadders MA**, Vauterin S, Platteau C, De Maeyer M, Vanhoorelbeke K, Huizinga EG, Deckmyn H (2006) Paratope determination of the antithrombotic antibody 82D6A3 based on the crystal structure of its complex with the von Willebrand factor A3-domain. *J Biol Chem*. 281:2225-31